Differential abnormalities of two spinal motoneuron populations in the SOD1 G93A neonatal mouse (model of the amyotrophic lateral sclerosis)

Félix Leroy

UNIVERSITÉ PARIS DESCARTES
CENTRE UNIVERSITAIRE DES SAINTS - PERES

Thèse de doctorat de l'université Paris Descartes

Spécialité
Neurosciences

Laboratory of Neurophysics and Physiology
Laboratoire de Neurophysique et Physiologie

Laboratoire de Neurophysique et Physiologie UMR 8119

ed3c

Ecole doctorale
Cerveau – Cognition – Comportement

Présentée par M. Félix Leroy

Pour obtenir le grade de

Docteur de L'Université Paris Descartes

Atteinte différentielle de deux populations de motoneurones spinaux chez le souriceau SOD1 G93A (modèle de la maladie de Charcot)

Soutenue publiquement le 6 décembre 2013

Devant le jury composé de:

M. Pascal Branchereau	Université Bordeaux 1	Rapporteur
M. George Mentis	Columbia University	Rapporteur
M. Frédéric Charbonnier	Université Paris Descartes	Examinateur
M. Stéphane Charpier	Université Pierre et Marie Curie	Examinateur
M. Boris Lamotte d'Incamps	Université Paris Descartes	Examinateur
M. Daniel Zytnicki	Université Paris Descartes	Directeur de thèse

Differential abnormalities of two spinal motoneuron populations in the SOD1 G93A neonatal mouse (model of the amyotrophic lateral sclerosis)

Doctorate PhD thesis defended by Mr Félix Leroy
On the 6th of december 2013

Remerciements

En premier lieu, je tiens à remercier George Mentis, Pascal Branchereau, Stéphane Charpier et Frédérique Charbonnier d'avoir accepté de faire partie de mon jury thèse.

Je remercie ensuite chaleureusement Daniel Zytnicki pour m'avoir encadré durant la thèse. Merci pour la patience et la confiance dont il a fait preuve à mon égard. Je remercie également Boris Lamotte d'Incamps de m'avoir encadré et appris d'innombrables choses en particulier en ce qui concerne la technique de patch-clamp et la préparation que nous utilisons.

Un grand merci à tous les membres de mon équipe, Marin Manuel, Rebecca Manuel, Nicolas Deslestrée et Clémence Martinot aux côtés desquels j'ai pris plaisir à travailler durant ces 3 années.

Je remercie de même les personnes de l'UMR 8119, en premier lieu Claude Meunier qui m'a accueilli au laboratoire, mais aussi Visou Ady, Arthur Leblois, Bill Wood, Hervé Suaudeau, Carole Sens ainsi que tous les autres…

Merci aussi à tous les membres de l'UMR 8118, où j'ai effectué les dissections et avec lesquels j'ai eu de nombreuses discussions stimulantes sur nos projets respectifs.

Merci aussi à Patrice Jégouzo pour son aide précieuse. Merci aussi à l'équipe de Frédéric Charbonnier qui m'a accueilli à bras ouvert dès que je passais leur porte. Merci à Jamilé Hazan pour ses conseils concernant la technique de RT-PCR. Merci aussi à Ali Jalil qui m'a enseigné les subtilités des anticorps.

Je souhaite remercier particuliérement ceux qui, en dehors de mes encadrants ont bien souvent relus mes bafouilles: CJ Heckman, Kathy Quinlan et Marin Manuel. Un grand merci spécialement à Philippe Asher pour son oreille attentive et ses relectures assidues.

Enfin, je remercie vivement mes parents, Patrick et Patricia Leroy, ma famille, mes amis et surtout mon épouse Laëtitia Herbaut qui me soutiennent depuis des années et sans qui rien n'aurait été possible.

Table of content

Table of figures

Introduction

Motoneurons are the link between the nervous system and the muscles. They are the final common pathways of every neural circuits involved in motricity. Since Charles Sherrington's work we know that all motoneurons share the ability to excite muscle fibers. In the adult mammalian, one motoneuron innervates many muscle fibers but each muscle fiber is innervated by only one motoneuron (Liddel & Sherrington, 1925; Redfern, 1970; Jansen & Flatby, 1990; Van Essen *et al.*, 1990). A motor unit comprises the motoneuron and all its target muscle fibers that usually share similar contractile properties.

Motoneurons receive tens of thousand of peripheral as well as central inputs (Henneman & Mendell, 1981; Kernell, 2006). Descending systems (corticospinal, vestibulospinal, rubrospinal and reticulospinal) project either directly or indirectly on the motoneurons modifying phasically (voluntary action) or tonically (serotonin liberation during locomotion) the motoneurons voltage. Peripheral inputs project directly, or indirectly, on motoneurons. The muscular mechanoreceptors (neuromuscular spindles, Golgi tendon organs) but also the joint and cutaneous receptors allow proprioceptive information to drive the motoneurons activity as well. Ultimately all these inputs are summed in the motoneurons soma and generate trains of action potentials eliciting the recruitment of motor units and the muscle contraction.

Far from being a linear integrator (Kernell, 2006), motoneurons exhibit numerous voltage-gated conductances allowing non-linear transformation of the inputs (membrane bistability, hysteresis of the response to triangular ramps). The most extendedly studied is the calcium persistent inward current that amplifies distal tonic inputs (Lee & Heckman, 1998a). Another kind of persistent inward current arises from a sodium component. Its faster time constant suggests a role in amplifying faster inputs (Li *et al.*, 2004; Harvey *et al.*, 2006; Theiss *et al.*, 2007). Other conductances active at membrane resting potential filter the cell membrane potential below firing threshold. This is the case of the H-current that creates, in conjunction with the membrane passive properties, a peak of resonance amplifying inputs of specific frequency (Manuel *et al.*, 2007).

1/ Different motoneuron sub-types in the adult mouse

The motoneuron population can be divided in many sub-populations in adults (Figure 1). γ -motoneurons innervate intrafusal fibers whereas α -motoneurons innervate extrafusal fibers and beta-motoneurons innervate both. γ- and β-motoneurons further divide between static and dynamic motoneurons according to the way they modulate the spindle activity. When investigating the properties of the motor units, Burke *et al.* (1971; 1973) defined three physiological types: fast and slow motor units according to the contraction time of the muscle fibers and within the fast motor units fatigue-resistant and fatigable motor units according to the way the contractile material of their muscle fibers is able or not to sustain repeated stimulations. Since each motor unit comprises a single motoneuron we may therefore talk about slow motoneurons (S motoneurons), fast fatigue-resistant motoneurons (FR motoneurons) and fast fatigue-fatigable motoneurons (FF motoneurons). The investigation of the motor unit properties was initially carried out in the cat but similar results were obtained in many other mammals (rat, rabbit, human, guinea-pig, (Kernell, 2006)). However some authors argued that, in the mouse, FR and FF motor units form a continuum rather than discrete populations, especially in rodents in which motor neuron size differences are less marked (Bakels & Kernell, 1993a, b) (Gardiner, 1993). In mammals every muscle embodies the three types of muscle units although in highly variable proportions. Thanks to the glycogen depletion method, Burke *et al.* (1971, 1973) further demonstrated that all the muscle fibers of a given motor unit exhibited the same histochemical profile. Furthermore, they found a correlation between the physiological types and the histochemical profiles: type S motor units have type I muscle fibers, type FR motor units have type IIA muscle fibers, and type FF motor units have type IIB muscle fibers (Figure 1). Therefore Burke *et al.* (1971, 1973) showed an exquisite correlation between the muscle unit contractile properties (contraction velocity and fatigue resistance) and the molecular identity of the fibers (difference in the amount of oxidative enzymes such as SDH or in the amount of myofibrillar ATPases, (Edstrom & Kugelberg, 1968), reviewed in (Schiaffino & Reggiani, 2011). Later on, staining of the different isotypes of the myosin heavy chain proteins was established (Schiaffino *et al.*, 1988) allowing to tighten the link between the contractile proteins and the muscle unit properties.

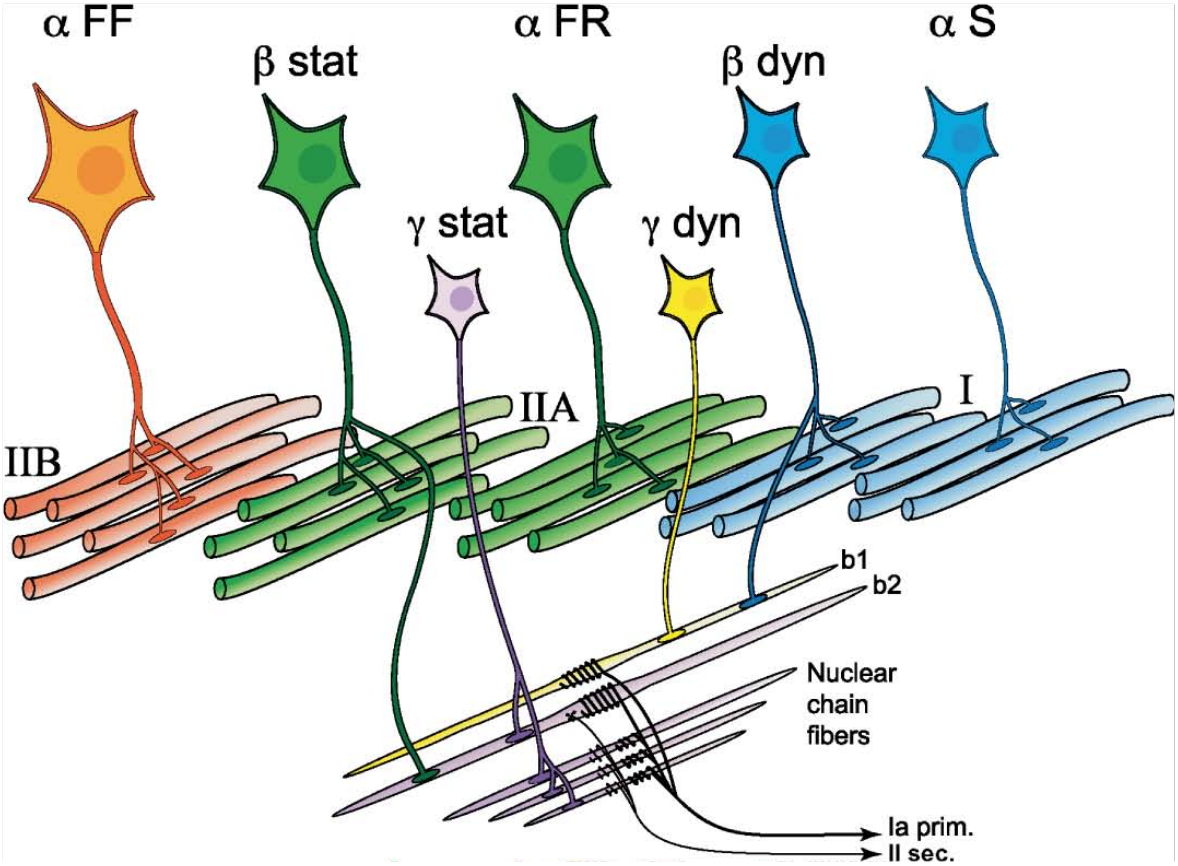

Figure 1: Schematic representation of the different types of motoneurons. The figure represents seven motoneurons innervating either extrafusal or intrafusal muscle fibers. FF-type alpha motoneurons are the biggest motoneurons (in term of soma size and axon diameter), and innervate a large number of type IIB extrafusal muscle fibers. FR alpha motoneurons are slightly smaller and innervate type IIA extrafusal muscle fibers. S-type alpha motoneurons are the smallest of the alpha motoneurons, they innervate fewer type I muscle fibers. Beta motoneurons are skeleto-fusimotor: they innervate both extrafusal and intrafusal muscle fibers. Beta static motoneurons innervate either type IIA or IIB extrafusal fibers and the intrafusal bag2 fiber. Beta dynamic motoneurons innervate type I extrafusal muscle fibers and the intrafusal bag1 fiber. Gamma motoneurons innervate exclusively intrafusal muscle fibers and are the smallest of the motoneurons. Gamma static motoneurons innervate the intrafusal bag2 fiber and/or the nuclear chain fibers. Gamma dynamic motoneurons innervate the intrafusal bag1 fiber. Note that in a muscle, the various types of extrafusal muscle fibers are mingled together and organized in a mosaic, while the intrafusal muscle fibers are much smaller than the extrafusal fibers and are ensheathed in the spindle capsule. Primary and secondary endings of the spindle encode parameters of the muscle stretches that are sent to the central nervous system via afferent fibers Ia and II. Adapted from Manuel & Zytnicki 2011.

The fact that different motoneurons impinge on different muscle units and that a given motoneuron connects exclusively to a homogenous muscle fiber population calls for a matching between a motoneuron and its efferent fibers characteristics (i.e the motoneurons electrophysiological properties need to be tuned to their output). Indeed, motoneurons properties are widely different. Among all characteristics, motoneurons of a given kind segregate according to their electrotonic size (evaluated by the measure of the input conductance, (Zengel *et al.*, 1985). In addition, Friese *et al.* (2009) showed that the average size of the soma already allowed to discriminate between γ - and α -motoneurons as early as P14 in the mice. Motoneuron size therefore increases from γ-motoneuron to α-FF motoneuron (γ < α-S < α-FR < α-FF).

Given the evidence indicating that α-motoneurons receive a common input (Mendell & Henneman, 1968; Henneman, 1985), Henneman *et al.* (1957) posited an orderly recruitment of the motor units based on the size principle. That is to say that considering a fixed input, the most electrotonically compact motoneurons will see their voltage rise more and will reach their firing threshold prior the less compact ones.

In the neonatal rodent, heterogeneity between motor units is already established (Close, 1967) and motor units present a biased composition in fiber types as early as E16 (Condon *et al.*, 1990). But what about putative differences between neonatal motoneurons electrical intrinsic properties? So far, we do not know how the functional properties of the different sub-types of spinal motoneurons maturate. It is well known that, in adult mammals, spinal motoneurons start to fire without any delay at the onset of a liminal current pulse (Kernell, 2006; Manuel *et al.*, 2009). In sharp contrast, at least two different firing behaviors were reported during the second postnatal week for the rat abducens motoneurons (Russier *et al.*, 2003) or the mouse spinal motoneurons (Pambo-Pambo *et al.*, 2009). Upon injection of liminal current pulses, the discharge starts at the current onset in some motoneurons but it is delayed in others.

The first part of my thesis aims at answering the following questions: *What are the currents underlying the different patterns of discharge in neonatal mice? Are the differences in firing patterns linked to diverse motoneurons functional sub-types?*

2/ Motoneurons are uneven when facing the ALS

The amyotrophic lateral sclerosis also called Charcot's disease or Lou Gehrig's disease is a neurological disease relatively frequent of cause unknown and somber prognosis. As Charcot stated it 140 years ago "the prognosis up to present, is of the gloomiest. There does not exist, so far as I am aware, a single example of a case where, the group of symptoms just described having existed, recovery followed". It is the most frequent motoneuron disease with a prevalence of 4/100000. Both sexes are concerned with a slight prevalence toward the males. Onset generally occurs around 50 years. The disease is characterized by a progressive degenerescence of

the spinal cord motoneurons as well as the motor cortex neurons and a destruction of the pyramidal tract (Goetz, 2000). So far only one drug has been approved by the FDA: the riluzole, an inhibitor of presynaptic glutamate release, only prolong the patient life by a few months. Superoxide Dismutase 1 (SOD1) is the most commonly mutated protein in cases of familial ALS (20%). However numerous different proteins and mutations have also been involved in ALS (Ling *et al.*, 2013). They will be reviewed in the chapter III.

The ALS symptoms usually begin with an obvious weakness and/or muscle atrophy. The majority of the cases experience "spinal onset" ALS, *i.e.*, symptoms starts in the arms or legs. Patients with the leg-onset form may suffer difficulties when walking or running or notice a tendency to stumble. Arm-onset patients may encounter increased difficulty with fine manual tasks such as buttoning their clothes, writing or play an instruments. In rare cases the affection remain confined to a single limb for a long time, this is the monomelic atrophy. Most of the other cases are "bulbar onset" ALS. These patients first notice difficulty of speaking clearly or swallowing. Speech may become nasal in character, slurred or softer. Other symptoms include difficulty of swallowing accompanied by a decrease in the tongue mobility. A very minor percentage of the patients suffer from "respiratory onset" ALS, where the intercostal muscles that support breathing degenerate primarily. Noteworthy, a few patients present symptoms similar to frontotemporal dementia and later include more typical ALS signs. Regardless of the part of the body first affected by the disease, muscle weakness and atrophy spread to other regions of the body as the disease progresses. In bulbar-onset ALS symptoms typically spread to the arms before the legs, whereas in limb-onset ALS, symptoms usually spread from the affected limb to the opposite limb before affecting a new body part. Furthermore some motor nuclei proved to be insensitive to the disease progression even during the latest stages. Clinical studies show that in most patients, ocular movement and voluntary control of eliminative functions remain unimpaired until terminal stages (Mitsumoto *et al.*, 2006). These functions are controlled by motor neurons of the oculomotor, trochlear, and abducens nuclei in the midbrain/hindbrain, and by Onuf's nucleus in the lumbosacral spinal cord, respectively. Post-mortem studies confirmed motoneurons from these motor pools remained intact (Schroder & Reske-Nielsen, 1984; Gizzi *et al.*, 1992; Mannen, 2000; Kaminski *et al.*, 2002). Correspondingly, mouse mSOD1

models also show almost complete resistance of oculomotor, trochlear, abducens (Ferrucci *et al.*, 2010) and Onuf's (Hamson *et al.*, 2002) nuclei.

To study the disease, a mutated version of the human SOD1 gene was introduced by transgenesis into the mouse genome (Gurney *et al.*, 1994). I used the G93A high expressor line SOD1 model to study the effect of ALS in neonatal mouse motoneurons. In this model, degeneration of the motoneurons starts at about 50 days (failing of the neuro-muscular junctions) and follows an order that depends on the motor unit type (Pun *et al.*, 2006; Hegedus *et al.*, 2008). Motoneurons innervating the fast-contracting and fatigable muscle fibers degenerate before those innervating the fast-contracting and fatigue-resistant fibers whereas those innervating the slow-contracting fibers are affected only during the final stages of the disease (Hegedus *et al.*, 2008).

Excitotoxicity, due to an excessive entry of calcium in the cell, is one of the main hypotheses to explain the motoneurons degenerescence. Excitotoxicity may come from intrinsic and extrinsic reasons. From the outside, a shift of the excitatory / inhibitory balance toward more excitation or a less efficient glutamate recapture by the astrocytes may induce an increase in the calcium entering the cell. From the inside, every time an action potential is emitted and travels along the axon, voltage-gated calcium conductances open and allow calcium to enter the cell. Therefore any modifications leading to broader or more numerous spikes will increase the total amount of calcium entering and might induce the death of the motoneuron. By definition the neuron is said hyper-excitable. Besides broadening of the spikes, critical changes in the electrophysiological properties include lowering of the recruitment threshold and/or increase of the spiking frequency for a given current density. Altogether any modifications of the intrinsic properties that lead to increase the number of spikes may induce hyperexcitability. In addition, evidence evidence indicates that motoneurons display low levels of calcium buffers (Lips & Keller, 1998). Several studies pointed out early alterations in the electrical and geometrical properties of cultured, spinal or hypoglossal motoneurons of embryonic and neonatal SOD1 mice. However, the results were somehow contradictory. In embryos, the excitability of the mutated motoneurons was higher than the WT motoneurons (Pieri *et al.*, 2003; Kuo *et al.*, 2005) and the dendritic length was shown to be reduced

(Martin *et al.*, 2013). In neonates, motoneurons were described as hypo-excitable by Bories *et al.* (2007) whereas for Pambo-Pambo *et al.* (2009) they were hyperexcitable. However, Quinlan *et al.* (2011) found that the excitability of motoneurons is homeostatically maintained despite an increase of their input conductance. This increase of input conductance was partly accounted for an over-branching of the dendritic tree (Amendola & Durand, 2008; Elbasiouny *et al.*, 2010). These discrepancies might be due to the fact that the spinal α-motoneurons are a heterogeneous population even at these early stages.

The heterogeneous vulnerability of SOD1 mutated motoneurons raises the possibility that, similarly to what happens in the adult, the sub-types found among the spinal motoneurons population in neonates are not affected in the same way by the SOD1 G93A mutation.

The second part of my thesis thereby aims at answering the following question: *Is it possible to identify in the neonatal mouse subsets of motoneurons specifically affected by the mutation?*

3/ Presentation of the work done

The common hypothesis underlying the questions defined above is that motoneurons electrical properties already clusterize in the neonatal mouse allowing the discrimination of different functional populations and that these populations are differentially affected by the disease.

To test this hypothesis I conducted patch-clamp recordings of P6-P10 L5 spinal motoneurons in an *in vitro* slice preparation (Lamotte d'Incamps *et al.*, 2012). The direct stimulation of the ventral rootlet allowed for identification of the motoneurons by the mean of the antidromic action potential. Experiments were conducted during the second postnatal week, a few days prior the mice begin walking. We thus hope to be able to disambiguate early causes of the ALS from downstream adaptations and coping mechanisms that might compensate early modifications. Furthermore, in the wild-type mouse we know very little regarding the motoneurons properties maturation.

In the first part of my work, I recorded wild-type (WT) motoneurons and found the two discharge patterns described previously (Pambo-Pambo *et al.*, 2009). In order to characterize the underlying currents, I conducted a series of voltage-clamp experiments coupled with pharmacology in order to decipher the currents underlying both discharge patterns. I found that the delayed firing motoneurons express two potassium currents not found in the other immediate firing motoneurons. These currents prevent the discharge before they inactivate, allowing the membrane potential to rise to the voltage threshold and the cell to fire.
This work gave birth to a manuscript entitled "**A subpopulation of neonatal mouse spinal motoneurones displays a delayed firing profile due to an A-like and a slow-inactivating potassium currents**" that has been recently submitted for publication.

In addition to exhibiting different discharge patterns, the delayed and immediate firing motoneurons display differences in their electrophysiological and morphological properties. Following the presentation of the first article I will detail three kinds of evidence (morphological, electrical and molecular) suggesting that the motoneurons exhibiting a delayed discharge in response to a liminal pulse of current innervate fast-contracting fibers whereas those with an immediate discharge innervate slow-contracting fibers.

In the second part of my work, I recorded motoneurons from SOD1 G93A mice as well as their non-mutant littermates. Mutant and WT motoneurons presented delayed and immediate firing patterns in the same proportions. Based on the known differential vulnerability to the disease between motoneurons of different sub-types I conducted the type-by-type comparison of the SOD1 mutation effect on the delayed firing motoneurons parameters on one side and immediate firing motoneurons on the other. I found that only the immediate firing motoneurons are hyperexcitable in the mSOD1 mice. The excitability of the delayed firing motoneurons is unchanged. A second manuscript entitled "**Only spinal motoneurons that display the "immediate firing" profile are hyperexcitable in SOD1 G93A neonatal mice**" was written and will be submitted shortly for publication.

4/ Thesis content

In the first chapter I will review what we know about the differentiation of the motor units and motoneurons leading to their extensive heterogeneity. In the second chapter I will summarize my results showing how the expression of specific potassium conductances in 66% of the wild-type motoneurons allows for the delayed firing pattern (in opposition to the left 33% of the motoneurons that fire at the pulse onset). The corresponding submitted article, that fully describes the results, is appended following the chapter 2. The second chapter continues presenting additional results to the first article that attempt to correlate the discharge patterns with known the motoneurons fast and slow subtypes. The third chapter will review the data regarding the impact of the SOD1 G93A mutation on the motoneurons properties. In the fourth chapter I will summarize my type-by-type analysis of the delayed and immediate motoneurons population. It will enlighten interesting opposite effects of the SOD1 mutation for each type of neonatal motoneurons. The corresponding article (to be submitted), that fully decribes the results, is appended following the chapter 4. Material and methods of the experiments are detailed in the two articles or in the protocol section at the end of the thesis. A global discussion on the work performed and its future developments completes this manuscript. After discussing the results concerning the maturation of the motor units and the differential effects of the SOD1 mutation, the discussion will open to consider whether a change in the cell excitation (i.e its synaptic inputs) could take place during the ALS and how this could be experimentally tested.

Chapter I: Differentiation of the heterogenous motoneuron populations

1/ Mature motoneurons intrinsic properties segregate

a/ According to their morphological parameters

Many of the motoneurons properties vary according to the motor unit type they belong to. Horseradish peroxidase stainings of cat motoneurons. Burke *et al.* (1981) have shown that the somas of motoneurons innervating FF motor unit tend to be are larger (50 - 80 µm) than those of motoneurons innervating FR motor units (50 - 70 µm), which themselves are larger than those of motoneurons innervating the S motor unit (45 - 70 µm). There is however an extensive overlap between the values. We know that γ-motoneurons are even smaller than the α slow motoneuron (Horcholle-Bossavit *et al.*, 1990). The difference seen in the average sizes can be expected to influence on many electrophysiological properties such as the axonal conduction velocity, input conductance and rheobase.

b/ According to their electrophysiological parameters

Zengel *et al.* (1985) realized a meta-analysis of 73 motoneurons recorded *in vivo* in the adult cat medial gastrocnemius that were type-identified based on the mechanical properties of their motor unit. They found that FF and FR motoneurons presented similar axonal conduction velocities (99 ± 1 m/s and 100 ± 1 m/s respectively) which was higher than that of S motoneurons (86 ± 1 m/s). Input resistances were comprised between 1.0 MΩ and 2.8 MΩ (1.6 ± 0.1 MΩ) for S motoneurons, between 0.4 MΩ and 1.6 MΩ (0.9 ± 0.1 MΩ) for FR motoneurons and between 0.1 and 1 (0.6 ± 0.1 MΩ) for FF motoneurons. Rheobase, defined as the minimum amount of current to inject during a 50 ms pulse to elicit firing, also varies between types being highest in FF motoneurons (21.3 ± 0.5 nA), intermediate in FR motoneurons (12.0 ± 0.4 nA) and lower in S motoneurons (5.0 ± 0.3 nA).

The overlap values of each individual electrophysiological parameters require using several parameters to properly classify a motoneuron. A single parameter could never reach a classification rate higher than 80% (Zengel *et al.*, 1985). Using the principal component analysis method Zengel *et al.* (1985) showed that a

classification criterion combining the input resistance and the AHP half-relaxation time they could correctly classify of 94% of their sample. Zengel *et al.* (1985) therefore chose boundaries in the input resistance and half-AHP duration spaces that allow for reliable motoneuron classification. A similar work on mouse motor units is currently underway in the lab as an *in vivo* mouse preparation was developed (Marin Manuel personnal communication). Preliminary results show that the electrophysiological properties of adult mouse motoneurons allow the characterization of three different groups of motoneurons. As observed in the cat, the motoneurons innervating the same type of muscle fibers share similar electrophysiological properties. Input conductance and AHP duration allow for a good discrimination of the motor unit type (Figure 2, Marin Manuel personal communication).

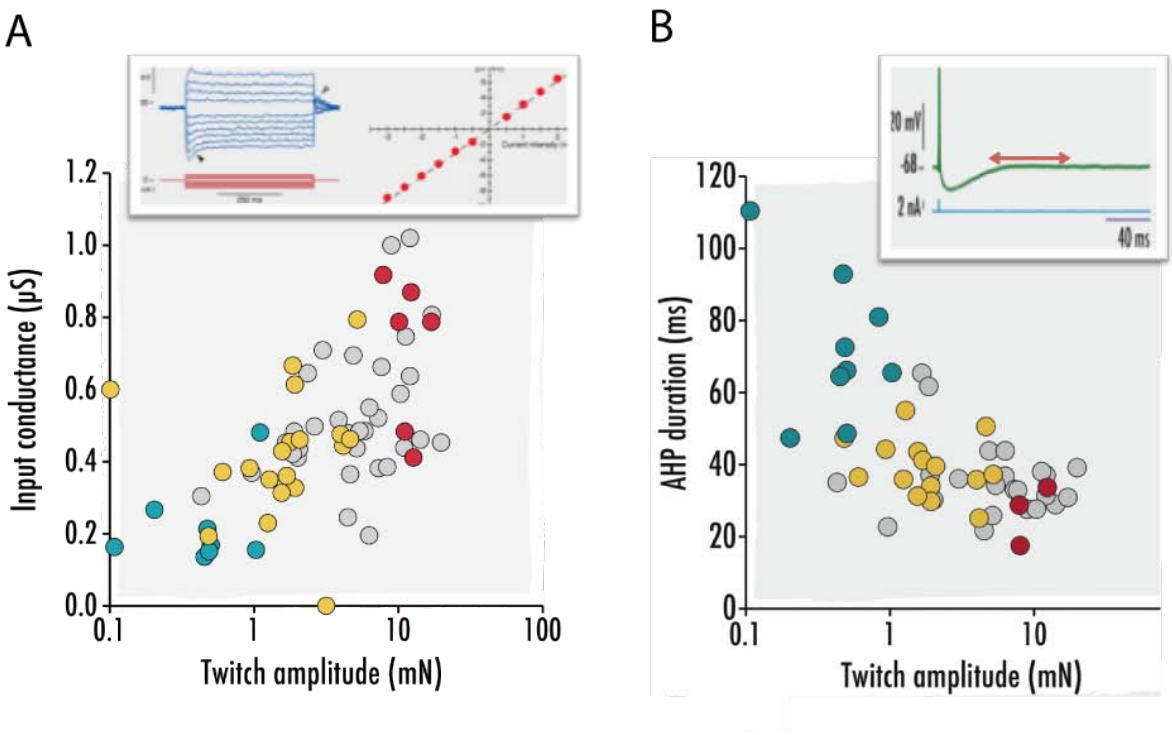

Figure 2: Motoneurons subtypes segregate according to their intrinsic properties. Plot of the input conductance **(A)** and the AHP duration **(B)** of in vivo adult motoneurons in function of the twitch amplitude of their motor units. S-type motoneurons in blue, FR-type motoneurons in yellow, FF-type motoneurons in red and non-identified motoneurons in grey. Inserts illustrate how each intrinsic property was measured. Personnal communication from Manuel et al.

2/ Henneman's "size principle" for mature motoneurons

The clusterization of the motoneuron electrophysiological properties allowed Henneman (1957) to forge the "size principle" to explain the orderly recruitment of motoneurons from the same motor pool. During the stretch reflex of a decerebrated cat sural triceps, the smaller motor units (S motor units) are recruited first. Henneman (1957) hypothesized that during a voluntary movement the smaller motor units exhibiting less force and longer contraction time (S motor units) are mobilized first followed by those producing more force and contracting more rapidly (FR and FF motor units). This was supported by many other experiments (Burke, 1981; Henneman & Mendell, 1981). If we assume that a common synaptic current drive for all α-motoneurons belonging to a common motor pool then because of their smaller input resistance the S motoneuron will reach its spiking threshold first. Then when the input increases the FR motoneurons will be recruited and ultimately the FF motoneurons. The longer time constant of S motoneurons also allows for an easier summation of the slow frequency synaptic inputs and favors similarly their selective recruitment at low frequencies. In this view, recruitment of different motor units starts by the smaller motor units of lesser force and longer contraction time allowing for a smooth gradation of the global force developed at the level of the entire muscle.

The "size principle" was posited at a time when motoneurons were thought to be passive integrators. We now know that the motoneuron membrane bears various voltage-dependant conductances allowing them to act as a non-linear integrators (Manuel *et al.*, 2007). However channels carrying the persistent inward currents are more strongly expressed on the slow type motoneurons which are the first recruited (Lee & Heckman, 1998a, b). Therefore this voltage-dependant conductance strengthens the orderly recruitment. Indeed, persistent inward currents were likely present during the experimental protocol Henneman used (Henneman, 1957). Some studies argued that motoneurons receive different inputs (Kanda *et al.*, 1977; Heckman & Enoka, 2012) and that the Henneman's principle should be supplemented by other principles such as an orderly recruitment among motoneurons supplying different muscles to better explain fast ballistic movements and smooth trajectories (Cope & Sokoloff, 1999) or "neuromechanical" principle to explain respiratory movements (Butler & Gandevia, 2008). Nevertheless, a multitude of studies in humans have shown the size principle to apply in multiple tasks,

muscles and movement speeds (Desmedt & Godaux, 1977; Jones *et al.*, 1994; Feiereisen *et al.*, 1997; Scutter & Turker, 1998), which fully validate it as a genuine physiological principle.

3/ Motor units differentiation

This section will briefly summarize the muscles and motoneurons development leading to the establishment of a functional adult motor unit in the mouse.

a/ Myogenesis

Myogenesis begins when stem cells originating from the somites migrate to the limb buds. They begin to synthesize myosin as early as E10 (Figure 3) in the mouse embryo (Jansen & Flatby, 1990). Myoblasts divide into primary myotubes. After a time lag myotubes are reached by motor axon nerves around E12. Myogenesis resume and a second wave of myogenesis build upon the first one adding the secondary myotubes (Figure 3). This second myogenesis ends around birth: before birth for respiratory muscles that will be used later on (the mice begin to stand around P10. The assembly of the secondary generation of myotubes requires innervation of the muscle and cholinergic activation of the primary fibers (Harris, 1981; McLennan, 1983). In rodents the early myotubes express both embryonic myosin heavy chain (MHC) and adult slow-type MHC. Many also express a distinct neonatal MHC (Weydert *et al.*, 1987). Primary generation myotubes remain mostly slow, while some eventually suppress the expression of slow-type MHC, to produce adult fast-type MHC instead. Such a transition is thought to be highly activity dependent. The second generation myotubes initially express embryonic and neonatal MHC. The majority develop into fast fibers. In slow muscles such as the soleus a more substantial fraction of the secondary myotubes develops into slow fibers (Narusawa *et al.*, 1987). The final numbers of fast and slow fibers and their distribution are characteristically different for each muscle and far from being fixed, reorganization occurs during the life upon injury or aging.

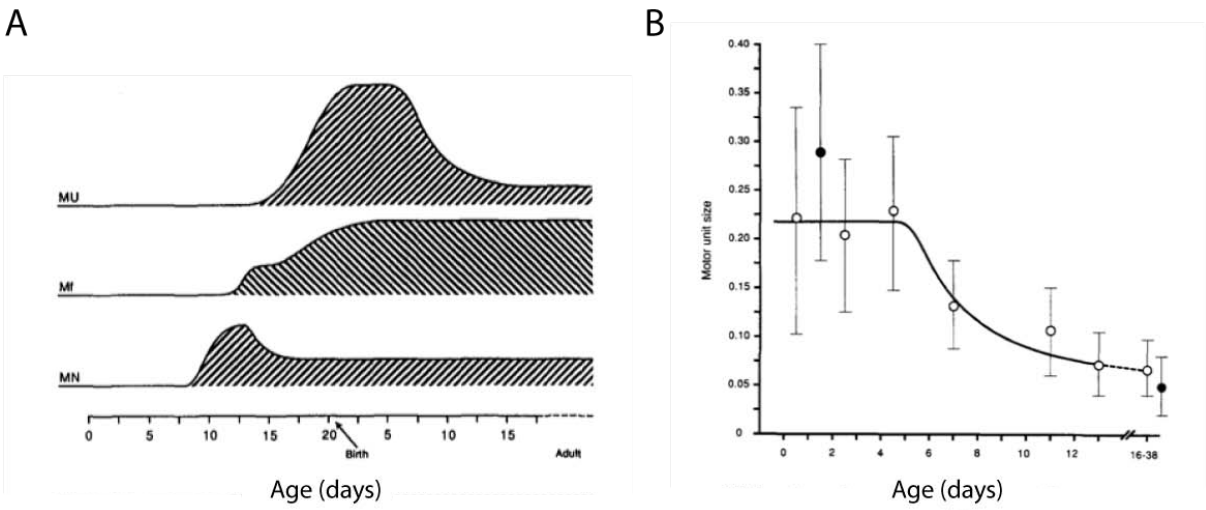

Figure 3: Summary of important events in the development of neuromuscular connectivity. **(A)** From top to bottom: size of motor units (MU), number of muscle fibers (Mf), number of motoneurons (MN) . Adapted from Jansen and Flatby 1990. **(B)** Figure 3. Reduction of motor unit size postnatally. Empty circles: Average value of unitary twitch contractions obtained by stimulating individual axons in ventral root filaments, expressed as fraction of maximal muscle twitch. Filled circles: Give corresponding values for unitary tetanic contractions at 0-4 days and 16-38 days. Bars give SD of values. The higher tetanic value in newborn is due to facilitation of terminals subthreshold for activating fibers after single shocks. The higher twitch value in juveniles is due to non-linear summation of twitches. From Fladby, 1987.

b/ Motor Columns

During development, newly postmitotic motoneurons are grouped into motor columns stretching along the rostrocaudal extent of the neural tube. This is due to gradients of diffusible molecules emitted from the neural tube which interact with the motoneuron transcription factors (reviewed in (Dasen & Jessell, 2009). For all mammals the motor columns are the following: the medial motor column (MMC), which projects to epaxial muscles of the dorsal body region, the hypaxial motor column (HMC), which projects to hypaxial muscles of the ventral body wall, and the lateral motor columns (LMC), which project to the limbs. The preganglionic column (PGC) innervates sympathetic ganglia and the smooth muscles. Within each column the ensemble of motoneurons innervating a single muscle is called a motor pool. It is interesting to note that in parallel to the distribution of motoneurons each motor pool comprises all the different functional sub-types described before. The presence of these two levels of diversity renders comparison between motoneurons of the same sub-type fully relevant only when operated within one motor pool. Once the motoneurons somas have reached their location in the spinal cord they begin sending their axons to innervate their target muscle. The motor axons exit the spinal cord through their segmental ventral roots and join their fellow motor axons belonging to the same motor pool but exiting from another segment in the lumbar plexus. The axons of the same motor pool then

fasciculate and travel along peripheral nerve trunks to leave these at specific branch points in order to reach the appropriate muscle.

c/ Formation of the neuromuscular junctions

The axon terminals reach the embryonic muscle prior to the fusion of the first myoblasts. Functional neuro-muscular junctions (NMJs) are formed shortly. In mammalian muscles, all NMJs are found located in a tightly regulated mid-part of the muscle fibers. Indeed, the medial part remain more or less fixed during the fiber contraction and the muscular action potential can propagate symmetrically toward both ends. Furthermore the close proximity between the different NMJs favors competition between them during the elimination of poly-innervation. The synapse formation and maturation requires intensive interactions between pre- and post-partners for correct alignment but also for motoneurons and fibers matching (Hall & Sanes, 1993). Evidence points out that future γ-motoneurons already connect to future intra-spindle fibers (Thompson *et al.*, 1990). Similarly, a few studies conducted on immature motor units (Thompson *et al.*, 1984; Flatby & Jansen, 1990) seem to indicate that most fibers are correctly grouped into muscle units prior the late events of axonal pruning and diminution of the muscle fiber poly-innervation.

d/ Motoneurons death

A massive developmental death begins when the axons reach the muscle embryos. From E12 in the mouse(Lance-Jones, 1982) and over the following week about half of the motoneurons will enter apoptosis and die (Figure 3A). Such a large loss is intriguing since all axons from a motor pool contact its appropriate muscle. One hypothesis is that the programmed death results from the wrong wiring within the muscle between inappropriate functional sub-types (mismatch between the motoneuron and fiber sub-types (Jansen & Flatby, 1990).

e/ Loss of the poly-innervation

In the adult each fiber is contacted by a single motoneuron. However around birth all muscle fibers are poly-innervated. All muscles therefore undergo a process of elimination of the poly-innervation. As a result the number of fibers in each motor unit decreases strongly. The size of motor units decreases accordingly (Figure 3B, (Jansen & Flatby, 1990). Dennis *et al.* (1981) measured in the rat intercostal muscle

the average number of NMJs present on each muscle fibers (Figure 4A). They observed an increase in the degree of poly-innervation followed by a plateau and then a decrease. However the degree of poly-innervation as well as the moment at which it begins to decrease vary extensively between muscles. In the rat diaphragm and intercostal muscles the degree of poly-innervation has peaked already a day before birth and is distinctly reduced at birth (Figure 4A, Bennett & Pettigrew, 1974; Dennis *et al.*, 1981). In the soleus, on the other hand, the expanded motor units appear to remain at a plateau until P10 with about 5 terminals converging on each fiber before stooping down quickly to 1 terminal by P15 (Figure 4B, (Brown *et al.*, 1976). Although different in time and intensity there are two process concomitantly at stake in the maturation of muscles around birth. On one hand new fibers (secondary myogenesis) are added and rapidly innervated and on the other hand supernumerary synapses are deleted. This situation can give rise to several scenarios depending on whether the events are disjoint or overlap. Due to the difficulty to properly follow the degree of poly-innervation around birth researchers tried to compare the rate of decrease in the poly-innervation. However the rate of decrease they measured only reflects the ratio of new contacts over the one being eliminated when only the number of axon terminals retracting truly matters. Additionally an important caveat was the absence of fiber type identification when assessing the poly-innervation. Some studies suggested that most NMJ were already type-matched prior the reduction of the poly-innervation. Callaway *et al.* (1989) measured the fractional decline in motor unit tension in the rabbit soleus and demonstrated a substantially higher initial degree of poly-innervation and rate of elimination for slow than for fast motor units.

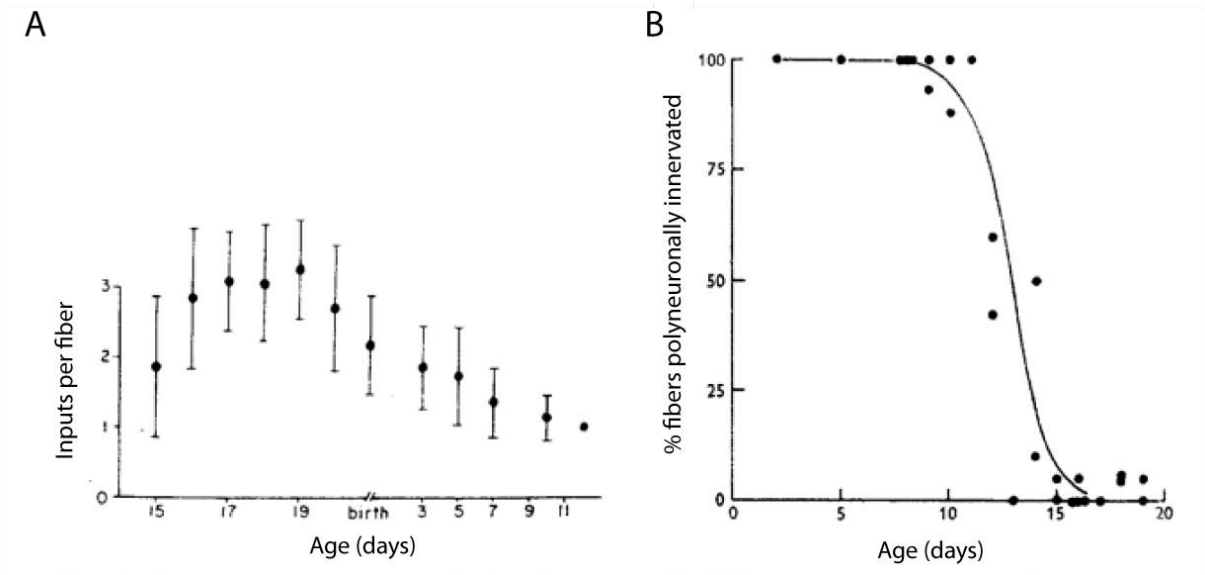

Figure 4: Polyneuronal innervation of muscle fibers. (A) Mean number of synaptic inputs per fiber of rat intercostal muscles. Each point gives the average and bars the SD of the number of unitary components of the epps from 30 - 60 fibers at each age (Dennis et al., 1981). **(B)** Frequency of polyneuronally innervated muscle fibers in the rat soleus over the postnatal period. Each point represents the average value obtained by graded nerve stimulation and intracellular recording from 20 or more fibers from each muscle (Brown et al., 1976).

Flatby and Jansen (1990) studied the composition in muscle fibers of the motor units of the mouse neonatal soleus at P2, P5 and P14. At P2 and P5 the muscle is still at its neonatal peak of polyneuronal innervation (on average 6 NMJ/fiber) while at P14 poly-innervation is virtually over. Stimulating one axon (i.e one motor unit) per experiment they were able to sample the muscle fibers connected to it. For recordings at P14 they used the glycogen depletion method. The group of Kugelberg (Edstrom & Kugelberg, 1968) first showed that in the adult individual motor axons innervate a homogenous group of muscle fibers. This was achieved by stimulating individual motor axons under anoxic conditions until the glycogen stores of their muscle fibers were depleted (Edstrom & Kugelberg, 1968).They could then identify the fibers histochemically on cross sections of the muscle using the periodic acid Schiff (PAS) reaction. However this method could not be used in immature muscle fibers at P2 and P5. The authors then randomly recorded muscle fibers and filled them with Lucifer Yellow when a plaque potential was recorded following the motor unit stimulation (Figure 5a,b and c). They plotted the histogram distribution of the fraction of fast fibers found in each recorded motor unit (Figure 5d). At P2 the histogram distribution is already slightly bimodal (Figure 5e) when an unimodal distribution would have been expected if the wiring were random (Figure 5d). Therefore already at P2, the motor units composition is already biased toward either

a majority of fast or a majority of slow fibers. The bimodal distribution refines at P5 and P14 (Figure 5f and 5g). Given to this biased composition motor units already displayed an emerging fast/slow cleavage in their contractile velocity as soon as P5. The authors concluded that most of the fast/slow separation of the muscle fibers takes place prior to the reduction in poly-innervation begins.

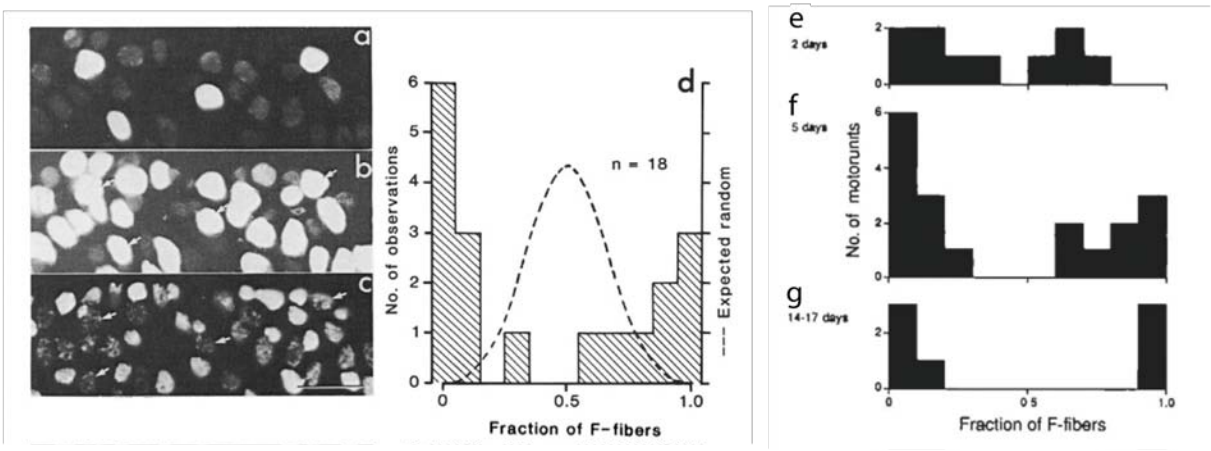

Figure 5: Neonatal motor unit are already largely homogenous in their fibers composition. (a) Part of cross-section from central region of a 5 day old mouse soleus muscle. Four fibres from the same motor unit labeled with Lucifer Yellow. **(b)** Same section, S fibres identified with antibody to slow myosin heavy chain and visualized with TRITC labelled secondary antibody. The faint signal from the S negative fibres is due to autofluorescence. The Lucifer-labeled fibres indicated by arrows are all S positive. **(c)** The neighbouring section, same field, reacted with antibody to F myosin. Labeling intensity distinguishes a strongly and a faintly labeled group of fibres. The strongly labeled group are virtually all negative to the S myosin antibody. The Lucifer-marked fibres (arrows) belong to the faintly labeled group. Scale 30 µm. **(d)** Histogram of motor units ranked according to fraction of F fibres in the labeled sample. The stippled curve gives the expected distribution if F and S fibres had been randomly innervated. From Fladby and Jansen, 1988. **(e, f, g)** Time course of the motor units homogeneization ins muscles fibers type. **(e)** 2 days, 10 motor units with an average of 10.2 (range 8- 3) fibers labeled in each. **(f)** 5 days, 18 motor units with an average of 10.8 (range 7-14) fibers labeled in each. **(g)** 2 weeks, 7 motor units with an average of 21.9 (range 16-38) labeled in each. The histograms show an increasing specificity of innervation during the neonatal period. Adapted from Fladby and Jansen 1990.

The following elimination of supernumerary NMJ would not be a major factor of the fast / slow fibers segregation but only a competition between motoneurons of the same sub-type to keep innervating the largest subset of fibers. Unfortunately, technical limitations precluded Flatby and Jansen from recording the properties of the motoneurons they stimulated. Although the total number of NMJs remains constant between P2 and P5 the histogram distribution shows an extensive refining in the motor unit composition. Presumably slow motoneurons loose synapses impinging on slow primary myotubes and slow secondary myotubes while gaining synapses on the neonatal secondary myotubes. Given that all primary myotubes are slow (Weydert *et al.*, 1987) and that we know that some slow motoneurons contact slow fibers at birth it is safe to assume that slow motoneurons innervate slow primary myotubes prior to the second myogenesis. We should keep in mind that activity-dependent transformation of the fibers is possible (reviewed in Schiaffino & Reggiani, 2011) and

cannot be entirely ruled out, although it probably only takes place during non-developmental remodeling following an injury.

To conclude, the formation and maturation of the motor unit is a highly controlled process leading to the correct wiring between matching motoneurons and muscle fibers. Motoneurons from a motor pool connect all to its muscle and within the motor pool the different motoneurons sub-types connect appropriately to their matching fibers. Assessing the properties of the motoneuron activating the recorded muscle units is the only way to properly correlate the two elements forming the motor unit. However technical limitation in the neonatal mouse have so far precluded performing simultaneous recordings from the muscle and the spinal cord. Such preparation remains to be developed. Thus no correlation has been made at an early age between the motor units and their motoneurons. Are the motoneurons properties already differentiated or do they differentiate later once the motoneurons are appropriately connected to their subset of homogenous muscle fibers? In the next section we will review the available data regarding the evolution of conductances, morphology and electrophysiological properties in the maturing motoneurons.

4/ Motoneuron maturation and differentiation

a/ Morphology

Initially, motoneurons precursors all begin growing dendritic tree once their somas finished migrating to the future place of the motor pool. The distribution of the somas is unimodal around birth and then becomes quickly bimodal reflecting the differentiation of gamma and alpha motoneurons (Horcholle-Bossavit *et al.*, 1990, for kitten; Friese *et al.*, 2009 for mice) Dendrite growth appeared to be proportional throughout the tree. Furthermore, the elongation was proportional to enlargement of overall spinal cord dimensions. The topology of cat and rat motoneuron dendritic tree is submitted to remodelling and pruning shortly after birth (Nunez-Abades *et al.*, 1994; Nunez-Abades & Cameron, 1995). The number of axon collateral changes as well for in the cat (Horcholle-Bossavit *et al.*, 1990). However, for mouse motoneurons dendritic trees, the topology remains similar from E17.5 to P11 (Li *et al.*, 2005; Martin *et al.*, 2013; personal observations). During the first post-natal weeks maturation mainly consisted of branch elongation and thickening throughout the whole dendritic

arborization, which appear to follow the significant overall growth of the surrounding tissue during this period. A small increase in number of nodes and terminals can be seen but overall mouse motoneurons dendritic tree mostly grow homogeneously in size (Li *et al.*, 2005; Martin *et al.*, 2013; personal observations).

Motoneuron morphology in adults is highly dependant of their motor pool as well as their functional sub-type. Dendrites initially projects in all directions to invade the surrounding space, but for motor pool close from the ventral horn boundary the most extensive branching takes place within the gray matter dorsal and medial to the somatic location (Li *et al.*, 2005; personal observations) when much less dendrites project rostro-caudally. Motor axons arise directly from the soma or from a thick proximal dendrite and then extend into the nearest ventral root (Li *et al.*, 2005; personal observations). Motor axons have one or two recurrent collaterals that branched profusely within the territory occupied by the dendrites of the same neuron, projecting notably to the Renshaw cells impinging back on the motoneurons (Li *et al.*, 2005; personal observations).

Cullheim *et al.*, 1987a, b) were among the first to study the size and topology of the type-identified motoneurons in adult mammals. Staining of the triceps surae alpha-motoneuron by HRP allowed reconstruction of the motoneuron and measurement of the membrane area. They showed that S-type motoneurons dendritic area was on average 22% smaller than F-type motoneurons although the populations overlap. The branching structures differed as well. S-type motoneurons were less prone to branching and expand more radially than F-type motoneurons. Overall the structural differences suggested that the F and S groups of α-motoneurons could be viewed as intrinsically distinct cell types and not as members of the same population with different sizes (Cullheim *et al.*, 1987a). In a companion paper the same authors tried to assess the ways in which dendrites occupy three-dimensional space. They concluded that despite considerable scatter, the results showed that the space occupied by the branches tends to be approximately the same in large and small dendrites, and in F and S cell groups (Cullheim *et al.*, 1987b). Further studies of adults motoneurons confirmed that the different motoneuron populations segregate relatively to their size in the following order (γ-motoneurons < α-S motoneurons < α-FR motoneurons < α -FF motoneurons). Extensive overlap between populations persists however all life long.

b/ Conductances

Motoneurons are endowed with a set of common voltage-dependent channels which include the fast sodium channels and the delayed rectifier potassium channels allowing the emission of action potentials (Barrett & Barret, 1976; Schwindt & Crill, 1984; Delgado-Lezama *et al.*, 1999). It also includes a calcium-dependent potassium channel responsible for the mAHP as well as a Ca^{2+} channel allowing calcium influx during the spikes. Drug sensitivity supports the idea that these channels are respectively the SK channel (Barrett & Barret, 1976; Schwindt & Crill, 1984; Delgado-Lezama *et al.*, 1999) and the N-type calcium channel (Perrier & Hounsgaard, 2000). Additionally motoneurons also express a non-specific cation channel generating the H-current (Ito & Oshima, 1965; Schwindt & Crill, 1984; Manuel *et al.*, 2009). Some motoneurons also exhibit additional currents such as the Ca^{2+} persistent inward current (Hounsgaard & Mintz, 1988), the Ca^{2+} transitory T-type current, the Na^{+} persistent inward current, the potassium A-current or the Ca^{2+} activated non-selective cationic current (Perrier & Hounsgaard, 1999). Among all currents identified in the motoneurons we will focus on three of them which expression has been shown to be modulated during development: the T-type calcium current, the transient potassium A-current, and the L-type Ca^{2+} current.

i/ T-type Ca^{2+} current

The T-type Ca^{2+} channel is a low-voltage activated Ca^{2+} channels (Figure 6C). It may induce a rebound of the membrane potential following prolonged hyperpolarization since it is inactivated at rest and de-inactivated upon hyperpolarization. Evidence for transient expression of T-type calcium channels in spinal motoneurons during development has been obtained from chick (McCobb *et al.*, 1989), mouse and rat (Figure 6A). In the mouse it has been detected in spinal motoneurons from E14 to P8 (Mynlieff & Beam, 1992a, b). In the rat, a T-type calcium current facilitated by serotonin was demonstrated in spinal motoneurons at P3-P4 (Berger & Takahashi, 1990) but it was never documented at later stages. It appears that its decline in spinal motoneurons matches the time of motoneuronal developmental death (McCobb *et al.*, 1989; Mynlieff & Beam, 1992a, b). However its expression persisted in the rat hypoglossal motoneurons (Berger *et al.*, 1995) and abducens (Russier *et al.*, 2003) much later after birth, suggesting a different role for this current in these motoneurons. Berger and Takahashi (Berger & Takahashi, 1990) proposed that the

early expression of T-channels in motoneurons could be responsible for the burst discharge pattern that characterizes intra-uterine motor activity. So far, this burst mechanism has only been confirmed for neonatal hypoglossal motoneurons (Berger *et al.*, 1995).

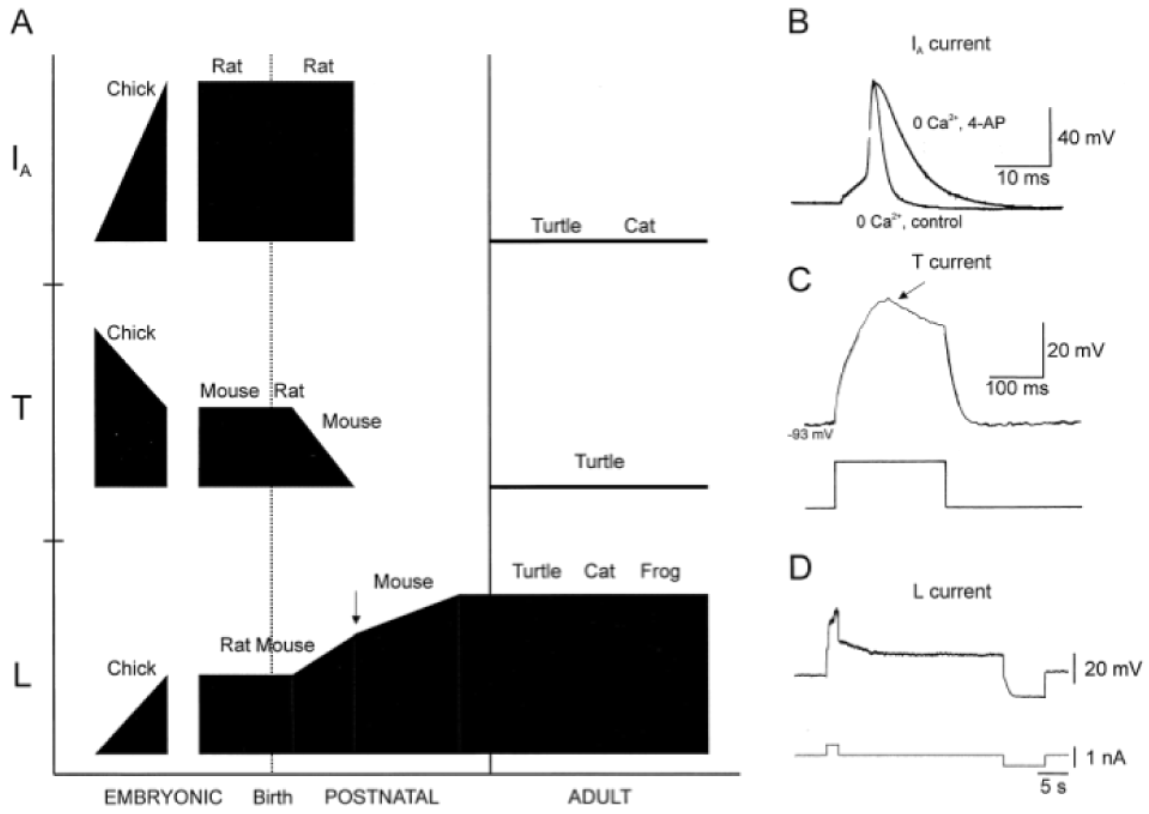

Figure 6: Ontogeny of I_A, T and L currents in motoneurons. (A) Summary of the time course of development of the three ionic currents during embryonic, postnatal and adult periods. **(B)** Effect of I_A antagonist 4-amino pyridine (4-AP) on action potential in rat spinal motoneuron at P2–P3 (Takahashi 1990). **(C)** T spike facilitation by 5-HT (10 µM) in rat spinal motoneuron at P3–P4 (Berger 1990). **(D)** Bistability mediated by L-type Ca^{2+} channel in motoneuron from adult turtle. Plateau potential facilitated by ACPD (40 µM). Contribution of I_{can} current excluded by replacing Na^+ with or N-methyl-D-glucamine chloride. Adapted from (Perrier 2000).

ii/ Potassium A-current

The fast transient outward A-current was originally described in the mollusc *Doridiae Anisodoris* by Connor and Stevens (1971). In vertebrates, it is mediated by numerous Kv isoforms including the Shaker-related Kv 1.4, the Shaw-related Kv 3.3 and Kv 3.4 as well as the Shal-related Kv 4.1, Kv 4.2 and Kv 4.3 (Pongs *et al.*, 1999). The addition of a β subunit to the α pore-forming subunits might also confers A-like properties to any α pore-forming subunit (Yao & Wu, 1999). Its activation requires a

period of hyperpolarization followed by a depolarization. Both the activation and the inactivation occur relatively quickly: a few milliseconds for the activation and a few tens of milliseconds for the inactivation. The A-current is suppressed by millimolar concentrations of 4-aminopyridine (4-AP, Figure 6B). The A-current is expressed in spinal motoneurons in the chick embryo as early as embryonic day 4 (E4) and the current density strongly increases at least until E11 (McCobb *et al.*, 1990). The A-current is also transiently expressed in motoneurons in the rat spinal cord from E14 until postnatal period P2–P8 (Safronov & Vogel, 1995; Gao & Ziskind-Conhaim, 1998; Svirskis & Hounsgaard, 1998; Alessandri-Haber *et al.*, 1999). No expression of the A-current was ever observed in adult spinal motoneurons of mouse, chick, rat, cat, frogs or turtle (Figure 6A). On the contrary, trigeminal motoneurons of adult guinea-pig also express the A-current (Conway *et al.*, 1988). Lappe and Nistri (1999) identified the A-current in hypoglossal motoneurons until P9. Russier *et al.* (2003) found the A-currrent to be expressed in a subset of the neonatal abducens motoneurons from P2 to P9. The rapid hyperpolarizing effect of the A-current makes it fit to shorten the spike duration (McCobb *et al.*, 1990; Svirskis & Hounsgaard, 1998), reduce the amount of calcium entering the neurons and perhaps spare them from apoptosis. In this view the A-current transient expression before birth would counterbalance the apoptotic effect of the T-type current. If a significant amount of A-current is de-inactivated prior to a pulse, the A-current may delay the discharge over a relatively short time (order of magnitude 30 ms). In neonatals, such an effect has been observed in spinal motoneurons (Gao & Ziskind-Conhaim, 1998; Perrier & Hounsgaard, 2000), as well as in brainstem motoneurons (Lape & Nistri, 1999; Russier *et al.*, 2003).

iii/ L-type Ca^{2+} persistent inward current

The Ca^{2+} persistent inward current carried by the L-type channels does not have a transient expression around birth but gradually appears after birth (Figure 6A). The L-type channels open during depolarizations and inactivate very little. They may therefore induce plateau potentials and bistability in the motoneurons, requiring a hyperpolarizing event to end the plateau (Figure 6D). In mouse and rat motoneurons L-type Ca^{2+} current is present at E14–15 (Mynlieff & Beam, 1992a; Hivert *et al.*, 1995)). In the mouse, the expression of L-type Ca^{2+} channels as measured by membrane current density continues to increase after birth (Mynlieff & Beam, 1992b)

and L-type channels contribute detectably to motor behavior after P7 (Jiang *et al.*, 1999). Indeed, plateau potentials resulting from the current activation have been found in adult cat and mouse spinal motoneurons (Schwindt & Crill, 1980; Bennett *et al.*, 1998; Kiehn & Eken, 1998; Lee & Heckman, 1998b; Jiang *et al.*, 1999). Similarly, the adult rats and humans motoneurons exhibit correlates of plateau potentials (Eken & Kiehn, 1989; Gorassini *et al.*, 1998; Kiehn & Eken, 1998). Indirect evidence suggests that plateau potentials contribute to motor behaviour by shaping motor output patterns and provide mechanisms for self-sustained activation of motor units (Kiehn & Eken, 1997, 1998; Delgado-Lezama *et al.*, 1999; Russo & Hounsgaard, 1999).

To conclude, in spinal motoneurons, the expression of the A-current and the T-type current starts during the early embryonic development and peaks during the motoneuronal death suggesting a regulatory role. Its role at later stages in trigeminal, hypoglossal or abducens motoneurons remains however elusive. In parallel the L-type channels expression increases slowly after birth and becomes stable around the time the animal engages in locomotor postural activity. The distinct set of conductances expressed at embryonic or adult stage may reflect distinct role for the motoneurons intrinsic properties. At a young age, these properties may be part of the signaling system that regulates growth, pathfinding, cell death, and formation of pre- and post-synaptic contacts (Perrier & Hounsgaard, 2000). In the adult, motor system is mature and the intrinsic properties need to be tuned to support the motoneurons functions. This led us to question whether all types of motoneurons belonging to a same pool express the same conductances in similar densities. Since they have to perform various functions it seems crucial their currents match their needs.

c/ Delayed firing in a subpopulation of neonatal motoneurons

So far, we do not know whether and how the functional properties of spinal motoneurons maturate at the same time as those of their muscle fibers. It is well known that, in adult animals, spinal motoneurons start to fire almost without any delay at the onset of a liminal current pulse (Kernell, 2006; Manuel *et al.*, 2009) for mice motoneurons). In sharp contrast, the firing behavior is heterogeneous during the second postnatal week (Russier *et al.*, 2003; Pambo-Pambo *et al.*, 2009; Zhu *et al.*, 2012). For liminal current pulses, the discharge starts at the current onset in some

motoneurons but it is delayed in others. Pambo-Pambo *et al.* (2009) worked on the mouse spinal cord slice preparation between p6 and p10. They reported that some neonatal spinal motoneurons fired at threshold with around 100 ms of delay and that this delay disappeared when 10 mM TEA and 4 mM 4-AP were applied. Zhu *et al.* (2012) reported that two weeks following birth, the spinal rat motoneurons exhibited several firing patterns. While 42% discharged at pulse onset, 30% presented delayed onset discharge. The remaining motoneurons displayed irregular firing patterns. Russier *et al.* (2003) analyzed the two populations of rat abducens neonatal motoneurons in a preparation of brainstem slices from P1 to P13. They observed two types of motoneurons according to their firing profile during prolonged depolarizations. The first type, accounting for 70% of the total, exhibited a burst of action potentials followed by an adaptation of the discharge (bursting discharge). Their firing pattern was similar to that of adult abducens motoneurons. They exhibited T-type as well as H-currents. The second population of abducens motoneurons displayed a delayed discharge, the was due to the potassium A-current and was observed only between P4 and P9. According to the authors, these motoneurons exhibited immature characteristics: simple AHP and no separated fast and medium AHPs, as well as a linear current–voltage relationship and a small input conductance. Given that the total number of abducens motoneurons remained unmodified and that only motoneurons presenting a bursting discharge were encountered after P9 the authors concluded that the expression of the A-current was transient and that motoneurons of the second type (delayed discharge) turn into the other type (bursting discharge) right before the rat begin using the muscles controlling the eye (P11-P12). Thus, the transient delayed firing pattern due to the A-current observed in a sub-set of neonatal motoneurons appears to be a common property of motoneurons. Noteworthy Lape and Nistri (1999) also identified a second slow inactivating potassium current that may also delay the discharge on a longer time-scale. During the second postnatal week, rat hypoglossal motoneurons exhibit either a decrementing or an incrementing firing pattern in response to square pulses (Viana *et al.*, 1995), while in adult spinal motoneurons, the firing frequency is always decreasing during a pulse (Brownstone, 2006). Similarly, facial motoneurons (Magarinos-Ascone *et al.*, 1999) of neonates also presented heterogenous firing behaviors and frequency adaptations. In general it seems that a sub-population of developing motoneurons express additional potassium currents modulating the

discharge onset and its adaptation. Since we know that muscle fibers are already differentiated and that the sub-types are grouped in homogeneous motor units during the second post-natal week we may wonder whether motoneurons from different types have different discharges and if this difference is required for the proper maturation of the system.

Besides these two patterns of discharge very little is known about the maturation of conductances within the same motor pool. Ramp-response analysis suggests that in the adult S-type motoneurons have more Ca^{2+} persistent inward currents than the F-type ones (Lee & Heckman, 1998a, b). This fits with the idea that slow motoneurons are engaged more often in postural activity (Burke, 1981) and need to sustain prolonged activation of their muscle fibers.

d/ Labelling of motoneuron molecular markers: dissecting the sub-populations

Research for molecular markers of different motoneuron types is of the utmost importance. Indeed when working on a slice preparation, the efferent muscle fibers are missing and an easy molecular tool would allow to establish a correlation between recorded cell and motor unit type. However, the detection of markers requires comprehensive analysis of the genes expressed by distinct cell populations and the difficulty to harvest sufficient amounts of mRNA from identified motoneurons have hindered this analysis for a long time.

Specific markers of γ- and α-motoneurons were recently discovered recently. The transcription factor Estrogen-related receptor 3 (Err3), an orphan receptor of the nuclear hormone, can separate γ- from α-motoneurons in the spinal cord. Its expression first localizes to the cell bodies and becomes restricted to γ-motoneurons during the first two postnatal weeks (Friese *et al.*, 2009). Adult γ-motoneurons also express higher levels than α-motoneurons of the glial cell line–derived neurotrophic factor receptor subunit GFRα1 as detected using reporter mice (Shneider *et al.*, 2009). Conversely, the neuron-specific nuclear protein named nuclear nuclei (NeuN, Mullen *et al.*, 1992) antigen is strongly expressed by α-motoneurons but not by γ-motoneurons (Friese *et al.*, 2009; Shneider *et al.*, 2009). More recently, the serotonin receptor 1d (5HT1d) was found to be expressed specifically by γ-motoneurons after P11 (Enjin *et al.*, 2012).

Concerning the fast and slow motoneurons, the first identified marker was the calcitonin gene (Calca) and its gene product calcitonin gene-related peptide (CGRP). Several studies showed a correlation between its expression and the amount of fast motoneurons within a motor pool (Forsgren *et al.*, 1993; Piehl *et al.*, 1993). γ -motoneurons appear to lack Calca expression as well. Building on this results Enjin *et al.* (2010) proved that the expression of another protein, the chondrolectin, colocalized with Calca (Figure 7A). Then Enjin *et al.* (2010) correlated Chodl expression with one of two distinct motoneurons populations recorded at the second post-natal week. Motoneurons from the two populations exhibited different half-AHP durations (Figure 7B and D), different rheobases (Figure 6E) and different input resistances (Figure 7F). As a result the two populations segregated along the AHP duration and rheobase axis (figure 7G) similarly to what has been demonstrated in the adult cat fast and slow motoneurons (Zengel *et al.*, 1985) and probably in the adult mouse motoneurons as well (figure 2). Finally Enjin *et al.* (2010) showed that motoneurons non-expressing Chodl expressed the estrogen-related receptor β (ERRβ) making it a putative slow motoneurons marker. In parallel in situ hybridization also showed that synaptic vesicle protein 2A (SV2A) was selectively localized in motor nerve terminals on slow (type I and small type IIA) muscle fibers. SV2A is broadly expressed at birth, then fast motoneurons downregulate its expression during the first postnatal week (Chakkalakal *et al.*, 2010). Lately the expression of the Ca^{2+}-activated K^+ channels 3 (SK3) was found to be restricted to putative slow motoneurons in the rat motoneurons (Deardorff *et al.*, 2013). However SK3 expression was weak during the first two weeks following birth. This new marker is particularly promising since SK channels carry the mAHP current and the slow motoneurons AHP is significantly longer than the fast motoneurons AHP in the adult cat, rat and mouse (Kernell, 2006; Manuel *et al.*, 2009). This new marker may therefore be the first to bear a causal relationship with a major electrophysiological property used as a discriminative criterion between populations.

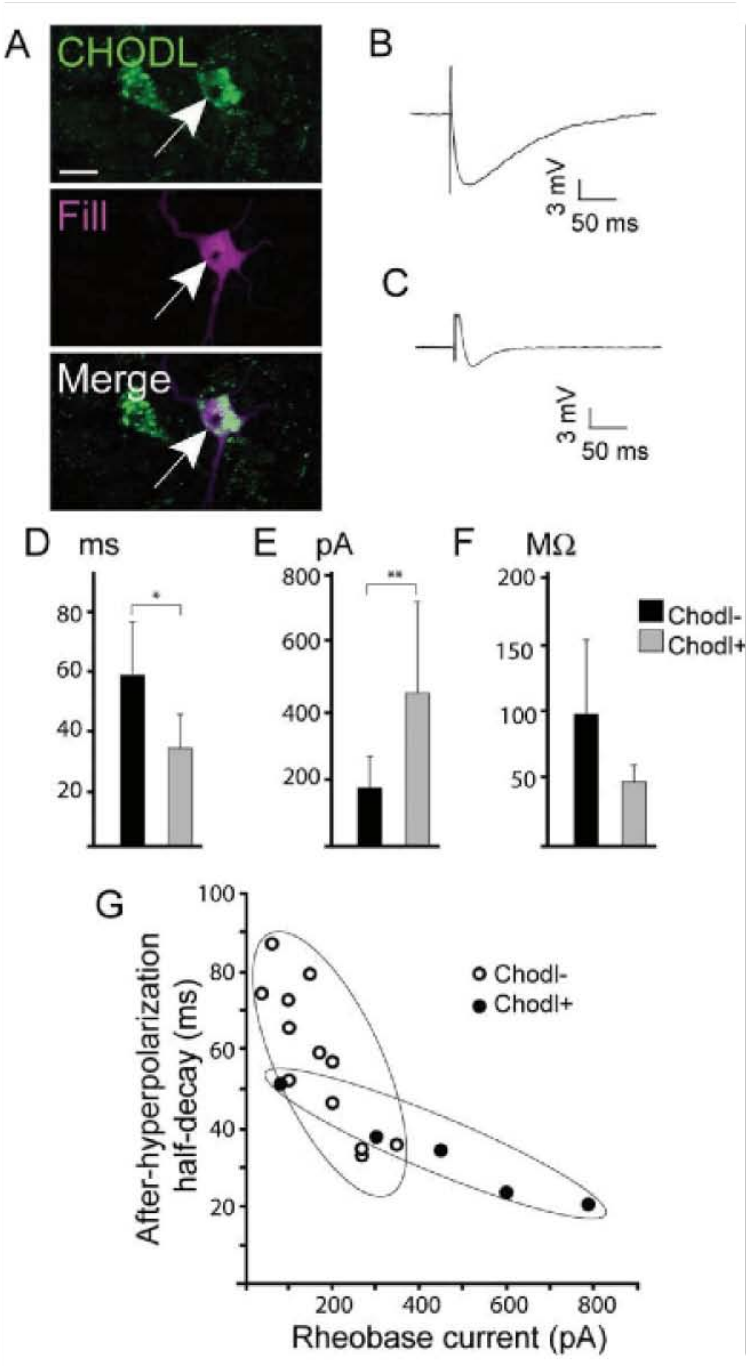

Figure 7: Chodl$^+$ cells have electrophysiological properties of fast motor neurons. (A) Chodl antibody staining of a motor neuron recorded and filled with biocytin. **(B,C)** Example traces of afterhyperpolarization of slow (**B**) and fast (**C**) motoneurons. **(D)** Mean after-hyperpolarization half-decay time for Chodl$^+$ and Chodl$^-$ motor neurons (Chodl+: 33 ± 12 ms; Chodl$^-$: 58 ± 18 ms; p = 0.02, n = 17 cells). **(E)** Mean rheobase current for Chodl$^+$and Chodl$^-$ motoneurons (Chodl$^+$: 444 ± 272 pA; Chodl$^-$: 168 ± 94 pA; p = 0.006, n = 17 cells). **(F)** Mean input resistance for Chodl$^+$ and Chodl$^-$ motoneurons (Chodl$^+$: 49 ± 12 MΩ Chodl-: 98 ± 55 MΩ; p = 0.07, n = 16 cells). **(G)** Scatterplot of motor neuron rheobase current versus after-hyperpolarization half-decay time. Chodl immunoreactivity indicated as Chodl$^+$ (filled circles) and Chodl$^-$ (open circles). Ovals enclose Chodl$^+$ and Chodl$^-$ groups. Values represent means ± SD. Scale bar = 20 µm in **A**. Adapted from Enjin et al 2009.

Conclusion

Motoneurons are subject to a profound reorganization of their intrinsic excitability during postnatal development. Evidence points out that the motoneuron sub-type is determined early on, probably before birth. The motoneurons grow in size during the entire animal life but in a hierarchical fashion. Size differences are noticeable in the weeks following birth.

The time window (P6-P10) that I have investigated during my thesis work is a period of intense shaping of the connectivity pattern within the muscle (reduction of poly-innervation and refinement of the motor unit homogeneity). During the second post-natal week the spinal cord is still immature (descending tracts are not functional) and the mouse cannot walk before P10. It is likely that the properties of the different motoneuron populations are still maturing leading to further differentiation between sub-types. Similarly to what had been done for the muscle fibers, I investigated how and when the differentiation between motoneuron electrophysiological properties arises. Heterogeneous firing is a common feature of neonatal motoneurons. Can we correlate the firing patterns with a subtype? What are the effects of the different activities on the respective maturation?

Chapter II: Two subpopulations of spinal motoneurons displaying different discharge profiles

1/ Introduction

The second postnatal week is crucial in the development of the mouse neuromuscular system. During this week, postural activity is acquired, allowing the locomotor behavior to switch from crawling to walking (Jiang *et al.*, 1999). This transformation calls for a remodeling of the sensory and the descending neural controls (Clarac *et al.*, 2004).The motor units also undergo extensive maturational processes in order to ultimately differentiate into three mature subtypes: the slow contracting motor units (S type), the fast contracting but fatigue resistant motor units (FR type) and the fast contracting and fatigable motor units (FF type; Burke, 1981).

During the second post-natal week the distal part of motor unit (the muscle unit composed of all muscle fibers innervated by a single motoneuron) is already differentiated. However, so far we do not know when and how the functional properties of spinal motoneurons maturate, particularly when and how the properties of slow motoneurons differentiate from those of fast motoneurons. It is well known that, in adults, spinal motoneurons start to fire without any delay at the onset of a liminal current pulse (Kernell, 2006; Manuel *et al.*, 2009), 2009 for mice motoneurons). In sharp contrast, the firing behavior is heterogeneous during the second postnatal week (Russier *et al.*, 2003; Pambo-Pambo *et al.*, 2009). For liminal current pulses, the discharge starts at the current onset in some motoneurons but it is delayed in others.

In a first time I characterized the currents underlying the delayed discharge exhibited by some of the spinal motoneurons and, I characterized their impact on the recruitment threshold and on the F-I relationship (article 1). The second part of this chapter presents arguments of electrophysiological, morphological and molecular nature to support the view that motoneurons with delayed firing might be fast motoneurons and motoneurons with immediate firing might be slow motoneurons.

2/ A-like and slow-inactivating potassium currents determine recruitment and firing properties in a subpopulation of spinal motoneurons in neonatal mice

Neonatal spinal motoneurons exhibit two discharge patterns upon injection of 5s-pulses at liminal intensities. For 34% of the motoneurons the discharge begins at pulse onset and is maintained until the end of the pulse (Article 1, Figure 1B2). For liminal intensities, the discharge continues irregularly. This is due to membrane oscillations (insert in Article 1 Figure 1B and Iglesias *et al.*, 2011) that occur in mouse motoneurons around spiking threshold (Article 1, Figure 1B2). For stronger stimulation the discharge becomes more regular (Article 1, Figure 1B3). The spiking frequency adaptation is decremental. The other 66% of the motoneurons exhibit a delay in the discharge for liminal pulse intensities (Article 1, Figure 1A2). Once started the discharge continues until the pulse end. The spiking frequency is incremental for liminal intensities. A curious slow membrane depolarization can be observed for subthreshold intensities of stimulation (Article 1, Figure 1A1). At suprathreshold intensities the discharge starts at pulse onset and the frequency adaption is decremental (Article 1, Figure 1A3). Discrimination between the two populations therefore requires careful assessment of the response for liminal intensities of stimulation upon injection of prolonged pulses.

In order to elucidate the currents behind these two discharge patterns, I switched to voltage-clamp mode. After identification of the motoneuron discharge pattern in current-clamp mode (Article 1, Figures 2A1 and B1), I applied voltage-pulses rising from holding voltage to the voltage previously reached at the pulse onset in current-clamp mode. Leak-subtracted current response yielded no voltage-dependent current for the immediate firing motoneurons (Figure 2B2). However the delayed firing motoneurons presented two outward currents of different kinetics (Article 1, Figure 2A2 white and black arrowheads). The fast one is likely the potassium A-current and acts to impede the cell from firing at pulse onset (Article 1, Figure 3). The slow current is also a potassium current blocked for high TEA concentrations (20 mM, Article 1, Figure 4) and the slow depolarization observed for sub-threshold stimulations is due to the inactivation of the slow outward current. Both potassium

currents counteract the membrane depolarization and prevent the cell from firing until they inactivate enough for the membrane potential to reach the cell voltage-spiking threshold. Subsequent acceleration of the discharge is due to the underlying membrane depolarization that continues until all slow current is inactivated.

Next, I characterized the F-I curves of the two motoneuron populations. Due to the slow time course of the second potassium current we injected current at the slow velocity of 0.1 nA/s (Article 1, Figure 5A1 and B1). Only at such low velocity would the F-I curve from stationary pulse match the one obtained from the ramp of current (Article 1, Figure 5 black triangles). The two populations display extensive differences in the F-I curves derived from slow current-ramp injection. Half of the immediate firing motoneurons exhibits a clockwise hysteresis (Article 1, Figure 5B2) similarly to what had been observed in some adult motoneurons (Manuel *et al.*, 2009) while the other half shows no hysteresis. Regarding the delayed firing motoneurons, two thirds present a F-I curve of a curious shape with the recruitment current higher than derecruitment current and ascending ramp firing at higher frequencies than the descending curve (Article 1, Figure 5A2). Inactivation of the slow potassium current is mostly responsible for this new behavior pushing back the onset of firing and then increasing the gain of the ramp until it completely inactivates (inflexion point, white arrow head). The last third display either clockwise hysteresis or none. We assumed that in these motoneurons the slow potassium current was not strong enough to dictate the F-I curve shape although the delayed firing pattern was clearly visible during 5 s pulses injections.

Finally I investigated the response in the delayed firing motoneurons to two consecutive slow ramps (Figure 6). In sharp contrast to the control F-I curve (Article 1, Figure 6A2) the second F-I curve displayed a counter-clockwise hysteresis with the onset and the end of discharge now occurring for the same current intensities and no inflexion point (Article 1, Figure 6B2). We concluded that the recruitment current now matched the de-recruitment as most of the slow potassium current was still inactivated at the ramp beginning. Repetitive stimulations may therefore facilitate the recruitment threshold of delayed firing motoneurons.

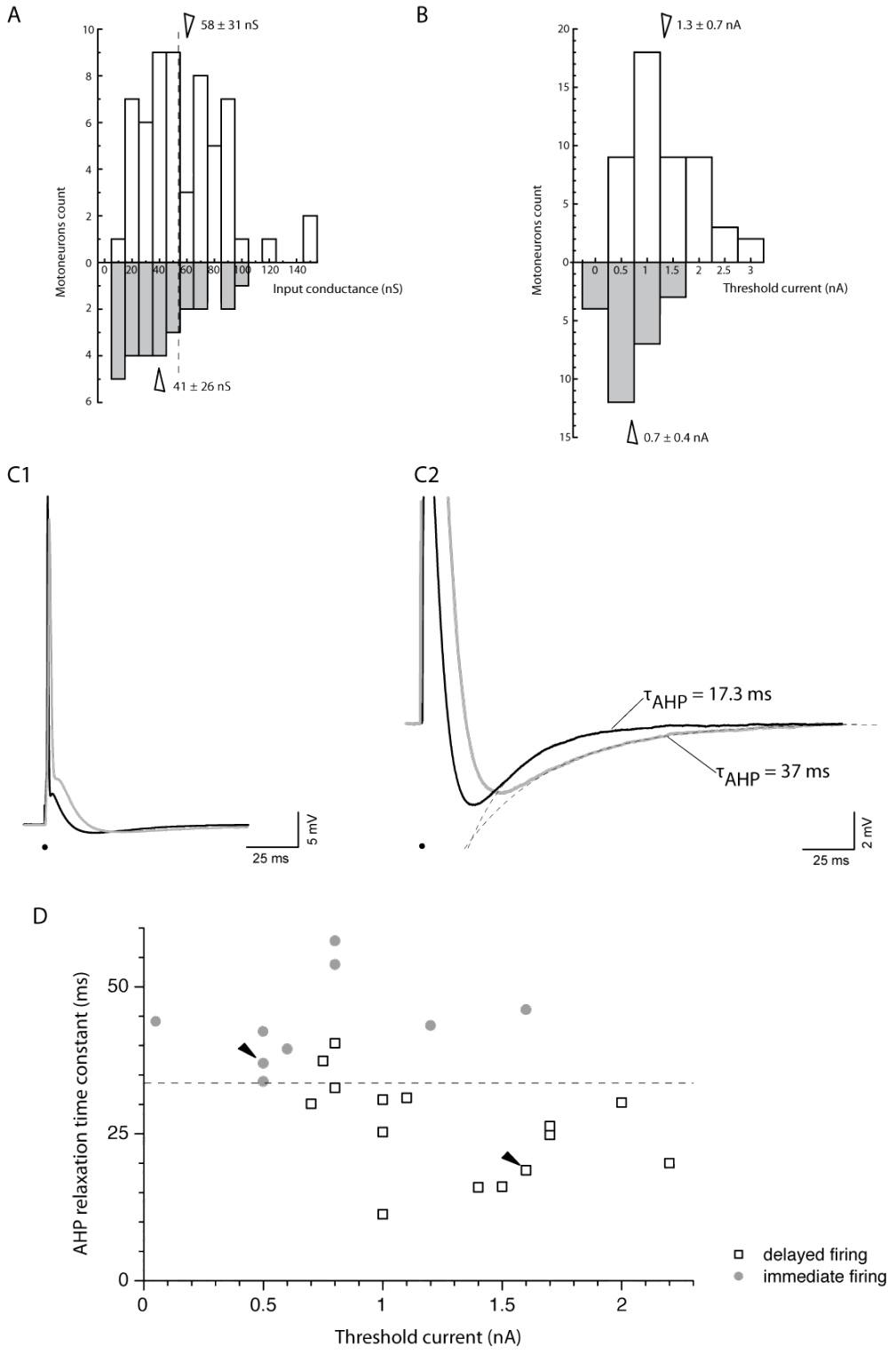

Figure 8: Electrical properties of delayed firing and immediate firing motoneurons strongly suggest that they are fast and slow type motoneurons. A: Distribution of the input conductances for the delayed firing (white) and the immediate firing (grey) motoneurons. The open arrows points to the average values of the input conductance of each group. **B**: Distribution of the threshold currents (5 s depolarizing pulses) for the delayed firing (white) and the immediate firing (grey) motoneurons. **C1-2**: Action potentials of a delayed firing (black) and an immediate firing (grey) motoneuron elicited by a 1 ms square pulse of current (black dot) (5 nA injected for the delayed firing motoneuron and 2.1 nA for the immediate firing motoneuron). Arrow in **C1** point at the peak of the grey trace.The mono-exponential fits (dotted line in **C2**) are the best estimate of the AHP relaxation. τAHP is the time constant of this fit. D: Clustering of delayed firing and immediate firing motoneurons when plotting τAHP against threshold current. Grey circles indicate immediate firing motoneurons and open squares delayed firing motoneurons. Arrowheads point at the motoneurons illustrated in **C2**.

3/ Correlation of the discharge patterns with fast and slow types

Can we ascribe known functional subtypes to the two discharge pattern populations? It is unlikely that they come from two different motor pools. This seem little possible given that somas of both types were consistently found intermingled along different segments all over the ventral cord . A second hypothesis could be to ascribe the γ-motoneuron subtypes to the immediate firing motoneurons exhibiting smaller somas. This hypothesis does not hold when comparing the average size of the immediate firing motoneuron somas with the average size of the γ-motoneuron somas at the same age (Friese *et al.*, 2009). Consequently we assumed that delayed and immediate firing motoneurons most likely correspond to F- and S-type motoneurons, respectively. Although the lack of muscle fibers connected to our recorded motoneurons prevented us from formal identification we based our assertion on several electrical, morphological and molecular arguments, all based on previous works linking motoneurons features with their functional subtypes as reviewed in the first chapter.

a/ Electrical and morphological evidence

Motoneurons were recorded in an *in vitro* slice preparation. Such preparation precludes to correlate the motoneurons properties with those of the motor units they innervate. Therefore in order to distinguish the sub-types of neonatal motoneurons I did a clustering analysis of the whole population and tried to see whether some clusters would show up along the parameters that were most relevant to discriminate between sub-types for adults motoneurons. Motoneurons exhibiting the delayed firing pattern of discharge and those exhibiting the immediate firing pattern display major differences in their electrical properties. These differences strongly suggest that they are indeed two different sub-populations. First, the distribution of their input conductances is not the same (Figure 8A). The mean input conductance is larger in the delayed firing motoneurons (58 ± 31 nS, N=59) than in the immediate firing motoneurons (41 ± 26 nS, N=27, p=0.01). Figure 8A shows that input conductances exceeding 55 nS (dashed vertical line) were much more frequently observed in the delayed firing motoneurons (46%) than in the immediate firing ones (26%). Second the immediate and the delayed firing motoneurons display differences in the distributions of their threshold currents (Figure 8B). The threshold currents ranged

from 0.4 nA to 3 nA (N=50) for the delayed firing motoneurons but they are shifted toward smaller values (0.05 nA to 1.7 nA, N=26) for the immediate firing motoneurons. The mean threshold current is then significantly different in the two sub-populations (1.3 ± 0.7 nA for the delayed firing motoneurons vs. 0.7 ± 0.4 nA for the immediate firing motoneurons; p=0.0001).Third, the AHP relaxation time is significantly shorter in the delayed firing motoneurons (26 ± 8 ms, N=18) than in the immediate firing ones (42 ± 27 ms, N=11, p=0.04, Figure 8C2). Indeed, similarly to the adult motoneurons, the AHP relaxation time allows discriminating quite well the delayed firing motoneurons (below 34 ms for most of them) from the immediate firing motoneurons (above 34 ms for most of them, Figure 8D).

Altogether, our electrophysiological data strongly suggest that delayed and immediate firing motoneurons are indeed two different sub-populations. They might very well be ascribed to F- and S-type motoneurons, respectively. This assumption is based on the fact that F type motoneurons display higher input conductance, higher threshold current and shorter AHP duration than S type motoneurons in adult cats (Zengel *et al.*, 1985), rats (Beaumont & Gardiner, 2002; Button *et al.*, 2006) and mice (Manuel and Heckman, SfN 2012).

The hypothesis that delayed firing and immediate firing motoneurons might be ascribed to F and S motoneurons is further supported by their morphological differences. We filled motoneurons of both types with neurobiotin (Figure 9A1 and B1) to reconstruct their dendritic tree (Figure 9A2 and B2). The delayed firing motoneurons (Figure 1B) had more branching points (40 ± 11, N=13 vs. 26 ± 11, N=9, p=0.02) and a longer total branch length (7480 ± 2750 µm, N=13 vs. 5360 ± 1200 µm, N=9, p=0.02) than the immediate firing neurons (Figure 9A). Figure 9C shows that the two populations tend to cluster when plotting the total dendritic tree against the number of branching points indicating that the dendritic tree of delayed firing motoneurons is generally larger and more complex than the dendritic tree of immediate firing motoneurons. Again, this is in keeping with the well-known morphological differences between F and S motoneurons in adults (Burke, 1982; Cullheim *et al.*, 1987a).

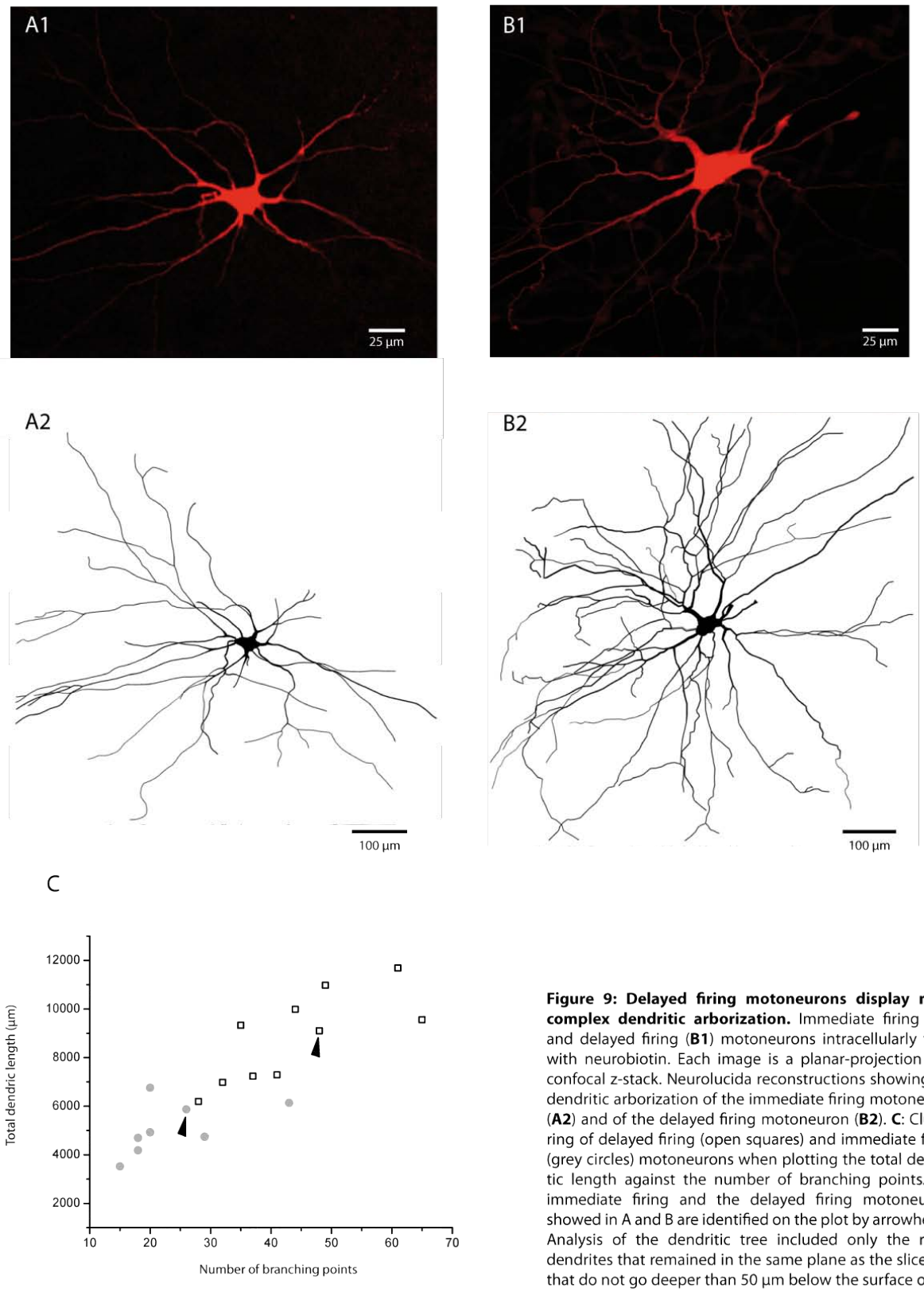

Figure 9: Delayed firing motoneurons display more complex dendritic arborization. Immediate firing (**A1**) and delayed firing (**B1**) motoneurons intracellularly filled with neurobiotin. Each image is a planar-projection of a confocal z-stack. Neurolucida reconstructions showing the dendritic arborization of the immediate firing motoneuron (**A2**) and of the delayed firing motoneuron (**B2**). **C**: Clustering of delayed firing (open squares) and immediate firing (grey circles) motoneurons when plotting the total dendritic length against the number of branching points. The immediate firing and the delayed firing motoneurons showed in A and B are identified on the plot by arrowheads. Analysis of the dendritic tree included only the radial dendrites that remained in the same plane as the slice and that do not go deeper than 50 µm below the surface of the slice.

b/ Molecular evidence

i/ RT-PCR on total spinal cord RNA

In order to ascertain the expression of multiple molecular markers (Chodl, Err-β, Err-γ and Calca) within a single motoneuron I tried setting up a multiple single-cell RT-PCR

analysis. The first step was designing the primers and testing their efficiency on a 1 ng sample of the whole spinal cord mRNA (Figure 10). The Northern-blot presented show selective amplification of the four genes in simplex or multiplex. However I failed to reliably amplify the mRNA harvested following motoneuron recordings, probably due to the lack of sensitivity of the multiplex RT-PCR given the small amount of mRNA harvested.

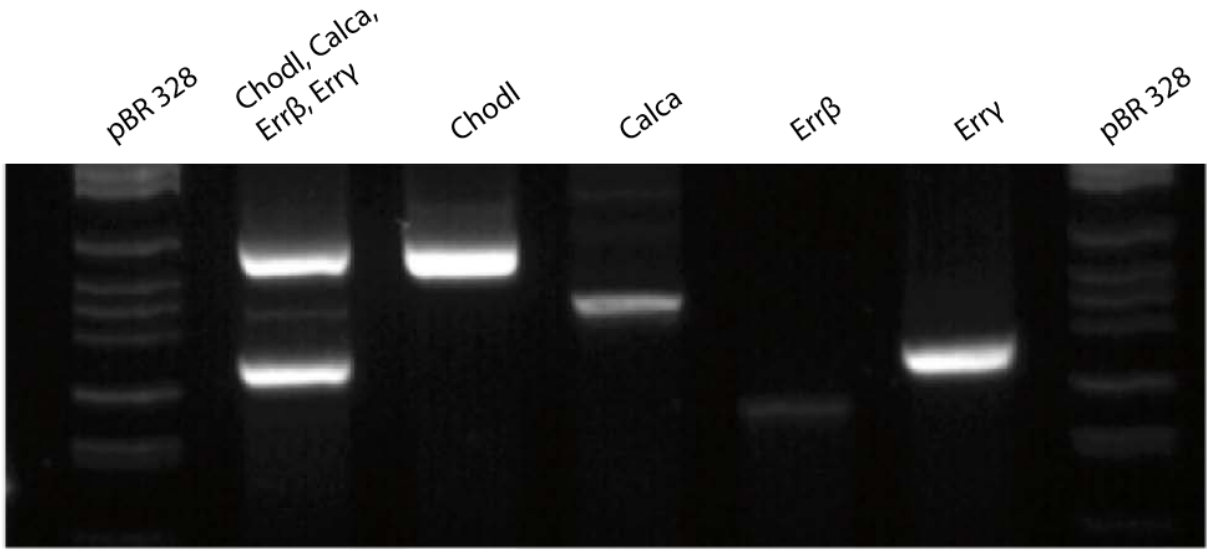

Figure 10: Setting of the single cell RT-PCR. Whole spinal cord RNA extract (1µg) was loaded with different primers either in simplex or in multiplex (Chodl, Calca, Errβ, Errγ)

ii/ NeuN and Err3 cannot discriminate α- from γ-motoneurons before P14

Friese *et al.* (2009) proved that after P14, NeuN expression restricted to α -motoneurons while Err-γ restricted to γ-motoneurons. To test whether this dichotomy occurred as well between immediate and delayed firing motoneurons we injected neurobiotin in type-identified cells and performed NeuN and Err-γ immunohistochemistry (see protocol section). Both type of motoneurons expressed NeuN jointly with a faint Err-γ (Figure 11 white arrowhead). Other nearby smaller nuclei expressed strongly Err-γ while presenting no expression of NeuN (Figure 11 asterisks). These smaller neurons were likely to be γ-motoneurons. After discussion with Sylvia Arber (personal communication) I concluded that Err-γ expression was decreasing in the recorded cells while NeuN remained strongly expressed. Furthermore the soma size of the recorded motoneurons presents a distribution shifted toward values larger than the distribution of γ-motoneurons soma size (data

not shown). Therefore the vast majority of recorded motoneurons were α - motoneurons.

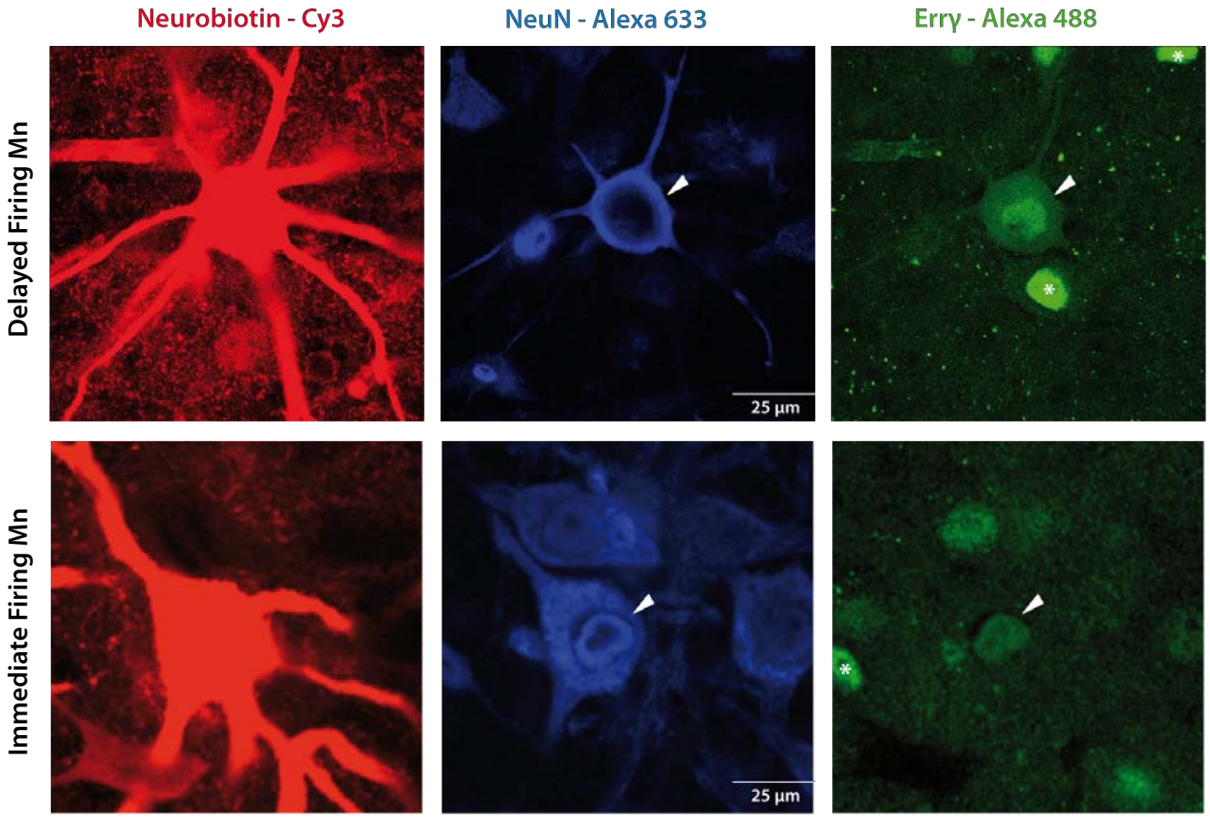

Figure 11: Immediate and delayed firing motoneneurons co-express NeuN and Erry. Following neurobiotin injection, NeuN and Erry immuno-histolabelling was performed. Neurobiotin was coupled to streptavidin conjugated Cy3, NeuN to alexa 633 and Erry to alexa 488. Recorded immediate (bottom) and delayed (top) firing motoneurons are indicated by white arrowheads. Note the strongly Erry labelled motoneuron (asterisk).

iii/ Chodl a putative marker of FF motoneurons

We recorded delayed and immediate firing motoneurons and injected them with 2% neurobiotin. After light PFA fixation, Rebecca Manuel performed the in situ hybridization of the Chodl protein (Figure 12 top). Neurobiotin was later coupled to Cy2-conjugated streptavidin (see protocol section). The analysis of the discharge pattern repartition showed that only a subpopulation of delayed motoneurons expressed Chodl (7/15, Figure 5 bottom). None of the recorded immediate firing motoneurons (n=9) expressed Chodl (Figure 12C bottom). Similarly to Enjin *et al.* (2010) we correlated Chodl expression with large threshold current and short half-AHP duration (Figure 7C). Only delayed firing motoneuron presenting the larger current thresholds current and the shorter AHP duration expressed Chodl. Experiments are currently underway in adult type-identified motoneurons to assert whether only FF but not FR or S motoneurons express Chodl. Should these

preliminary results be confirmed, we could assume that immediate firing motoneurons are slow-motoneurons while delayed are fast-motoneurons. The probe to test the restriction of Err-β expression to immediate firing motoneurons is currently under development as well as the the probe to test whether Calca expression is restricted to delayed motoneurons.

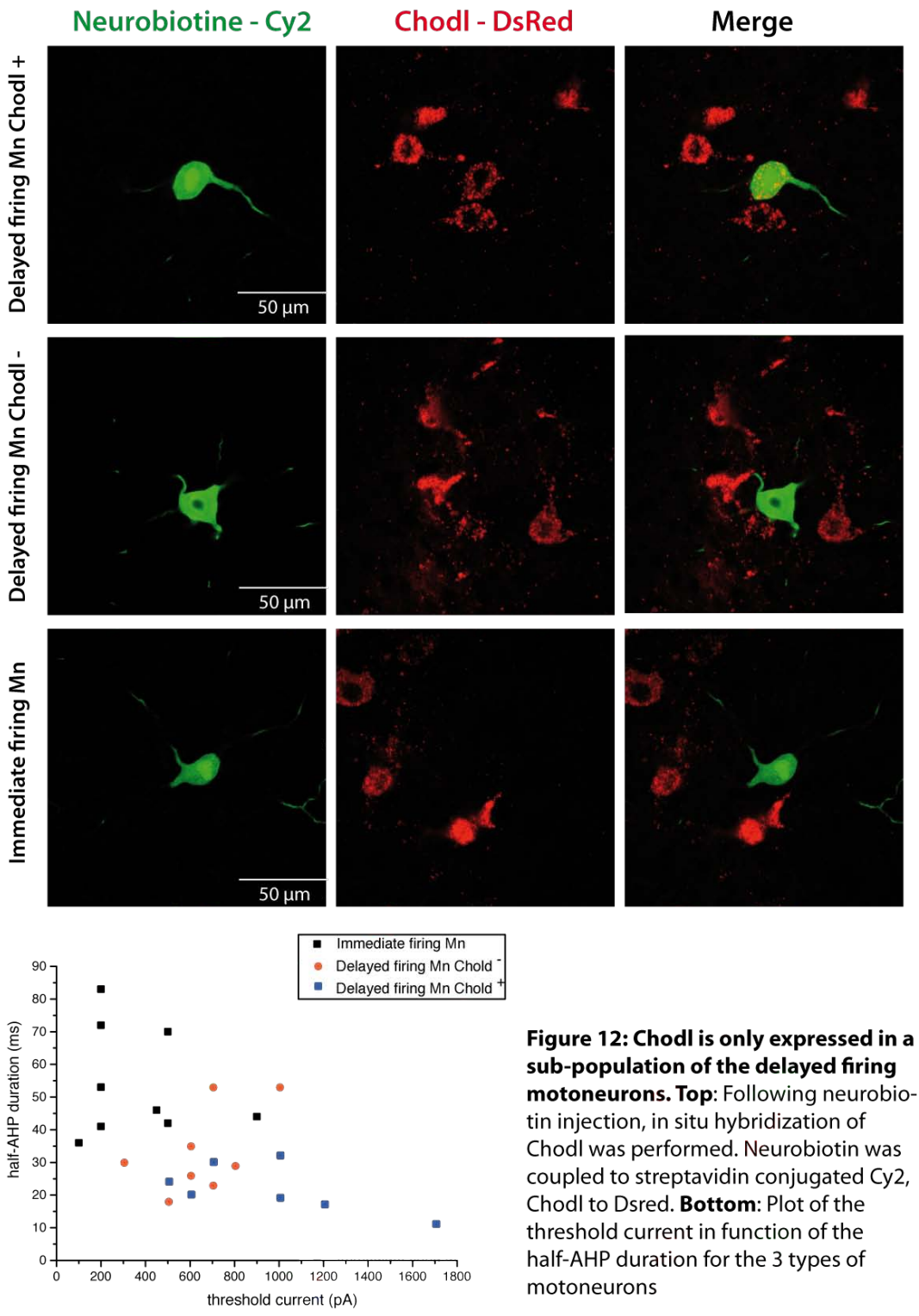

Figure 12: ChodI is only expressed in a sub-population of the delayed firing motoneurons. Top: Following neurobiotin injection, in situ hybridization of ChodI was performed. Neurobiotin was coupled to streptavidin conjugated Cy2, ChodI to Dsred. **Bottom**: Plot of the threshold current in function of the half-AHP duration for the 3 types of motoneurons

4/ Conclusion

Spinal motoneurons display two firing patterns due to the expression of the A-current and a slow potassium current in the delayed firing motoneurons only. This led to strong qualitative differences in the F-I curves of the two populations. The very slow kinetics of the slow potassium current led the delayed firing motoneurons to lower their recruitment current upon consecutive stimulations. We may infer that repetitive stimulation leaving little time for the slow current to de-inactivate will produce a lowering of the rheobase and facilitate spiking. The slow current would therefore act as an integrator of the past activity (last 30 s) and its progressive long-lasting inactivation would have a facilitating effect on the discharge. On the other end the immediate firing motoneurons do not exhibit the additional potassium currents and therefore fire at pulse onset and do not integrate inputs over long ranges.

The extensive body of evidence presented above suggest that delayed and immediate firing motoneurons are respectively fast and slow motoneurons. A formal proof is however lacking due to the lack of muscle fibers in our preparation. Furthermore although the use of putative type-specific molecular markers yields interesting results, they need to be complemented with recordings in the adult using the *in vivo* preparation that was developped in the lab (Manuel *et al.*, 2009).

Article 1

A subpopulation of neonatal mouse spinal motoneurones displays a delayed firing profile due to an A-like and a slow-inactivating potassium currents

Félix Leroy, Boris Lamotte d'Incamps and Daniel Zytnicki
Laboratoire de Neurophysique et Physiologie, Université Paris Descartes, Centre National de la Recherche Scientifique (UMR 8119), 45 rue des Saints-Pères, 75006 Paris, France

Running title: Currents underlying the delayed firing in spinal neonatal motoneurones

Key words: spinal motoneurones, electrical properties, whole-cell recording

Total number of words: 5170

Corresponding author: Daniel Zytnicki
Laboratoire de Neurophysique et Physiologie, UMR 8119
Université Paris Descartes, UMR 8119, 45 rue des Saints-Pères, 75006 Paris, France e-mail: Daniel.Zytnicki@parisdescartes.fr

Table of Contents category:
Neuroscience – cellular/molecular

Key points summary

- In neonatal mice, two populations of spinal motoneurones are observed: most motoneurones discharge with a delay in response to a threshold pulse of current (delayed firing pattern), whereas others discharge at the pulse onset (immediate firing pattern).
- We have investigated which currents are responsible for the delayed firing pattern.
- We demonstrated that an A-like potassium current, which acts on a short time scale, together with a slow-inactivating potassium current, which acts on a longer time scale, are responsible for the delay of the discharge.
- These currents decrease the motoneurone excitability and shape the F-I function (i.e., the relationship between discharge frequency and intensity of injected current in the cell).
- We discuss how these potassium currents might contribute to the maturation of motor units in neonates.

Word count: 125

Abstract

In the second postnatal week, the locomotor behaviour of mice transforms from crawling into walking. This is made possible by profound changes in motor units. Yet, how the discharge properties of spinal motoneurones evolve during the post-natal maturation and whether they have an effect on the motor unit maturation remains an open question. In neonates, the spinal motoneurones display two modes of discharge. For threshold pulses, 66% of the motoneurones have a discharge that start at the current onset and adapts during the pulse ("immediate firing motoneurones"), but in the 33% other motoneurones the firing is delayed and then accelerates throughout the pulse ("delayed firing motoneurones"). Though the delayed firing pattern is quite common in spinal motoneurones of neonates, the ionic mechanisms that elicit this mode of discharge have received little attention. In the present work, we deciphered the ionic currents that underlie the delayed firing pattern by combining whole cell patch clamp recordings in both current- and voltage-clamp modes. We showed that it is caused by a combination of an A-like potassium current that acts on a short time scale and a slow-inactivating potassium current that delays the discharge on a much longer

time scale. We then investigated how these two potassium currents contribute to the recruitment threshold and how they shape the F-I function of delayed motoneurones in neonatal mice. We revealed that the slow inactivating potassium current induces memory effects that have a strong impact on the motoneurone excitability and on its discharge.

Introduction

The second postnatal week is a milestone for the development of the mouse neuromuscular system. During this week, postural activity is acquired, allowing the locomotor behaviour to switch from crawling to walking (Jiang *et al.*, 1999). This transformation calls for a remodelling of the sensory and the descending neural controls (Clarac *et al.*, 2004). Motor units also undergo extensive maturation (Thompson *et al.*, 1984; Jansen & Flatby, 1990) in order to ultimately differentiate into three mature subtypes: slow-contracting , fast-contracting but fatigue-resistant and fast-contracting and fatigable motor units (Burke, 1981). The time course of motor unit maturation depends on their type: during the second post-natal week, the slow muscle fibres already express their mature myosin heavy chain isoform whereas the fast contracting fibres will express theirs later (Agbulut *et al.*, 2003; Schiaffino & Reggiani, 2011). At birth, muscle fibres are heavily poly-innervated (Brown *et al.*, 1976; Jansen & Flatby, 1990). Synapse elimination begins at the end of the first week and by the end of the second post-natal week each fibre is innervated by a single motoneurone (Brown *et al.*, 1976; Jansen & Flatby, 1990). How the discharge properties of spinal motoneurone evolve during the post-natal maturation and whether they have an effect on the motor unit maturation remains an open question.

The firing behaviour is heterogeneous during the second postnatal week as revealed by patch-clamp recordings in slices (Russier *et al.*, 2003; Pambo-Pambo *et al.*, 2009). In P1-13 rat, most abducens motoneurones responded to a current pulse with a bursting pattern with frequency adaptation, whereas the discharge of the other motoneurones was delayed and displayed a progressive acceleration of the frequency (Russier *et al.*, 2003). The delayed firing pattern was only transiently observed between P4 and P9 in rat abducens motoneurones (Russier *et al.*, 2003). Similarly, two modes of discharge initiation have also been observed in mouse spinal motoneurones at P6-P10 (Pambo-Pambo *et al.*, 2009). For liminal current pulses, the discharge starts at the current onset in some motoneurones (immediate firing pattern) but it is delayed in others (delayed firing pattern). We do not know how long the delayed firing pattern is expressed in spinal motoneurones since it is difficult to record them in vitro after P10. However, only the immediate firing pattern was observed in *adult* spinal motoneurones recorded in vivo at about P30 (Manuel *et al.*, 2009). This suggests a transient expression of the delayed firing pattern during the first post-natal month. It is then

likely that this pattern of motoneurone discharge plays some functional role in the post-natal development of motor units. Even though the delayed firing pattern seems to be a common feature of neonatal mouse motoneurones, the ionic mechanisms that elicit this mode of discharge in spinal motoneurones have received little attention.

In the present work we identified the ionic currents that underlie the delayed firing pattern by combining whole-cell patch-clamp recordings in both current- and voltage-clamp modes. We showed that this discharge pattern is caused by a combination of an A-like potassium current that acts on a short time scale and a slowly inactivating potassium current that delays the discharge on a much longer time scale. We then investigated how these two potassium currents contribute to the recruitment threshold and how they shape the F-I function of delayed motoneurones. We revealed that the slow inactivating potassium current induces memory effects that have a strong impact on motoneurone excitability and discharge.

Methods

Animals and slices preparation

The experiments were performed in accordance with European directives (86/609/CEE and 2010-63-UE) and the French legislation. They were approved by Paris Descartes University ethics committee. Slices were prepared as described by Lamotte d'Incamps *et al.* (2012). 6 to 10 day old C57BL/6J mice (Janvier) were anesthetized with an i.p. injection of 0.1 ml of pentobarbital sodium (25 mM). An intracardiac perfusion was performed using ice cold low Na solution (concentrations in mM: KCl 3, NaH_2PO_4 1, sucrose 230, $NaHCO_3$ 26, $CaCl_2$ 0.8, $MgCl_2$ 8, glucose 25, ascorbic acid 0.4, kynurenic acid 1, Na-pyruvate 2) bubbled with 95% O_2 and 5% CO_2 (pH 7.4). After decapitation, a laminectomy was performed at about 4°C in the same solution. After sectioning the roots, the spinal cord was transferred to a K-gluconate solution (K-gluconate 130, KCl 15, EGTA 0.05, HEPES 20, glucose 25, kynurenic acid 1, Na-pyruvate 2, adjusted to pH 7.4 with KOH), then embedded into a 2% agar solution at 38°C (prepared with K-gluconate solution), which was then cooled down as quickly as possible. After solidification, the agar block containing the spinal cord was glued in the chamber of the slicer and 400 µm thick slices of the lumbar spinal cord were cut in K-gluconate solution. The slices were cut obliquely (35°) relative to the axis of the spinal cord to conserve the integrity of the motoneurone axons and thus allow the antidromic identification of the motoneurones. The slices were transferred into artificial cerebrospinal fluid (ACSF) containing (in mM): NaCl 130, KCl 2.5, $CaCl_2$ 2, $MgCl_2$ 1, NaH_2PO_4 1, $NaHCO_3$ 26, glucose 25, ascorbic acid 0.4, Na-pyruvate 2, bubbled with 95% O2 and 5% CO2 (pH 7.4). The transfer was made in ACSF at 34°C. After 30 minutes the slices were brought to room temperature (18-24°C).

Electrophysiology

The recording chamber was continuously perfused with ACSF at a rate of 1 - 2 ml/min, at room temperature. The slices used were those containing a ventral rootlet of sufficient length to be mounted on a suction stimulation electrode, a glass pipette with a tip size adapted to the diameter of the rootlet (40 - 170 µm) and filled with ACSF. Single biphasic stimulation of the VR (1 - 50 V, 0.1 - 0.3 ms) was used to elicit antidromic action potential in the recorded cells of the ventral cord. The motoneurones were found in the ventral horn and patched in whole-cell configuration under visual control using a video-camera (Scientifica, Uckfield, UK). We targeted cells in the ventral horn with a soma area in the 550-1000 μm^2 range, i.e. larger than the soma area of gamma motoneurones at P14 {Friese*,* 2009}. Identification of the cell as motoneurone was based on the recording of an antidromic action potential following stimulation of the ventral root. We retained for analysis motoneurones exhibiting a resting potential equal or below -50 mV, and an overshooting action potential.

Patch pipettes had an initial open-tip resistance of 3 to 6 MΩ. The internal solution contained (in mM): K-gluconate 140, KCl 6, HEPES 10, EGTA 1, $CaCl_2$ 0.1, Mg-ATP 4, Na_2GTP 0.3. The pH was adjusted to 7.3 with KOH, and the osmolarity to 285 - 295 mOsm. Prior to any other drug, synaptic currents were suppressed by adding 2 µ M NBQX (2,3-dioxo-6-nitro-1,2,3,4-tetrahydrobenzo(f)quinoxaline -7-sulphonamide) to block the AMPA receptors, 50 µM D-APV (D(−)-2-Amino-5-phosphonopentanoic acid) to block NMDA receptors, 1 µ M strychnine to block glycinergic receptors and 3 µM gabazine to block GABAergic receptors. All synaptic blockers were purchased from Abcam (Cambridge) as well as TTX, Oxotremorine and XE991 dihydrochloride. TEA (Tetra-ethyl-amonium), 4-AP (4-Amino-Pyridine) and Cd^{2+} were acquired from Sigma (St Louis). An AxoClamp 700B (Molecular Devices) amplifier was used for data acquisition. Whole-cell recordings were filtered at 3 kHz, digitized at 10 kHz using a CED 1401 acquisition system and monitored using Signal 5 software (Cambridge Electronic Design Limited, Cambridge, England). The bridge resistance compensation was applied in current-clamp mode. In voltage-clamp, series resistance compensation was used (50-80%). Furthermore, in voltage-clamp mode, five successive traces were averaged and were subsequently leak-subtracted (the leak current in response to a small pulse, 10 times smaller than the test pulse, was multiplied by 10 and was subtracted from the test response). Liquid junction potential (15 mV) was corrected offline.

Data analysis

Analysis of the recordings was performed using custom programs in Signal 5 (Cambridge Electronic Design Limited, Cambridge, England). Input conductance was the inverse of the slope of the I-V curve obtained by injecting small 500 ms pulses of currents (-100 pA to +20

pA, 30 pA steps repeated 10 times). The *threshold current* was the minimal current required to elicit a discharge in response to a 5 s square pulse (the current was incremented by 50 - 100 pA steps). We measured the *voltage spiking threshold* on the first spike of the 5 s pulses as the voltage at which the first derivative reached 10 mV/ms. We also measured the *recruitment current (I_{on})* for which the first action potential was fired during a 0.1 nA/s current ramp (average of three trials).

Results

Most spinal motoneurones exhibit a delayed discharge in response to a threshold pulse of current at P6-P10

At P6-P10, spinal motoneurones displayed two types of responses during long lasting pulses of depolarizing currents. Figure 1A illustrates a typical example observed in 59 of the 89 motoneurones (66%) recorded. Upon injection of a 1.3 nA square pulse of 5 seconds duration, the response displayed a slow depolarization (arrow) but the voltage did not reach the threshold for spiking (Figure 1A1). When the current intensity was increased to 1.4 nA, the motoneurone still did not discharge at the onset of the pulse (Figure 1A2), but the membrane potential depolarized slowly (not visible at this scale), pushing the motoneurone towards its spiking threshold (-48 mV). The motoneurone started to fire only 1.5 s after the onset of the pulse and then the discharge frequency increased throughout the rest of the pulse (1.4 nA was then considered the threshold current for this motoneurone). For higher current intensities, the motoneurone was more depolarized and the delay of the first spike decreased. When the current was large enough (2 nA in Figure 1A3) the motoneurone discharged at the onset of the pulse and its firing frequency now decreased throughout the pulse. In these motoneurones that exhibited a delay in their response for a liminal pulse, the latency of the first spike was on average 1.5 seconds (0.3 - 4.9 s). Overall, the majority of spinal motoneurones recorded at P6-P10 displayed a remarkable delay of firing when the current intensity is just supraliminal. We called them “delayed firing motoneurones”.

The 30 remaining motoneurones (34%) did not exhibit any delay in their responses to a square current pulse as illustrated in Figure 1B. In this example, the motoneurone reached its firing threshold (-59 mV) when a 0.1 nA current pulse was injected (Figure 1B1). It fired two spikes at the onset of the current pulse. The firing was then sparse with only two more spikes before the end of the pulse. When the intensity of the current was increased to 0.3 nA, the firing started at the pulse onset at a frequency of about 30 Hz (Figure 1B2). It then declined and became very irregular after approximately 1.6 s. The irregularity of the discharge was due to the alternation of oscillations and full-blown spikes as shown in the insert (mixed mode oscillations, Iglesias et al., 2011). At higher current intensities, the mixed

mode oscillations disappeared and the neuron displayed a regular discharge throughout the pulse duration with a decreasing firing frequency (Figure 1B3). Firing frequencies that increase during the pulse were never observed in this motoneurone sub-population. We named these motoneurones “immediate firing motoneurones”. Remarkably, the delayed firing motoneurones have on average a larger input conductance, a more depolarized voltage threshold for spiking and a larger threshold current than the immediate firing motoneurones (see table 1).

The delayed firing pattern is due to two potassium currents that act at two time scales

To understand what are the underlying currents that account for the behaviour observed around spiking voltage threshold in the delayed firing motoneurones, we compared the responses of motoneurones to 5 s voltage steps near spiking threshold in voltage-clamp mode. After application of synaptic blockers, the motoneurone subtype was identified in current-clamp using a threshold current pulse (Figure 2A shows a delayed firing motoneurone and figure 2B an immediate firing motoneurone from the same experiment). We switched to voltage-clamp mode (0.2 µM TTX was added in the bath to block the sodium current) and applied voltage steps from a holding potential of -110 mV to -65 mV (the voltage reached at the pulse onset in both motoneurones in current-clamp mode, Figures 2A2 and 2B2). During the voltage jump, the delayed firing motoneurone displayed an outward current with two distinct components (Figure 2A2, dark trace). The first component displayed a quick activation and inactivation and developed about 0.3 nA at its peak (filled arrowhead). This fast outward current likely explains why the motoneurone was not able to discharge in current-clamp at the pulse onset. The second component of the outward current was weaker (only 0.1 nA at the peak, open arrowhead). It displayed a slow activation and an even slower inactivation. This slow inactivation accounted for the slow depolarization that progressively brought the motoneurone towards its firing threshold and is likely responsible for the long delay before firing onset. When the voltage step was further increased to -35 mV (above the spiking threshold of both motoneurones), the peaks of the fast and slow components increased and they were superimposed on a steady outward current (dashed line). This steady current corresponds to the activation of the delayed rectifier current at a higher voltage than the threshold voltage for spiking.

In sharp contrast virtually no outward current was visible at the voltage-spiking threshold in the immediate firing motoneurone (Figure 2B2, dark trace), which explains why this motoneurone fired at pulse onset. When the voltage step was increased to -35 mV, a strong delayed rectifier was again present (4.9 nA, plateau on grey trace). We reproduced this

experiments in 8 motoneurones (5 delayed firing and 3 immediate firing motoneurones) and we made similar observations as in figure 2.

The fast and slow components observed in the delayed firing motoneurones proved to be two independent currents. Indeed only the fast component was sensitive to the level of the holding potential preceding the depolarizing jump). This is illustrated in Figure 3A. A voltage step from -110 mV to -45 mV produced a fast outward current of more than 0.6 nA (dark trace), while the same step from a holding of -65 mV elicited a fast outward current of less than 0.2 nA (dashed trace). This observation was consistently made in three delayed firing motoneurones. In order to investigate the impact of the fast current, that acts only at a relatively short time scale, on the discharge of the delayed firing motoneurones, we induced firing with a current pulse that was just larger than the threshold pulse (1 nA in the example shown in figure 3B1 and 3B2, current-clamp recording). In these conditions, the first spike latency was longer (77 ms, Figure 3B1) following a hyperpolarizing pre-pulse (voltage held at -95 mV) than following a depolarizing pre-pulse (8 ms, Figure 3B2, voltage held at -65 mV). The longer latency was due to the fact that more fast current was available because of its prior de-inactivation by the hyperpolarizing pre-pulse. This experiment was repeated in five delayed firing motoneurones and the latency of the first spike was always larger when conditioning the response with a -95 mV pre-pulse than with a -65 mV pre-pulse (Figure 3B3). Moreover, in voltage-clamp mode, only the fast current was abolished after a bath application of 5 mM 4-AP (Figure 3C). On average, the application of 5 mM 4-AP reduced the fast component by 63% (n = 5). The effect of bath application of 5 mM 4-AP was further demonstrated on other delayed firing motoneurones recorded in current clamp-mode. In the example shown in Figure 3D, the latency of the first spike decreased from 100 ms (Figure 3D1) to 5ms (Figure 3D2) after 4-AP application. This experiment was repeated in three delayed firing motoneurones in which the latency of the first spike was always longer before, than after, application of 5 mM 4AP (Figure 3D3). Altogether, the de-inactivation of the fast current upon hyperpolarization and its suppression by 5mM 4-AP strongly suggest that the fast current is a potassium A-current (Lape & Nistri, 1999; Russier *et al.*, 2003).

While the A-like current was selectively abolished by 4-AP, the remaining slow component was nearly suppressed by 20 mM TEA (Figure 4A) indicating that the later component was also carried by potassium ions. This experiment was repeated in four delayed firing motoneurones in which bath application of 20 mM TEA reduced the slow potassium current by 70%. However, neither 50 µM oxotremorine nor 50 µM XE991 (not shown) had an effect on it. Thereby this current was not a M-current. It compared rather with the slowly activating, even more slowly inactivating potassium current described by Lüthi et al. (1996) in CA3 pyramidal cells of rat hippocampus. It was responsible for the long delay of the discharge that we observed in our experiment in current clamp mode (Figure 4B1) since this long delay

was totally abolished by bath application of 20 mM TEA (Figure 4B2). Such a high dose of TEA probably blocked, not only the slow-inactivating potassium current but also the A-current (Aguayo & Weight, 1988; Denton & Leiter, 2002) explaining why there was no short delay left at the pulse onset. Indeed the delayed firing pattern was somehow converted into immediate firing pattern (no delay in the first spike, decreasing firing frequency).

The two potassium currents shape the F-I function of the delayed firing motoneurones

Since they lower the motoneurone excitability, the potassium currents play a major role in shaping the F-I function of the delayed firing motoneurones. The response to a slow triangular ramp of current shown in Figure 5A was recorded in the same delayed firing motoneurone as in Figure 1A. The stationary F-I relationship can be fairly well approximated provided that the ramp velocity was as low as 0.1 nA/s. At this very slow velocity, the ascending branch of the F-I function was superimposed to the stationary F-I curve obtained with the long current pulses (upward triangles, Figure 5A2 and see also Figure 5B2). Prior to the inflexion point (open arrowhead), the pulse response (Figure 1A2) displayed an increasing spike frequency resulting from the inactivation of the slow potassium current. After the inflexion point, the pulse responses no longer displayed this feature (see Figure 1A3) indicating that the slow potassium current was no longer shaping the firing response. On the response to the slow triangular ramp, the recruitment current (1.25 nA) was larger than the de-recruitment current (0.89 nA, Figure 5A2). This was most likely due to the activation of the slow potassium currents that delayed the recruitment of the motoneurone. The behaviour illustrated in Figure 5A has never been observed in immediate firing motoneurones.

Conversely, the immediate firing motoneurone illustrated in Figure 5B (same motoneurone as in Figure 1B) displayed a lower recruitment current (0.06 nA) than de-recruitment current (0.32 nA, Figure 5B2). We have recently shown that such a F-I function can be caused by a very slow inactivation of the sodium current (Iglesias et al., 2011; Miles et al. 2005). A slow inactivation of the sodium current is likely to be also at work in this motoneurone as suggested by the decreasing of the size of the action potentials throughout the ascending phase of the ramp (Figure 5B1). However, the delayed firing motoneurone on Figure 5A also displayed some sodium inactivation suggesting that its F-I function results from the combined inactivation of both the slow potassium and slow sodium currents.

The slow potassium current plays a critical role in setting the recruitment current of delayed firing motoneurons, as demonstrated in Figure 6. Figure 6A shows another delayed firing motoneurone for which the recruitment current was substantially higher (0.56 nA) than the de-recruitment current (0.15 nA). However, in response to a second triangular ramp that started 2 seconds after the end of the first one (Figure 6B), the recruitment current was much

lower (0.10 nA) and was close to the de-recruitment current that was the same in both ramps. This strongly suggests that at the end of the first triangular ramp the slow potassium current had fully inactivated and that the delay of 2 seconds before the next ramp was not long enough to allow it to de-inactivate. As a consequence, the motoneurone is more excitable at the onset of the second ramp than at the onset of the first one. In order to get rid of this memory effect, we had to wait at least 30 seconds between two successive ramps indicating again that the memory effect was due to a slow current.

In these conditions, the recruitment currents during the slow ramps are quite close to the threshold current during the long square pulses, and again they are on average larger in delayed firing than in immediate firing motoneurones (Table 1). In 39 out of 51 delayed firing motoneurones (76%), the recruitment current was higher than the de-recruitment current as in Figure 5A. This reflects the influence of the slow potassium current. In 6 others (12%), the response was not hysteretic (recruitment and de-recruitment currents were the same, ascending and descending branches superimposed, not shown) suggesting that the influence, on the recruitment threshold, of the slow potassium and slow sodium currents were compensating each other. In the remaining 6 delayed firing motoneurones (12%), the recruitment current was lower than the de-recruitment current suggesting a stronger inactivation of the slow sodium current (Iglesias et al., 2011). The responses of the immediate firing motoneurones were much simpler because they are not endowed with the slow potassium current. 20 immediate firing motoneurones have been investigated. 11 of them displayed the pattern illustrated in Figure 5B (recruitment current lower than de-recruitment current, and substantial reduction of the spike height suggesting strong sodium inactivation) whereas the other 9 had ascending and descending branches that were superimposed (identical recruitment and de-recruitment currents, little reduction of the spike height, not shown).

Discussion

We have shown that, at P6-P10, a majority of spinal motoneurones display a delayed firing pattern in response to long square pulses of current. The delayed discharge is caused by the combined action of a fast A-like current and a slow-inactivating potassium current. These potassium currents contribute to shaping the F-I function of the delayed firing motoneurones. The slow-inactivating current is responsible for memory effects that have a strong impact on motoneurone excitability.

Transient expression of A-like and slow-inactivating potassium currents during postnatal development

The delay of motoneurone discharge is due to two potassium currents that act at two different time scales. The transient fast A-like current acts by delaying the discharge over a relatively short time (about 30 ms in our experimental conditions). Similar current has been observed in spinal motoneurones of neonatal mice (Gao & Ziskind-Conhaim, 1998; Perrier & Hounsgaard, 2000) as well as in brainstem motoneurones (Lape & Nistri, 1999; Russier *et al.*, 2003). The slow-inactivating potassium current is responsible for the long delay of the discharge (several seconds). Such slow currents have also been observed in other types of neurons such as the adult rat hippocampus neurons (Storm, 1988; Lüthi *et al.*, 1996) and the thalamic relay neurons (Huguenard & Prince, 1991) where they coexist with the A current. However, the A-current and the slow-inactivating potassium current only have a transient expression in spinal motoneurones of neonates since both of them are lacking in adult spinal motoneurones (Kernell, 2006; Barrett *et al.*, 1980). Delays in the discharge have never been observed in adult spinal motoneurones, which fire always at the onset of liminal pulses (Kernell, 2006; Manuel *et al.*, 2009; Meehan *et al.*, 2010). Furthermore, the delayed firing pattern was only transiently observed between P4 and P9 in rat abducens motoneurones (Russier *et al.*, 2003). The transient expression in neonates of the delayed firing pattern is then consistent with the transient expression of the A-like current and the slow-inactivating potassium current.

The potassium currents determine the firing properties of the delayed firing motoneurones

The potassium currents can deeply shape the firing properties of motoneurones. First, they delay the discharge. During liminal pulses, we observed delays that could last several seconds after the pulse onset. These delays are longer than those (about 100 ms) reported by Russier et al. (2003) and Pambo-Pambo et al. (2009). Second, the inactivation of the slow potassium current elicits an acceleration of the discharge. Such acceleration has been observed only in the delayed firing motoneurones (Russier *et al.*, 2003; Pambo-Pambo *et al.*, 2009 and present work). However, we have shown that the acceleration pattern may convert into a deceleration pattern (frequency adaptation) when the injected current is increased past the inflection point of the F-I curve. This suggests that for higher voltages the current inactivates more rapidly and it no longer plays any consistent role in the discharge pattern. In contrast, the immediate firing motoneurones never display an acceleration of the discharge. In adult motoneurones, the firing frequency is always decreasing during a pulse (Viana *et al.*, 1995; Brownstone, 1986; Manuel *et al.*, 2009). This again suggests that the delayed firing pattern is only expressed during a restricted window of the post-natal period. Third, the slow potassium current shapes the F-I function of the delayed firing motoneurones during triangular ramp of currents. In these cells, the F-I function mostly depends on the interaction

between the slow inactivation of the potassium current and the slow inactivation of the sodium current. The F-I functions of the immediate firing motoneurones are more stereotyped since the slow potassium current is lacking in these cells. In adults, spinal motoneurones were found to display a variety of F-I functions (Hounsgaard *et al.*, 1988; Lee & Heckman, 1998; Bennett *et al.*, 2001; Button *et al.*, 2006). The shape and the hysteresis of these functions depend on the slow currents that are expressed, notably calcium persistent inward currents and a classification in four types was proposed by Bennett et al. (2001). However, this classification cannot apply to motoneurones of neonatal mice since the delayed firing motoneurones are not endowed with the same panoply of currents as adult motoneurones. Moreover, persistent inward currents are weak in motoneurones of neonatal mice (Quinlan *et al.*, 2011).

Impact of the potassium currents on the recruitment of the delayed firing motoneurones

On average, the delayed firing motoneurones have larger input conductances than the immediate firing ones. As a consequence their recruitment requires a larger synaptic drive than the recruitment of immediate firing motoneurones. This trend is favoured by the presence of potassium currents that contribute to decrease their excitability. This is likely why the delayed firing motoneurones exhibit, on average, more depolarized voltage thresholds for spiking than the immediate firing motoneurones. The A-like current would increase the recruitment threshold for brief synaptic inputs (several tens of milliseconds) whereas the slow potassium current would increase the threshold during steady synaptic inputs. Potassium currents might then help to ensure an orderly recruitment of neonatal motoneurones. However, we demonstrated that the recruitment threshold of the delayed firing motoneurones may be reduced when the intervals between the slow current ramps is short. This is likely due to the fact that the slow potassium current remains inactivated thus enhancing the motoneurone excitability. This “memory effect” lowers the recruitment threshold of delayed firing motoneurones. Slow synaptic activation of the delayed firing motoneurones repeated at short intervals is then likely to decrease their recruitment threshold and to increase their firing probability. However, we do not know whether delayed firing motoneurones are recruited frequently enough so that the memory effect may take place in physiological conditions.

The potassium currents might contribute to the maturation of motor units in neonates

A link between the discharge properties of the motoneurone and their muscle targets cannot be established in our experimental conditions. However, it is likely that all cells were alpha motoneurones since their soma areas were larger (550 - 1000 μm^2) than the soma areas of gamma motoneurones at P14 (Friese *et al.*, 2009). Furthermore the delayed and immediate

firing motoneurones are likely to co-exist in same motor pools since we have frequently encountered the two types in close proximity in the same slice. Given that delayed firing motoneurones present, on average, larger input conductances and higher recruitment currents we may assume they are bound to be F type motoneurone whereas immediate firing motoneurones become S type. This hypothesis remains however to be experimentally tested.

Under this assumption, the lower recruitment probability of the delayed compared to the immediate firing motoneurones would contribute to the maturation of their motor units. First, the motoneurones activity has an impact on the maturation of the myosin heavy chain isoforms (Lowrie *et al.*, 1989; Goldspink *et al.*, 1992; Picquet *et al.*, 1998, Agbulut *et al.*, 2009). Furthermore, the slow muscle fibres already express their mature myosin heave chain isoform at the end of the first week whereas the fast fibres express theirs later (Agbulut *et al.*, 2003; Schiaffino & Reggiani, 2011). One can speculate that this differential rate of maturation originates from the differential activity between immediate and firing motoneurones. Second, the motoneurones activity has also an impact on the rate of elimination of supernumerary neuromuscular junctions (Thompson, 1985). Indeed, increasing the neuromuscular activity by chronically applying electrical stimulation dramatically increases the rate of loss of synaptic contacts (O'Brien *et al.*, 1978). Conversely, reducing proprioceptive inputs to motoneurones (Benoit & Changeux, 1975) or reducing inputs to muscle fibres by partial axotomy (Brown *et al.*, 1976) delays the elimination of poly-innervation. As a result, motor units whose activity was reduced by TTX had larger territories than those whose axons remained active (Callaway *et al.*, 1989). This was further supported by experimental and theoretical works suggesting that motoneurones with less active neuromuscular junctions had larger motor units than motoneurones with more active ones (Callaway *et al.*, 1987; Barber & Lichtman, 1999; Nowik *et al.*, 2012). One may wonder whether the larger F motor unit territories would result from the lower activity of the delayed firing motoneurones.

References

Agbulut O, Noirez P, Beaumont F & Butler-Browne G. (2003). Myosin heavy chain isoforms in postnatal muscle development of mice. *Biology of the cell / under the auspices of the European Cell Biology Organization* **95,** 399-406.

Aguayo LG & Weight FF. (1988). Characterization of membrane currents in dissociated adult rat pineal cells. *The Journal of physiology* **405,** 397-419.

Barber MJ & Lichtman JW. (1999). Activity-driven synapse elimination leads paradoxically to domination by inactive neurons. *The Journal of neuroscience : the official journal of the Society for Neuroscience* **19,** 9975-9985.

Barrett EF, Barrett JN & Crill WE. (1980). Voltage-sensitive outward currents in cat motoneurones. *The Journal of physiology* **304,** 251-276.

Bennett DJ, Li Y & Siu M. (2001). Plateau potentials in sacrocaudal motoneurons of chronic spinal rats, recorded in vitro. *Journal of neurophysiology* **86,** 1955-1971.

Benoit P & Changeux JP. (1975). Consequences of tenotomy on the evolution of multiinnervation in developing rat soleus muscle. *Brain research* **99,** 354-358.

Brown MC, Jansen JKS & Van Essen D. (1976). Polyneural innervation of skeletal muscle in new-born rats and its elimination during maturation. *The Journal of physiology* **261,** 387-422.

Brownstone RM. (1986). Beginning at the end: repetitive firing properties in the final common pathway. *Progress in neurobiology* **78,** 156-172.

Burke RE. (1981). *Motor units: anatomy, physiology, and functional organization*. Am. Physiol. Soc., Bethesda, MD.

Button DC, Gardiner K, Marqueste T & Gardiner PF. (2006). Frequency-current relationships of rat hindlimb alpha-motoneurones. *The Journal of physiology* **573,** 663-677.

Callaway EM, Soha JM & Van Essen DC. (1987). Competition favouring inactive over active motor neurons during synapse elimination. *Nature* **328,** 422-426.

Callaway EM, Soha JM & Van Essen DC. (1989). Differential loss of neuromuscular connections according to activity level and spinal position of neonatal rabbit soleus motor neurons. *The Journal of neuroscience : the official journal of the Society for Neuroscience* **9,** 1806-1824.

Clarac F, Brocard F & Vinay L. (2004). The maturation of locomotor networks. *Progress in brain research* **143,** 57-66.

Denton JS & Leiter JC. (2002). Anomalous effects of external TEA on permeation and gating of the A-type potassium current in H. aspersa neuronal somata. *The Journal of membrane biology* **190,** 17-28.

Friese A, Kaltschmidt JA, Ladle DR, Sigrist M, Jessell TM & Arber S. (2009). Gamma and alpha motor neurons distinguished by expression of transcription factor Err3. *Proceedings of the National Academy of Sciences of the United States of America* **106,** 13588-13593.

Gao BX & Ziskind-Conhaim L. (1998). Development of ionic currents underlying changes in action potential waveforms in rat spinal motoneurons. *Journal of neurophysiology* **80,** 3047-3061.

Goldspink G, Scutt A, Loughna PT, Wells DJ, Jaenicke T & Gerlach GF. (1992). Gene expression in skeletal muscle in response to stretch and force generation. *The American journal of physiology* **262,** R356-363.

Hounsgaard J, Hultborn H, Jespersen B & Kiehn O. (1988). Bistability of alpha-motoneurones in the decerebrate cat and in the acute spinal cat after intravenous 5-hydroxytryptophan. *The Journal of physiology* **405,** 345-367.

Huguenard JR & Prince DA. (1991). Slow inactivation of a TEA-sensitive K current in acutely isolated rat thalamic relay neurons. *Journal of neurophysiology* **66,** 1316-1328.

Jansen JKS & Flatby T. (1990). The perinatal reorganization of the innervation of skeletal muscle in mammals. *Progress in neurobiology* **34,** 39-90.

Jiang Z, Carlin KP & Brownstone RM. (1999). An in vitro functionally mature mouse spinal cord preparation for the study of spinal motor networks. *Brain research* **816,** 493-499.

Kernell D. (2006). The motoneuron and its muscle fibers. *Oxford, UK: Oxford UP*.

Lamotte d'Incamps B, Krejci E & Ascher P. (2012). Mechanisms shaping the slow nicotinic synaptic current at the motoneuron-renshaw cell synapse. *The Journal of neuroscience : the official journal of the Society for Neuroscience* **32,** 8413-8423.

Lape R & Nistri A. (1999). Voltage-activated K+ currents of hypoglossal motoneurons in a brain stem slice preparation from the neonatal rat. *Journal of neurophysiology* **81,** 140-148.

Lee RH & Heckman CJ. (1998). Bistability in spinal motoneurons in vivo: systematic variations in rhythmic firing patterns. *Journal of neurophysiology* **80,** 572-582.

Lowrie MB, More AF & Vrbova G. (1989). The effect of load on the phenotype of the developing rat soleus muscle. *Pflugers Archiv : European journal of physiology* **415,** 204-208.

Lüthi A, Gahwiler BH & Gerber U. (1996). A slowly inactivating potassium current in CA3 pyramidal cells of rat hippocampus in vitro. *The Journal of neuroscience : the official journal of the Society for Neuroscience* **16,** 586-594.

Manuel M, Iglesias C, Donnet M, Leroy F, Heckman CJ & Zytnicki D. (2009). Fast kinetics, high-frequency oscillations, and subprimary firing range in adult mouse spinal motoneurons. *The Journal of neuroscience : the official journal of the Society for Neuroscience* **29,** 11246-11256.

Meehan CF, Sukiasyan N, Zhang M, Nielsen JB & Hultborn H. (2010). Intrinsic properties of mouse lumbar motoneurons revealed by intracellular recording in vivo. *Journal of neurophysiology* **103,** 2599-2610.

Miles GB, Dai Y, Brownstone RM. (2005). Mechanisms underlying the early phase of spike frequency adaptation in mouse spinal motoneurones. *The Journal of physiology* **566 (Pt 2)**:519-32.

Nowik I, Zamir S & Segev I. (2012). Losing the battle but winning the war: game theoretic analysis of the competition between motoneurons innervating a skeletal muscle. *Frontiers in computational neuroscience* **6,** 16.

O'Brien RA, Ostberg AJ & Vrbova G. (1978). Observations on the elimination of polyneuronal innervation in developing mammalian skeletal muscle. *The Journal of physiology* **282,** 571-582.

Pambo-Pambo A, Durand J & Gueritaud JP. (2009). Early excitability changes in lumbar motoneurons of transgenic SOD1G85R and SOD1G(93A-Low) mice. *Journal of neurophysiology* **102,** 3627-3642.

Perrier JF & Hounsgaard J. (2000). Development and regulation of response properties in spinal cord motoneurons. *Brain research bulletin* **53,** 529-535.

Picquet F, Stevens L, Butler-Browne GS & Mounier Y. (1998). Differential effects of a six-day immobilization on newborn rat soleus muscles at two developmental stages. *Journal of muscle research and cell motility* **19,** 743-755.

Quinlan KA, Schuster JE, Fu R, Siddique T & Heckman CJ. (2011). Altered postnatal maturation of electrical properties in spinal motoneurons in a mouse model of amyotrophic lateral sclerosis. *The Journal of physiology* **589,** 2245-2260.

Russier M, Carlier E, Ankri N, Fronzaroli L & Debanne D. (2003). A-, T-, and H-type currents shape intrinsic firing of developing rat abducens motoneurons. *The Journal of physiology* **549,** 21-36.

Schiaffino S & Reggiani C. (2011). Fiber types in mammalian skeletal muscles. *Physiological reviews* **91,** 1447-1531.

Storm JF. (1988). Temporal integration by a slowly inactivating K+ current in hippocampal neurons. *Nature* **336,** 379-381.

Thompson WJ. (1985). Activity and synapse elimination at the neuromuscular junction. *Cellular and molecular neurobiology* **5,** 167-182.

Thompson WJ, Sutton LA & Riley DA. (1984). Fibre type composition of single motor units during synapse elimination in neonatal rat soleus muscle. *Nature* **309,** 709-711.

Viana F, Bayliss DA & Berger AJ. (1995). Repetitive firing properties of developing rat brainstem motoneurones. *The Journal of physiology* **486 (Pt 3),** 745-761.

Competing interests

The authors declare no competing interests.

Author contributions

FL performed and designed the experiments, analysed and interpreted the data and wrote the article. BLI conceived and designed the experiments and analysed the data. DZ interpreted the data and wrote the article.

Funding

Financial supports provided by the Agence Nationale pour la Recherche (HYPER-MND, ANR-2010-BLAN-1429-01), the NIH-NINDS (R01NS077863) and the Thierry Latran Fundation (OHEX Project) are gratefully acknowledged. Felix Leroy is recipient of a “Contrat Doctoral” from the Ecole Normale Supérieure, Cachan.

Acknowledgements

The authors wish to thank Pr. CJ Heckman and Drs Marin Manuel & Katharina Quinlan for helpful comments and careful scrutinizing of the manuscript and Ms. Rebecca Manuel for mouse breeding.

Table and Figure Legends

Table 1: Comparison of electrophysiological properties between Delayed firing and Immediate firing motoneurones.
In each cell is given the average value ±SD, the range of values, and the number of observations. *Mann-Whitney U test* (two-tailed) were used to assess the difference between two samples. The p values from the Mann-Whitney U test are given in the last column. The means of each properties displayed differ significantly.

Figure 1: Delayed and immediate firing patterns of discharge
A1-3: Responses of a delayed firing motoneurone to long lasting pulses (5 seconds) of increasing amplitude. Bottom: injected-current (square pulses in nA), middle: voltage-response (in mV) and top (A2, A3 only): instantaneous firing frequency (Hz). In A1, the horizontal dashed line and the arrowhead point out the progressive depolarization of the membrane potential. **B1-3:** Responses of an immediate firing motoneurone to long lasting pulses of increasing amplitude. Same organization as in A. The insert is an enlargement of a small portion (rectangle) of the voltage in B2 showing the oscillations (arrowhead) between the spikes.

Figure 2: Delayed firing motoneurones exhibit a fast and a slow outward currents
A1 and **B1**: Voltage-responses of a delayed **(A1)** and an immediate firing **(B1)** motoneurone to a long lasting current-pulse at liminal intensities (current-clamp mode). Bottom: injected-current, and top: voltage-response. Note that the voltage was about -65 mV at the pulse onset (voltage threshold -53 mV for the delayed firing motoneurone and -65 mV for the immediate firing one). **A2** and **B2**: Current-responses of the same delayed **(A2)** and immediate **(B2)** firing motoneurone to voltage-pulses from -110 mV to -65 mV or -35 mV. Bottom: voltage-command and top: current-response. Note the fast (filled arrowhead) and the slow (open arrowhead) outward currents in A2. They are virtually lacking in B2.

Figure 3: The fast outward current is an A-like current
A: Voltage-jumps to -45 mV from different holding potentials (-110 mV : solid lines and -65 mV : dashed-lines) in a delayed firing motoneurone (voltage-clamp mode). Bottom: voltage-command and top: current-response. **B1-2:** Voltage-responses from the same motoneurone following two different pre-pulses (note that the pulse inducing the discharge remains unchanged). Bottom traces injected-current and top traces voltage-response. Arrowheads point at the first spike latency. **B3** Plot of the first spike latency in function of the voltage the motoneurones were maintained at (dashed line: motoneurone in B1-2). **C:** Voltage-clamp recording before (dashed line) and after 15 min of 5 mM 4-AP (solid line). **D1-2:** Voltage-responses from the motoneurone to the same pulse before (**D1**) and after (**D2**) 5 mM 4-AP application. Arrowheads point at the first spike latency. **D3:** Plot of the first spike latency of three different motoneurones before and after 5 mM 4-AP application (dashed line: motoneurone in D1-2).

Figure 4: The slow outward current is blocked by TEA
A: Slow outward current activated by a long lasting voltage step in a delayed firing motoneurone (voltage-clamp recording). Grey line: control record with 5 mM 4-AP in order to abolish the fast outward current. Black line: record 15 min after a TEA bath application (20 mM). Bottom: voltage command, top: current-responses. **B1:** Response of a delayed firing motoneurone to a threshold stimulation in control condition (no drugs, current clamp mode). Note the 3 s delay before firing onset and the increasing firing frequency. Bottom: injected-current, middle: voltage-response and top: instantaneous firing frequencies (in Hz). **B2:** Same motoneurone recorded following 15 minutes of TEA application (20 mM) (same arrangement as B1). Under these conditions, the motoneurone discharged at the pulse onset and its discharge frequency is decrementing during the pulse.

Figure 5: Firing behaviour of delayed firing (A) and immediate firing (B) motoneurones in response to a slow triangular ramp of current

A1 and **B1**: Responses to triangular ramp of currents (slope ± 0.1 nA/s). Bottom: injected-current, middle: voltage-response and top: instantaneous firing frequency (Hz). The dashed vertical lines indicate the recruitment and the de-recruitment currents. The two motoneurones are the same as in Figure 1. **A2** and **B2**: Instantaneous firing frequency plotted in function of the injected current during the ascending (empty squares) and descending (filled circles) ramps. The stationary F-I curve calculated from the square-pulses (Figure 1) is also plotted (filled upward triangles, at each intensity the frequency is the averaged frequency over the last second of the pulse). The filled arrowheads point at the stationary frequencies computed from the traces shown in Figure 1. The open arrowhead points at the inflexion point of the ascending branch.

Figure 6: Memory effect of the slow outward current
A1 and **B1**: Consecutive current-injections (triangular ramp, slope ± 0.1 nA/s) in the same motoneurone. The ramp in B started 2 seconds after the completion of the ramp in A. Bottom: injected-current, top: voltage-response. **A2** and **B2**: Instantaneous firing frequency during the ascending (grey squares) and descending (black circles) ramps. Arrow points the lowering of the recruitment current between A and B.

Table 1

	Delayed firing MNs	Immediate firing MNs	*Mann-Whitney U test*
Input conductance (nS)	52 ± 28 10 / 151 N=59	33 ± 23 6 / 98 N=30	0.0006
Voltage threshold (mV)	-48 ± 7 -62 / -31 N=59	-60 ± 7 -75 / -41 N=30	0.0008
Threshold current (nA)	1.20 ± 0.61 0.30 / 2.80 N=59	0.59 ± 0.40 0.05 / 1.60 N=29	<0.0001
Recruitment current on ramp (nA)	1.08 ± 0.65 0.15 / 2.87 N=51	0.62 ± 0.47 0.07 / 1.96 N=20	0.001

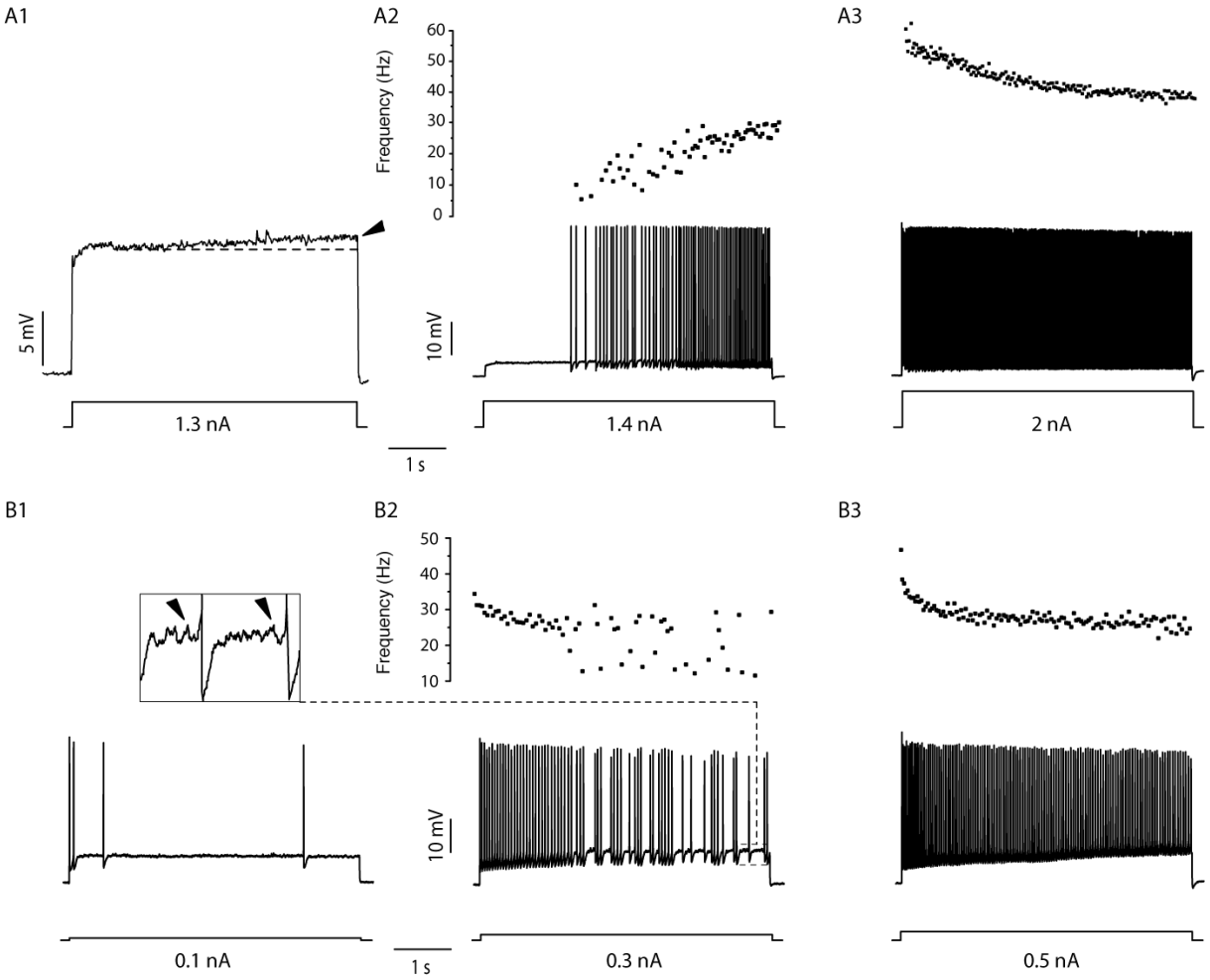

Article 1 Figure 1

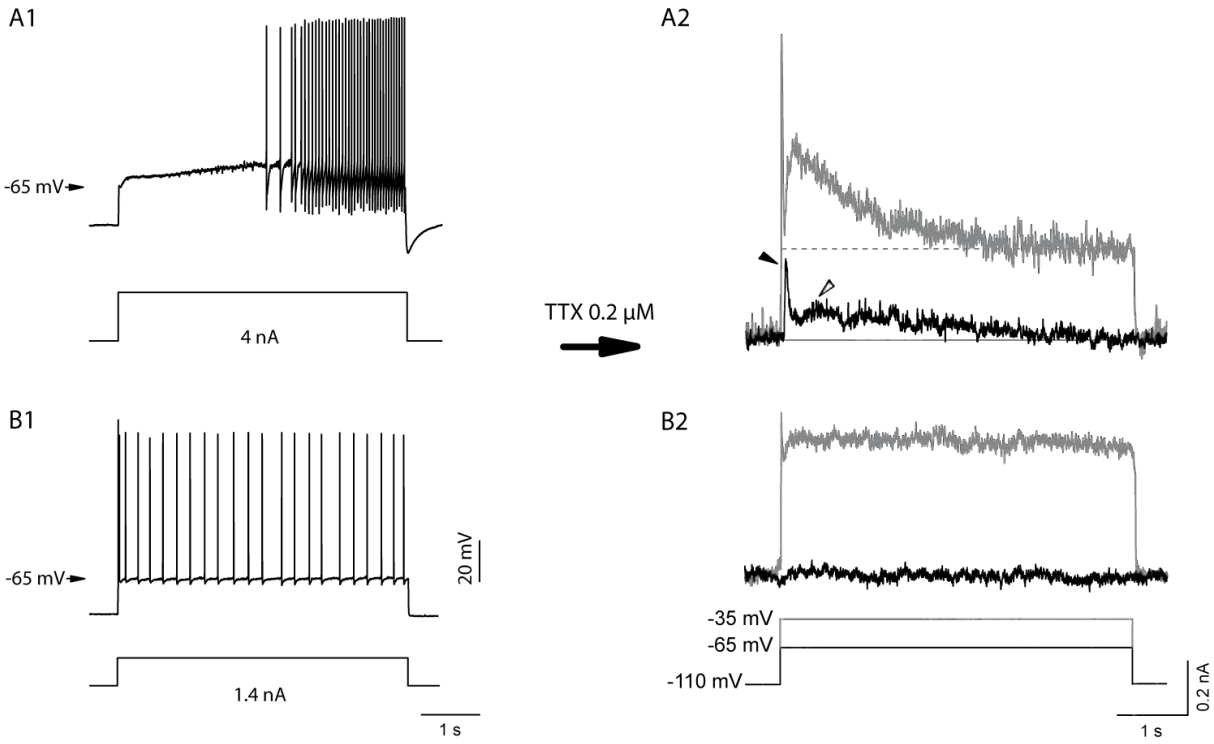

Article 1 Figure 2

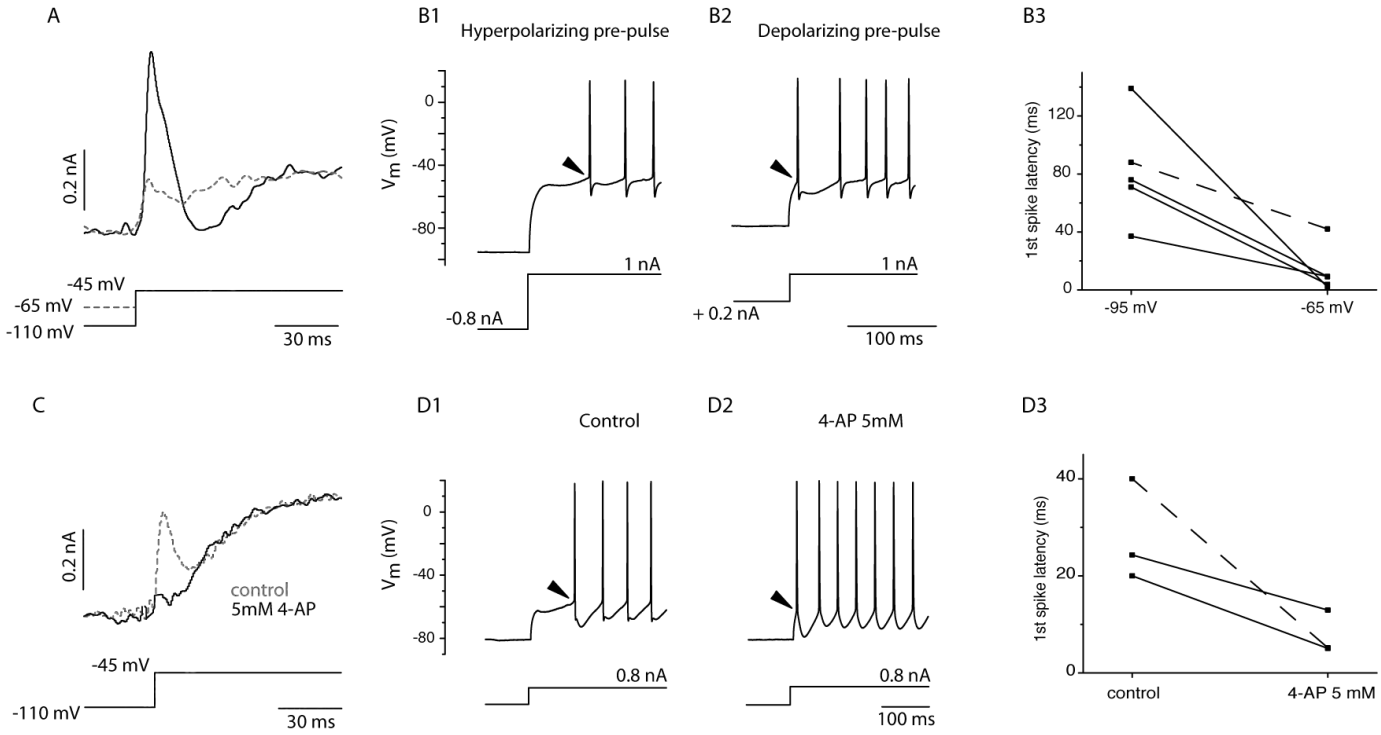

Article 1 Figure 3

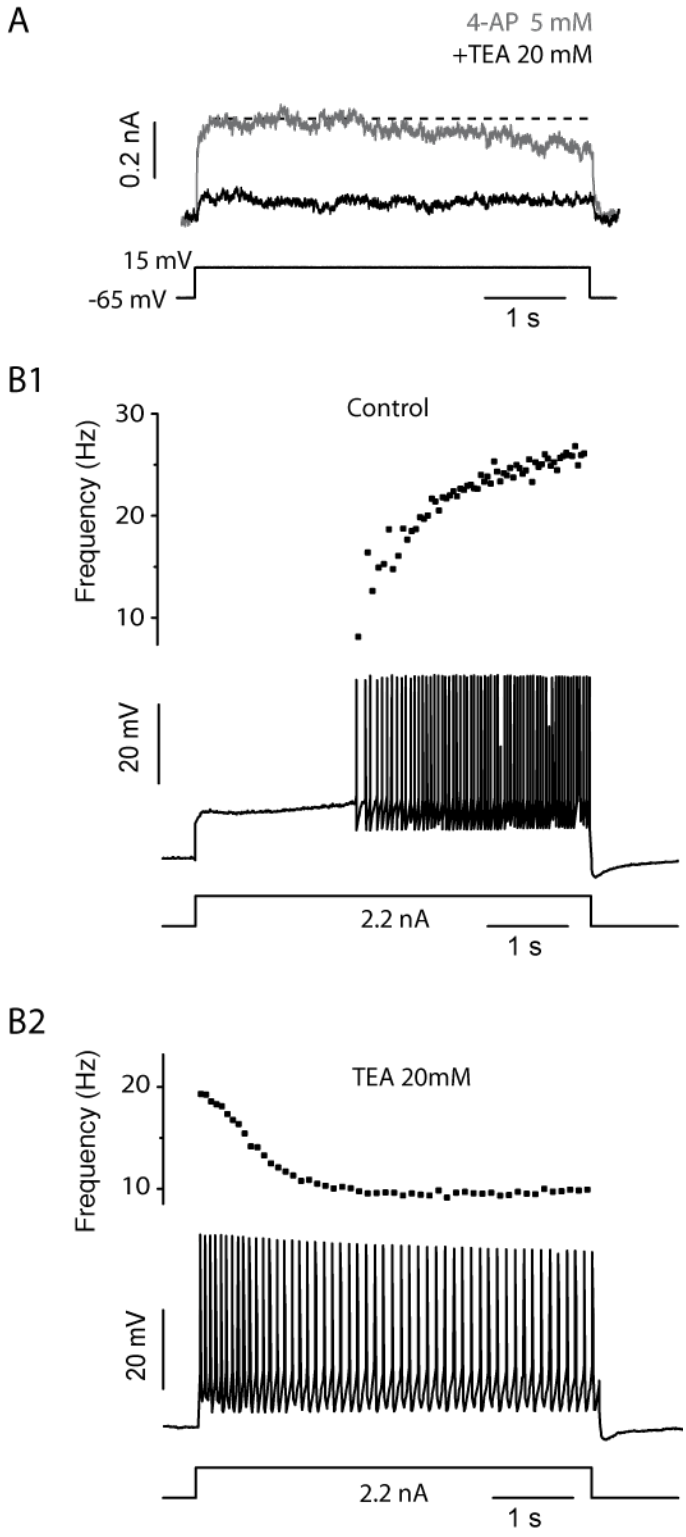

Article 1Figure 4

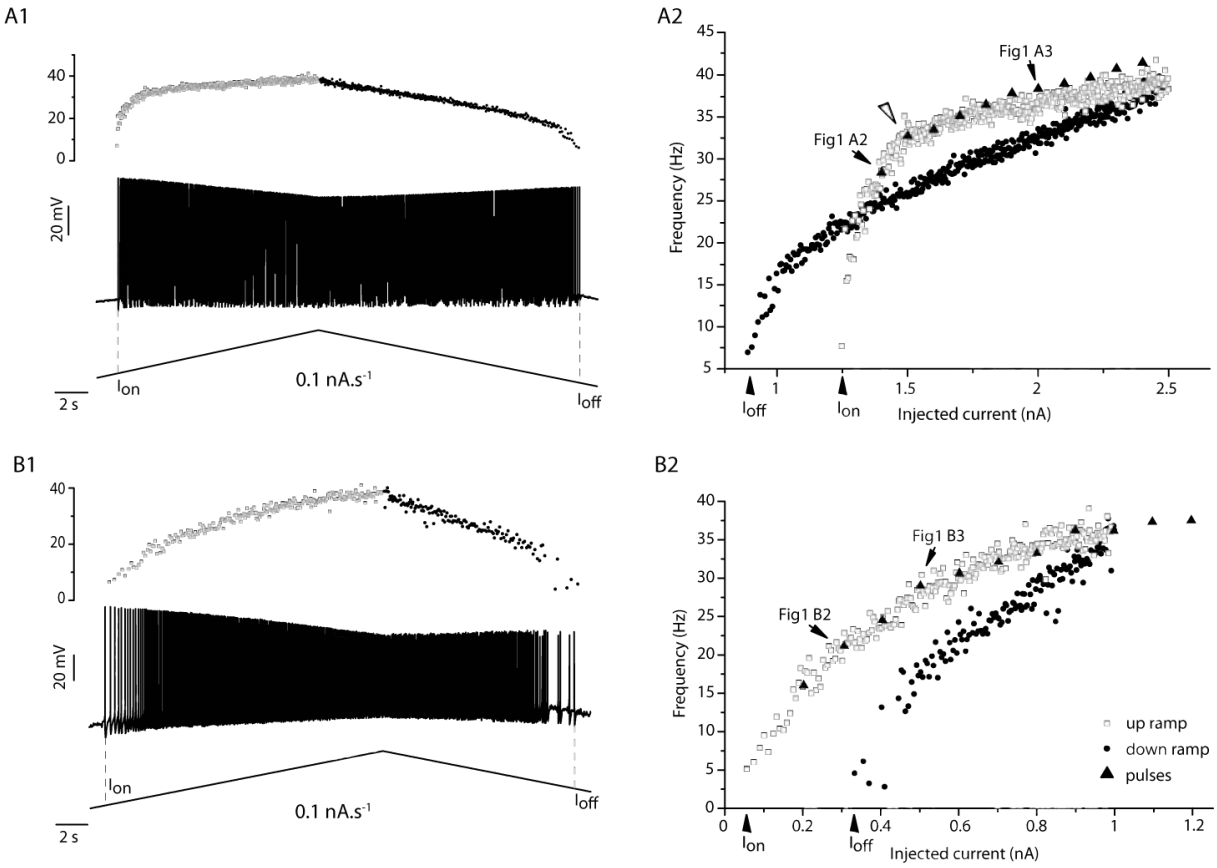

Article 1 Figure 5

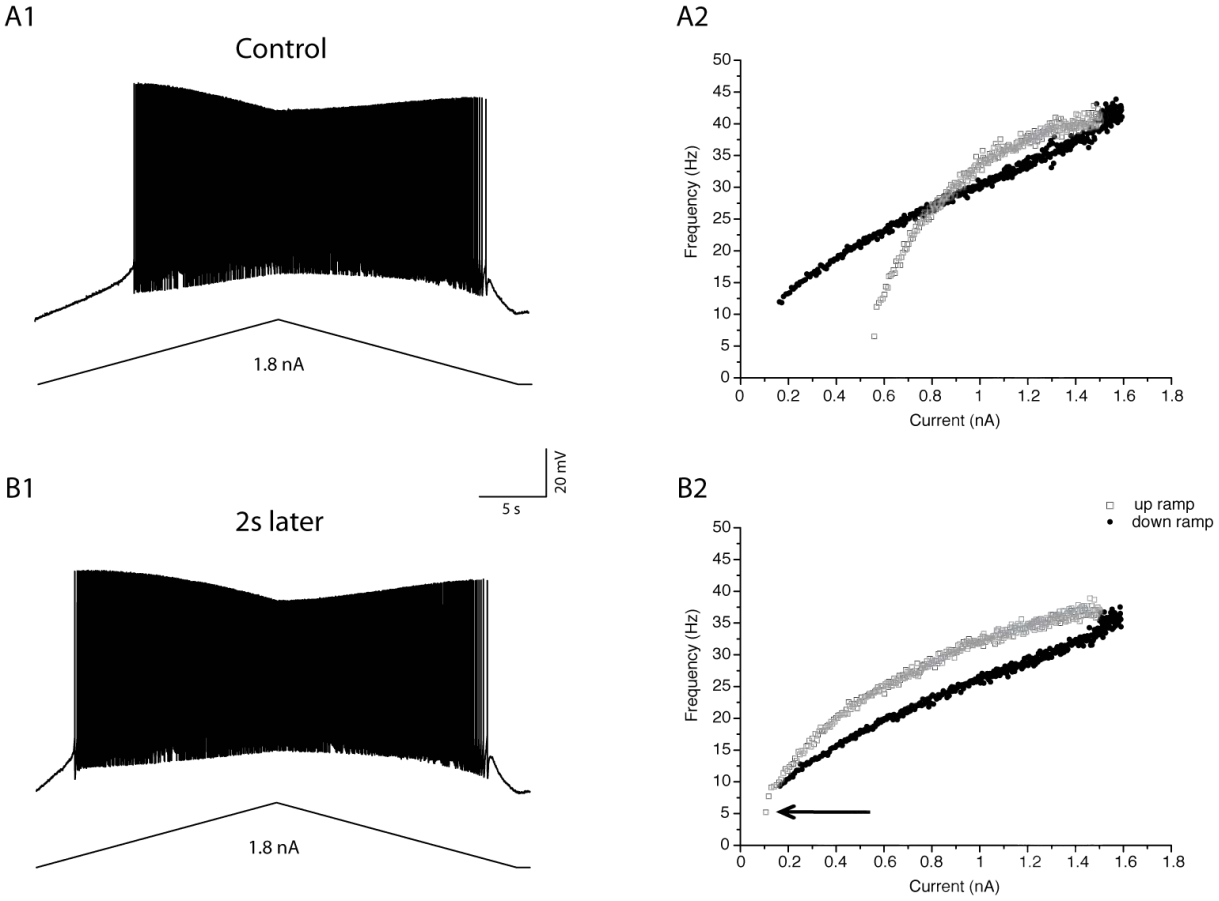

Article 1 Figure 6

Chapter III: heterogeneous vulnerability of the motoneurons during the ALS

1/ Mutations conferring the ALS and mouse models

The most common mutated protein in the familial cases of ALS (fALS) is the superoxide oxide dismutase protein. More than 140 point mutations have been detected in the primary structure of SOD1 in ALS patients. Noteworthy most of these mutations did not induce a loss of function in the protein activity but rather a misfolding of the protein (Turner & Talbot, 2008). This suggests the protein misfolding is involved in the disease (reviewed in Boillee *et al.*, 2006a). Although SOD1 is expressed ubiquitously in most cell types, the ALS is characterized by a selective degeneration of the motor neurons. The insertion of the human mutation G93A of the SOD1 protein in the mouse genome (Gurney *et al.*, 1994) reproduces most of the pathology of human sporadic and familial ALS (Wong *et al.*, 2002). The high-expressor line G93A SOD1 transgene will be further refered to as the mSOD1 transgene. Conditional expression of the transgene proved however that the full disease phenotype required expression of the mutation in other cell types than motoneurons such as astrocytes and microglia (Papadimitriou *et al.*, 2010). Based on the SOD1 gene excision from selected sub-types it is thought that the onset of the disease is driven by mSOD1 produced by motoneurons (Boillee *et al.*, 2006b; Yamanaka *et al.*, 2008; Wang *et al.*, 2009) and NG2+ oligodendrocyte precursors (Kang *et al.*, 2013). Progression on the other hand depends on mSOD1 coming from astrocytes (Yamanaka *et al.*, 2008) and microglia (Boillee *et al.*, 2006a). The figure 13 recapitulates the different contributions of mSOD1 within different cell types. The alterations induced by mSOD1 are thus both cell-autonomous and non-cell autonomous manners (Boillee *et al.*, 2006a).

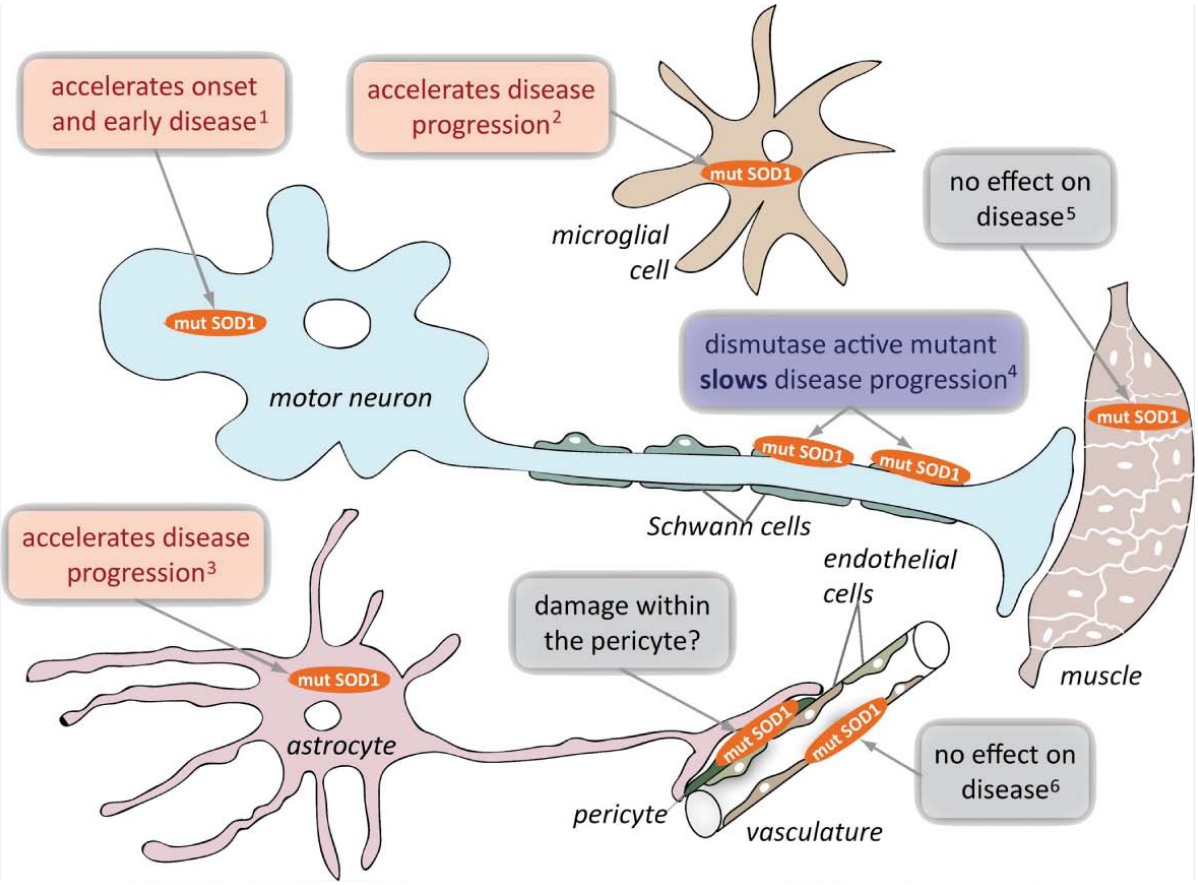

Figure 13: Contribution of mutant SOD1 within different cell types in ALS. Despite the apparent selectivity for motoneurons, multiple lines of evidence indicate that nonneuronal cell types contribute to pathogenesis and disease progression in SOD1-mediated neurodegeneration. Mutant SOD1 expression in motor neurons directs the onset and development of early disease, but does not influence its progression. In contrast, mutant SOD1 expression in microglia or astrocytes accelerates disease progression without affecting its onset. Expression of a dismutase-active mutant SOD1 specifically in Schwann cells was found to slow disease progression, but the role of a dismutase-inactive mutant in these cells has not been tested. Mutant SOD1 expression within muscle or endothelial cells does not affect ALS onset or progression, although some reports suggest that muscle might be a direct target of mutant SOD1 toxicity. Lastly, the vasculature is damaged very early in disease, leading to loss of tight junctions between endothelial cells and microhemorrhages, but whether any of this is from mutant SOD1 within pericytes, the terminal astrocyte, or coming from cells outside the vasculature is not established. **1** Ralph *et al.* 2005, Boillée *et al.* 2006, Jaarsma *et al.* 2008. **2** Beers *et al.* 2006, Boillée *et al.* 2006, Wang *et al.* 2009. **3** Yamanaka *et al.* 2008b. **4** Lobsiger *et al.* 2009. **5** Holzbaur *et al.* 2006, Miller *et al.* 2006, Dobrowolny *et al.* 2008, Towne *et al.* 2008. **6** Zhong *et al.* 2009. Adapted from Ilieva *et al.* 2009.

Other SOD1 mouse models based on different mutations (SOD1 G85R) or using low-expressor instead of the high-expressor used originally for the G93A mutation model have been produced and allow comparing the progression of the disease in milder mouse models. Furthermore, many other mutated proteins have been linked to the ALS (VAPB, Angiogenin, Alsin, Senataxin, Dynactin, FUS/TDP 43). Many are linked to mRNA maturation processes (reviewed in Ling *et al.*, 2013). New mouse models expressing these mutated proteins have been developed to investigate the disease progression. In 2011, the hexanucleotide repeat expansions located at the locus C9orf72 was linked to a specific form of ALS combined with frontotemporal dementia (DeJesus-Hernandez *et al.*, 2011). This mutation may represent as much as 6% of cases of ALS among Europeans.

2/ Evolution of the disease

Most of the changes observed at the systemic, spinal cord and motor units level are summarized in the Figure 14.

a/ Sequence of behavioral and systemic changes in mSOD1 mice.

The earliest behavioral symptoms were detected at P10. They consisted in a delayed righting reflex and errors in forelimb placement (van Zundert *et al.*, 2008). Changes in gait and running speed do not become evident before P50 (Veldink *et al.*, 2003; Wooley *et al.*, 2005). This age matches the beginning of FF motoneurons degeneration. Muscle strength dropout is therefore more evident in muscles containing a large proportion of FF motor units. In fast-twitch muscles such as the tibialis anterior, the extensor digitorum longus and the medial gastrocnemius muscles, the motor unit isometric forces declined from 40 days of age (Hegedus *et al.*, 2007). This is still 50 days before reported overt symptoms and motoneuron loss. By P90 motor units from all muscles begin to degenerate but again particularly in fast muscles (Hegedus *et al.*, 2007). The first signs of muscle paralysis are visible around P100, followed by complete hindlimb paralysis around P125. At the last stages, the rapidly evolving process of degeneration leads to forelimb paralysis around P135 and death of the animal soon after (Chiu *et al.*, 1995).

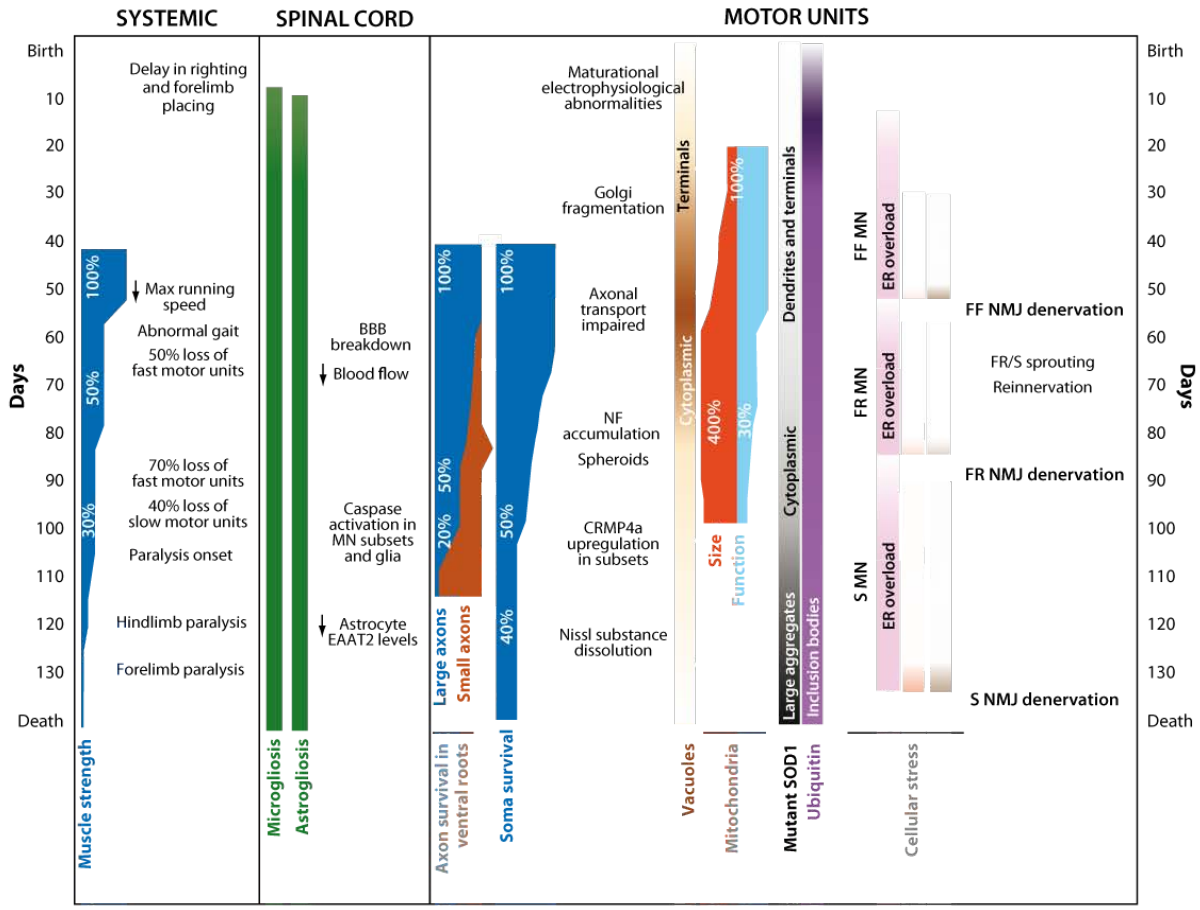

Figure 14: Time course of neurodegeneration in the SOD1G93A mouse model of amyotrophic lateral sclerosis (ALS). The diagram provides an overview of the complex ballet of cellular and molecular mechanisms that lead over six months to the death of this severe model of ALS. Many changes occur before muscle strength is reduced by half, including initial alterations in electrophysiology and behavior followed by ubiquitination and ER stress in susceptible FF motor neurons leading to axonal dieback and microgliosis and astrogliosis in the spinal cord. These are accompanied by subcellular changes such as Golgi fragmentation and mitochondrial swelling. During the following months, these changes become exacerbated and generalized to other motor units, leading to extensive motor neuron loss and muscle paralysis. Indicated stages (scale in days) represent those in the G93A high-expressor line. Some parameters have not been studied at earlier stages, so the indicated dates represent the latest possible onset. The overall layout progresses from systemic and behavioral changes on the left toward molecular and cellular changes in motor units on the right. Adapted from Kanning et al 2010.

b/ Sequence of cellular changes in mSOD1 mice.

Several events precede the muscle denervation. Microgliosis begins around P30 (Saxena *et al.*, 2009) and astrocytosis around P50 (Fischer *et al.*, 2004). However the time at which astrocytes and microglia begin to emit toxic factors susceptible to affect motoneurons remains unknown. Rupture of the blood brain barrier and a

reduction of blood flow occur around P60 (Zhong et al. 2008) but reduction in capillary length is detected far earlier (from P7, see Yoshikawa *et al.*, 2009).
Although other cellular types are affected by the disease, most changes concern the motoneurons. Studies on cultured motoneurons revealed a defect in axonal transport (both anterograde and retrograde, (Kieran *et al.*, 2005; De Vos *et al.*, 2007), an increased sensitivity to Fas-ligand (apoptotic pathway, see Raoul *et al.*, 2002) and an impaired mitochondrial function (De Vos *et al.*, 2007). Overall, alteration of specific death pathways and the transport of their effectors are an early effect of expression of mSOD1. In neonatal motoneurons, abnormal microvacuoles and swollen mitochondria were observed in the cytoplasm at P14 (Bendotti *et al.*, 2001). Additionally, vacuolization of the mitochondria in the axon terminals (Gould *et al.*, 2006), fragmentation of the Golgi apparatus a P30 (Mourelatos *et al.*, 1996) and accumulation of ubiquitin (Vlug *et al.*, 2005; Saxena *et al.*, 2009) were also reported in young mouse motoneurons prior to any decrease in muscle strength or innervation.

During early adulthood (P50-P90) the impairment of retrograde (Ligon *et al.*, 2005) and anterograde (Zhang *et al.*, 1997; Pun *et al.*, 2006) transports in motoneurons leads to the accumulation of neurofilaments (Tu *et al.*, 1996). In parallel swelling of the endoplasmic reticulum, mitochondria and cytoplasm continues (Kong & Xu, 1998) (Kong & Xu 1998, Martin et al. 2007) as well as a deficiency in mitochondrial function (Martin *et al.*, 2007). The alteration of motoneuron axons and terminals likely elicits the impairment and retraction of the synapses. Indeed, during the early adulthood (P50 and above), the ALS progression has been initially characterized by a progressive degeneration of NMJ, denervation and reinnervation of motor endplates through a process of axonal dieback and compensatory sprouting (Schaefer *et al.*, 2005). Similarly motoneurons axon collaterals projecting to Renshaw cells degenerate from P60 (Wootz *et al.*, 2013). VACHT immunoreactive boutons opposed to Renshaw cells presented a ring-like appearance with little or no reactivity in the center instead of the regular filled circle shape. In this study, VAChT-IR displacement was due to swollen mitochondria, degenerated structures or neurofilaments accumulation located in the motoneurons axon terminals. This strengthens the link between molecular defects and changes of the motoneurons projections.

During the late stages of the disease, after P100 when the paralysis becomes obvious the molecular modifications include alterations of the ubiquitin proteasome system (Cheroni *et al.*, 2009), ubiquitin/SOD1 aggregates in the cytoplasm (Sumi *et al.*, 2006; Kato, 2008) and dissolution of the Nissl substance in surviving motoneurons (Martin *et al.*, 2007). Late stages alterations are particularly difficult to interpret, since it is hard to separate what is causing the disease from adaptative strategies adopted by the cell. Most changes mentioned here are not detected in all motoneurons simultaneously but rather in a progressive way reflecting differential susceptibility to the disease of the different motoneuron subtypes. For example, vacuolization and swelling of mitochondria can be detected in the most vulnerable motoneurons (FF motoneurons) as early as P14 (Bendotti *et al.*, 2001; Yoshikawa *et al.*, 2009).

c/ Sequence of electrophysiological and morphological changes in the SOD1 mouse motoneurons

Unless specified otherwise, all results presented here come from spinal motoneurons recordings between P0 and P10 in the SOD1 G93A high expressor line mouse model.

i/ Morphological and passive properties

In neonatal mice, Bories *et al.* (2007) and Quinlan *et al.* (2011) found a decrease in the input resistance. However in another study the input resistance remained stable (Pambo-Pambo *et al.*, 2009). Another crucial property is the membrane resting potential that hyperpolarizes after birth (Quinlan *et al.*, 2011). It remains stable according to some studies (Bories *et al.*, 2007; Quinlan *et al.*, 2011) but decreases in Pambo-Pambo *et al.* (2009). However no changes in the passive properties (input resistance, membrane resting potential) could be detected in cultured cell preparations (Kuo *et al.*, 2004) or hypoglossal motoneurons (van Zundert *et al.*, 2008). In order to look for a morphological correlate to the modification of the input resistance many studies intracellularly filled the recorded motoneurons and reconstructed them At the embryonic age of E17.5 Martin *et al.* (2013) found an increase in motoneuron resistance due to a shortening of the terminal dendritic segments. The group of Durand found that at P3-P4 motoneurons exhibited longer terminal segments (Filipchuk & Durand, 2012). Later at P7-P8 the motoneurons

displayed an over-branching starting at 100 µm from the soma. However the authors did not correlate these modifications with any electrical properties. Moreover the analysis was conducted on small groups of reconstructed motoneurons (only 3 motoneurons WT at P3-P4) and may require repetition. In hypoglossal motoneurons, an early pruning of dendrites was detected at P4 (van Zundert *et al.*, 2008) which contrasts with the overbranching seen in spinal motoneurons. New results from my lab indicate that adults SOD1 motoneurons input conductance increases (Delestrée *et al.*, SfN 2012). In any case new studies of the motoneurons passive properties in the neonate need to be undertaken in order to clarify the situation.

ii/ Active properties

Active properties such as the persistent inward currents (PICs) shape the output of the motoneurons (Button *et al.*, 2006). The F-I curve embodies most characteristics of the motoneuron output (rheobase, gain, hysteresis etc). Most studies agreed on an increase in Na^+ and Ca^{2+} PIC (Kuo *et al.*, 2004; Kuo *et al.*, 2005; van Zundert *et al.*, 2008; Pambo-Pambo *et al.*, 2009; Quinlan *et al.*, 2011). However Pambo-Pambo *et al.* (Pambo-Pambo *et al.*, 2009) concluded to a decrease in PIC density. The evolution of the shape of the action potential was similarly controversial. While normal spike development leads to a narrowing of the spike (Quinlan *et al.*, 2011), it was found to be slowed down (van Zundert *et al.*, 2008; Pambo-Pambo *et al.*, 2009) sped up (Quinlan *et al.*, 2011) or unchanged (Bories *et al.*, 2007) depending on the study. Similarly, the gain of the mutated F-I curves were sometimes increased (Kuo *et al.*, 2004), sometimes decreased (Pambo-Pambo *et al.*, 2009) or sometimes unchanged (Bories *et al.*, 2007; Quinlan *et al.*, 2011).

iii/ Synaptic inputs

Another obvious way to induce excitotoxicity is to increase the motoneuron excitation while its intrinsic excitability remains intact. Hyper-excitation requires a modification of the synaptic input and a shift of the inhibition/excitation balance toward the second. Van Zundert *et al.* (2008) reported an enhanced frequency of spontaneous excitatory and inhibitory transmission in hypoglossal motoneurons. The analysis of the inhibitory inputs in a dissociated motoneuron culture preparation showed that the glycinergic but not the GABAergic transmission was impaired (Chang & Martin, 2011). Glycine-evoked current density was significantly smaller as well as the

averaged current densities of spontaneous glycinergic miniature IPSCs (mIPSCs). The reduced transmission likely originated from the downregulation of Glycine receptor mRNA expression and corresponding decrease in surface postsynaptic Glycine receptor. So far this result has not been reproduced in any acute spinal cord preparation.

3/ excitotoxic hypothesis and other theories

The numerous observations summarized above and others have led scientists to draw many hypotheses regarding the origin of the disease. Ilieva *et al.* (2009) recapitulated the different hypothesis explaining the origin of the disease in mSOD1 mice (Figure 15):

- mishandling of glutamate resulting in excitotoxicity
- ER stress
- Proteasome inhibition
- Damages in mitochondria
- Aberrant secretion of mSOD1 causing extracellular toxicity
- Extracellular superoxide activity
- Axonal disorganization and disrupted transport
- Microhemorrhages of spinal capillaries

These hypotheses are not exclusive and several parallel processes may be required to lead to specific motoneuron degeneration. We must keep in mind that, so far the mutant-driven toxic mechanisms that drives the disease remain elusive. Although the SOD1 mutations have been known since 1993 (Rosen *et al.*, 1993) no consensus has emerged regarding their toxicity. Proper assessment of the chain of events leading to the motoneuron degeneration has been hindered by the many alterations in the cell chemistry that are not directly involved in the disease development but are rather epiphenomena. I will detail the excitotoxic hypothesis as it is the one the appears most promising and can be easily tackled with using electrophysiology

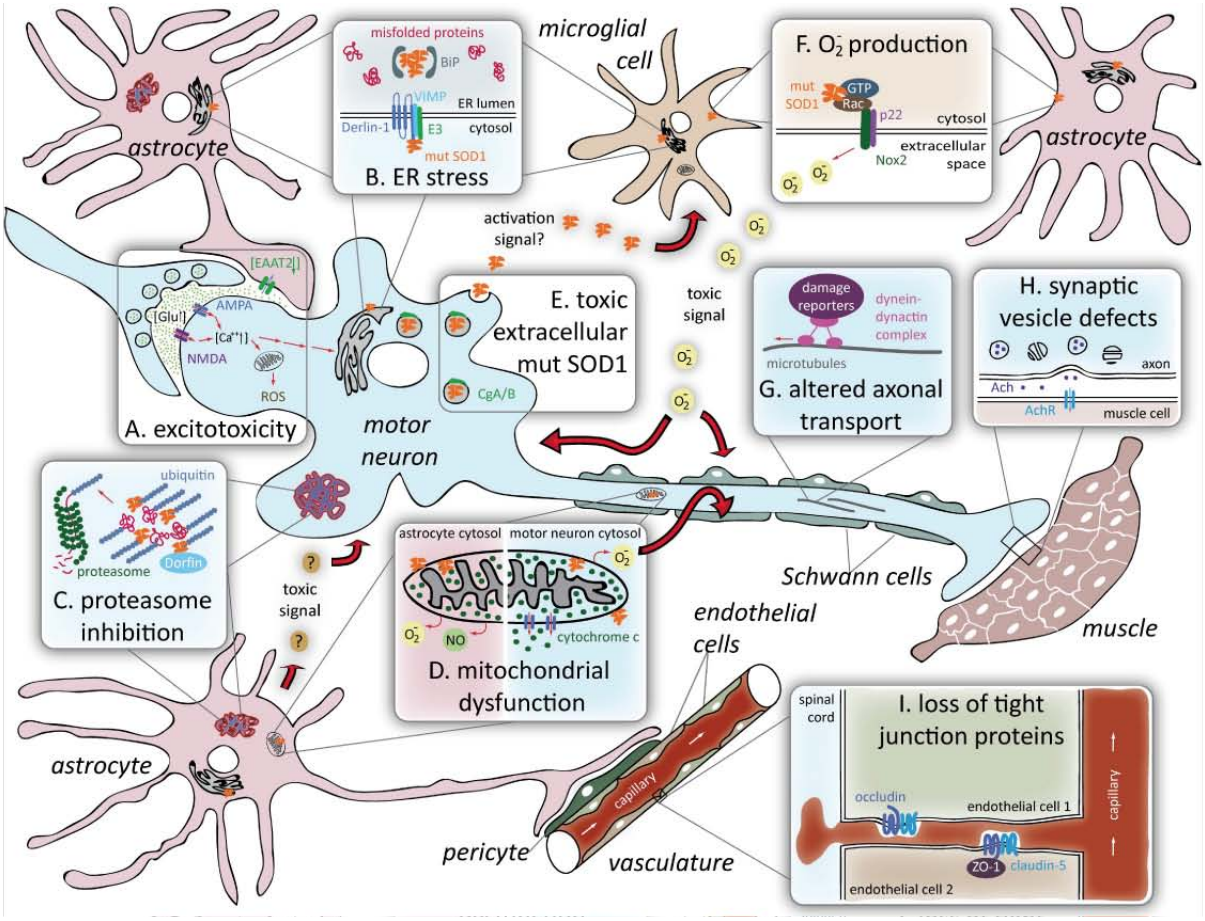

Figure 15: Proposed mechanisms of toxicity in SOD1-mediated ALS. (**A**) Excitotoxicity is the hyperactivation of motor neurons resulting from failure to rapidly remove neurotransmitter glutamate from synapses due to deficiency in the glutamate transporter EAAT2 in the neighboring astrocytes. (**B**) ER stress is induced by abnormal interactions of mutant SOD1 with ER proteins (see text for details). (**C**) Proteasome inhibition due to "overload" of the proteasome degradation pathway with ubiquitinated misfolded protein aggregates may damage astrocytes and motor neurons. (**D**) Mitochondrial dysfunction mediated by mutant SOD1 deposition on the mitochondrial membrane provokes release of cytochrome c in motor neurons, whereas in astrocytes it leads to nitro oxidative stress. (**E**) Toxic extracellular mutant SOD1 is secreted from motor neurons and astrocytes (not depicted) after interaction with components of neurosecretory vesicles. (**F**) Superoxide production from microglia or astrocytes can damage neighboring motor neurons. (**G**) Altered axonal transport including an increase in retrogradely transported stress-related proteins was reported in mutant SOD1-expressing motor neurons. (**H**) Synaptic vesicle defects such as stalling and loss from distal synapse in vulnerable motor neurons is an early event in ALS. (**I**) Loss of tight junction proteins within capillary endothelial cells results in the disruption of the blood–spinal cord barrier and the occurrence of microhemorrhages within the spinal cord well before disease onset. Adapted from Ilieva et al 2009.

Excitotoxicity is due to an excessive entry of calcium in the cell. It is one of the main hypothesis to explain the motoneuron degeneration given that motoneurons are known to have low level of calcium buffer (Lips & Keller, 1998). Many events leading to excitotoxicity have been referenced both in familial and sporadic ALS. The astrocyte glutamate transporter EAAT2 was proved deficient (Rothstein *et al.*, 1995;

Bruijn *et al.*, 1997; Howland *et al.*, 2002; Yang *et al.*, 2009). This could lead to a failure to rapidly recapture glutamate from the synaptic cleft and lead to hyper-excitation. The intrinsic hyper-excitability, defined as a lowering of the recruitment threshold and an increase of the spiking frequency, could elicit an increase in calcium entry and therefore possibly the death of the motoneurons. Whether the excitotoxicity is the main cause of the degeneration or not, we must keep in mind that the validation of any hypothesis should also explain the selective neuronal death when the mutation is ubiquitously expressed?

4/ Differential vulnerability of the motoneurons to the disease

a/ Subtype-Specific Differences in Disease Susceptibility in mSOD1 Motoneurons

Numerous observations revealed the disease did not similarly affect the motoneurons within a single motor pool. Thus the analysis of the ventral root reported a preferential loss of large caliber axons (Kong & Xu, 1998; Fischer *et al.*, 2004). Careful observation of muscle innervation showed a complete synchronous loss of FF terminals to IIB fibers in the triceps surae at P50 (Frey *et al.*, 2000) followed by an asynchronous dieback of FR motor units (Pun *et al.* 2006) whereas S motor units (and probably γ-motoneurons) remained little affected until the last stages (Pun *et al.*, 2006). Additionally 90% of the motoneurons expressing CGRP (fast motoneurons marker) died for only 50% of the total motoneuron number (Kong & Xu, 1998; Fischer *et al.*, 2004). Hegedus *et al.* (Hegedus *et al.*, 2007) confirmed the sequential loss of motoneurons from FF to S based on electrophysiological studies and fiber type analysis (Figure 16 left panel). Additionaly there could be a possible switch from FF to FR type prior to FF motoneurons death (Kieran *et al.*, 2005; Hegedus *et al.*, 2008; Gordon *et al.*, 2010). We must however keep in mind that the apparent resistance of FR and S motoneurons might reflect a higher sprouting capacity to reinnervate new targets lacking their FF innervation (Duchen & Tonge, 1973; Frey *et al.*, 2000). In human, EMGs showed that denervation precede motoneurons loss (Fischer *et al.*, 2004) and twitch force of fast motor units is affected earlier in patients with sporadic ALS (Dengler *et al.*, 1990). Therefore the few available correlates on human support results of the mouse models and marked differential vulnerability of different motor neuron subtypes is likely a feature common to all forms of ALS.

At the cellular level, fast axon terminals exhibit marks of stress (Wootz *et al.*, 2004; Kieran *et al.*, 2005; Kikuchi *et al.*, 2006; Atkin *et al.*, 2008), stalling synaptic vesicles when slow terminals display none of these modifications (Figure 16 right panel). Additionally, the terminal Schwann cells surrounding the NMJs of fast terminals over-express the semaphorin 3A (Sema3A) protein compared to the Schwann cells surrounding slow terminals (De Winter et al. 2006). In muscles Sema3A is only expressed by terminal Schwann cells and act as a repulsive protein, suggesting that localized over-expression of Sema3A in a subset of fast fibers could participate in the FF motor unit degeneration. Changes in the expression of other proteins such as reticulon-4A (Jokic *et al.*, 2006), galectin-1 (Kato *et al.*, 2001) and N-terminal fragment of amyloid precursor (Nikolaev *et al.*, 2009) may also be involve in the sprouting, pruning or dieback mechanisms that take place during the ALS.

b/ Pool-Specific resistance to neuro-degeneration in ALS

Motoneurons from different motor pool present also differential vulnerability to the ALS with some motoneuron pools completely oblivious to the disease. Although all voluntary movement is lost in late-stage ALS, clinical studies showed that the ocular movement and voluntary control of eliminative functions remain unimpaired until terminal stages (Mitsumoto *et al.*, 2006). The motor pool controlling these muscles are the abducens, trochlear and oculomotor nuclei located in the midbrain/hindbrain, and by Onuf's nucleus at the level of the lumbosacral spinal cord. The clinical observations were later confirmed by post-mortem analysis revealing that the resistant motor pools were virtually intact (Schroder & Reske-Nielsen, 1984; Gizzi *et al.*, 1992; Mannen, 2000; Kaminski *et al.*, 2002). This was reproduced in mouse model for abducens, trochlear and oculomotor motor pools (Ferrucci *et al.*, 2010) and Onuf's motor pool (Hamson *et al.*, 2002). So far the molecular differences between resistant and sensitive motor pool remain elusive. Although level of calcium-buffering proteins such as calbindin-D28K and parvalbumin was reported to be higher in SOD1 mouse model (Alexianu *et al.*, 1994; Obal *et al.*, 2006), the overexpression of parvalbumin in motoneurons did not yield to any lifespan improvement (Beers *et al.*, 2001).

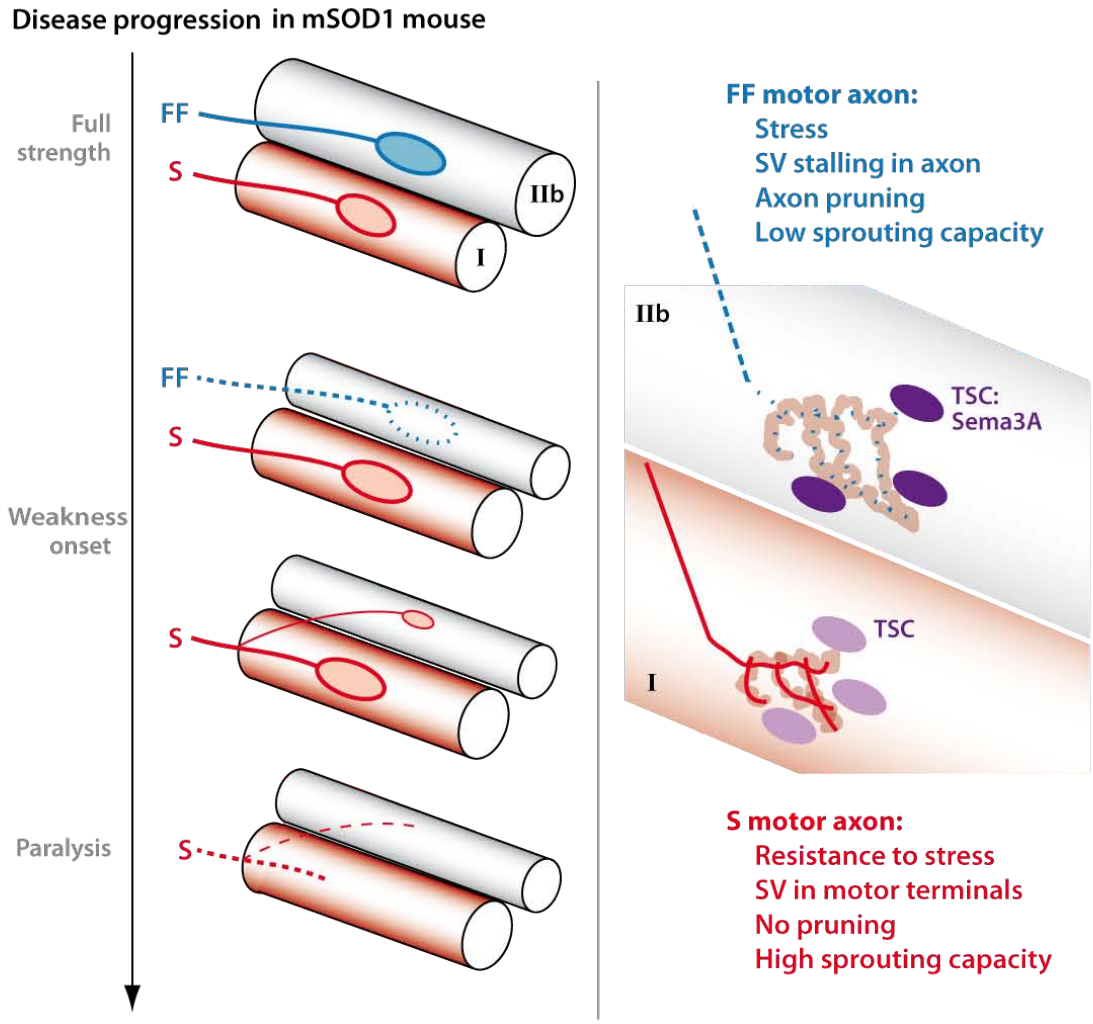

Figure 16: Neuromuscular junction phenotypes in fast-fatigable (FF) and slow (S) motor units in mutant SOD1 mice. Left panel: In healthy adult mice, although there is a limited degree of synaptic remodeling, slow Type I and FF Type IIb/x fibers remain stably innervated by S and FF motor neurons, respectively. During the presymptomatic period in SOD1G93A mice, there is selective dieback of FF motor axons. However, denervated endplates can, for a period, be reinnervated by axonal regrowth or sprouting from either FR or S motor neurons (only S shown for simplicity). At late stages, even S axons die back. Right panel: Differences between FF and S neuromuscular junctions and terminal axons at late presymptomatic stages. In addition to the indicated axonal characteristics, terminal Schwann cells at FF NMJs express higher levels of Sema3A. SV, synaptic vesicles.

Conclusion

As for many neurodegenerative diseases the major following questions are still debated. What are the mutant-driven toxic mechanisms that trigger the degenerescence? What explanation is there for the selective neuronal death from a ubiquitously expressed mutant? In this chapter we presented results obtained mostly

while studying the high-expressor line SOD1 G93A mutation. New mouse models (FUS or TDP43 mice) are becoming readily accessible and many observations such as the differential motoneuron vulnerability concur. Thus, although the use of mouse models may seem controversial in a disease of such complex etiology the multiplication of different models will eventually allow pinpointing the common alterations in the motoneurons machinery leading to degeneration and death. Alternatively other studies focus on improving the motoneuron resistance to the disease rather than understanding it. One possibility would be to increase the expression level of the motoneuron survival protein (Veldink *et al.*, 2005) or to express the correct amount of wild-type SOD1 using viral injection.

Chapter IV: Electrical and morphological properties of spinal motoneurons are differentially affected depending upon their firing pattern in SOD1 G93A neonatal mice

1/ Introduction

As reviewed in the previous chapter, several alterations of the motoneurons electrical and morphological properties have been reported in the SOD1 G93A neonatal mice (mSOD1). Most studies on embryonic motoneurons agreed on the hyper-excitability of these cells (Pieri *et al.*, 2003; Kuo *et al.*, 2005; Martin *et al.*, 2013). The result of neonatal motoneurons are however somewhat conflictual and not always coherent with the excitotoxicity hypothesis. Even though van Zundert *et al.* (2008) or Kuo *et al.* (2005) reported hyper-excitability, Bories *et al.* (Bories *et al.*, 2007) found the motoneurons hypo-excitable and Pambo-Pambo (2009) saw no changes while Quinlan *et al.* (2011) found a homeostatic adjustment of the motoneurons. The electrical properties affected are even more heterogenous between the studies. Concerning the morphology, over-branching was reported in neonatal spinal motoneurons (Amendola & Durand, 2008; Elbasiouny *et al.*, 2010). Conversely other studies reported early pruning of the dendrites in neonatal hypoglossal motoneurons (van Zundert *et al.*, 2008) as well as shortening of the dendrites terminal segment of embryonic spinal motoneurons (Martin *et al.*, 2013).

One factor that has not been taken into account so far is that motoneurons, even in neonatal animals, do constitute a heterogeneous population. They innervate different muscle fiber types and also display different patterns of discharge underlied by different panoplies of currents (see chapter II). This mirrors the known heterogeneous vulnerability between fast and slow motoneurons observed in the adult (Pun *et al.*, 2006; Hegedus *et al.*, 2007). Therefore we posited that the previous contradictory results originate from the ill-comparison between heterogenous population differentially affected by the disease. In other words, the heterogeneous vulnerability raises the possibility that, similarly to what happens in the adult, the sub-

types found among the spinal motoneuron population are not affected in the same way by the SOD1 G93A mutation. Is it possible to identify subsets of motoneurons differentially affected by the mutation?

2/ Results

mSOD1 spinal motoneurons divide between delayed and immediate firing motoneurons in similar proportions than WT motoneurons during the second post-natal week (Article 2 Figure 1). Consequently, I conducted the analysis comparing the four following groups: WT delayed firing motoneurons, mSOD1 delayed firing motoneurons, WT immediate firing motoneurons and mSOD1 immediate firing motoneurons. Primarily, I observed that the two types of mSOD1 motoneurons had, on average, different input conducatnces and threshold currents. This was similar to the WT delayed and immediate firing motoneurons. These properties include the input conductance, the threshold current during square pulses, the recruitment current during slow ramps and the voltage threshold (Article 2 table 1, article 2 figure 2). Type-by-type comparison is therefore relevant and was pursued along the rest of the article. Then I compared the relationship between input conductance and threshold current. WT and mSOD1 delayed motoneurons followed similar relationship (Article 2 figure 2A1). However for mSOD1 immediate firing motoneurons the relationship had a much smaller gain than for the WT immediate firing motoneurons (Article 2 figure 3A2). Consequently the threshold and recruitment currents were significantly smaller for mSOD1 immediate firing motoneurons than for their WT counterparts (Article 2 table 1). I then carefully analyzed the voltage-spiking thresholds and found that it was more hyperpolarized by 5 mV in average in mSOD1 immediate firing motoneurons compare to to WT immediate firing motoneurons. The lower voltage-spiking threshold likely accounts for part of the decrease in threshold and recruitment currents. Overall, this indicates that the immediate firing motoneurons, but not the delayed firing ones, are more excitable in the mSOD1 mice than in the WT mice during the second post-natal week.

I also analyzed and compared the repartition of F-I curves types between the four groups. F-I curves were classified in 3 types (Article 2 figure 3). Type A comprises

ramps producing a linear F-I curve with no hysteresis. Type B comprises ramps which F-I curves presented a clockwise hysteresis (onset for lower current than the offset). Type C comprises curves exhibiting lower offset than onset. F-I curve type distribution was similar when comparing mSOD and WT immediate firing motoneurons in one side and mSOD1 and WT delayed firing motoneurons in the other side (Article 2 figure 3). Therefore no change seems to take place in the firing pattern of mSOD1 motoneurons.

Controversial reports concerning the action potentials led me to analyse them type by type as well. Action potentials of delayed firing motoneurons are narrower and their AHPs are accordingly shorter than in immediate firing motoneurons (Article 2 table 3 and figure 4). This holds true both in WT and mSOD1 mice. No effect of the mutation could be observed in the shape of the action potential and its AHP either in delayed or immediate firing motoneurons (Article 2 table 3).

The last part of this work compares the morphology of reconstructed motoneurons (Article 2 figure 5). As previously reported in this thesis delayed firing motoneurons overbranch compared to immediate firing motoneurons (Article 2 figure 5 and table 3). This is also the case between mSOD1 delayed and immediate firing motoneurons (Article 2 figure 5 and table 3). When comparing populations presenting the same discharge patterns we observed that most mSOD1 delayed firing motoneurons display a similar dendritic tree topology compared to the WT delayed firing motoneurons (Article 2 figure 6A1 and table 3). Only one out of the 15 reconstructed motoneurons overbranches. This motoneuron was excluded from the subsequent analysis.
The mSOD1 delayed firing motoneurons exhibited a total dendritic length 11% longer (Article 2 table 3) than for the WT. This was in accordance with the dendritic path trajectories and terminal segment being 10% longer (Article 2 figure 6A1). Overall, dendrites of delayed firing motoneurons probably endure a 10% elongation. Regarding the immediate firing motoneurons their average total dendritic length is 35% smaller (Article 2 figure 6A2 and table 3) than the WT while the number of branching points remains stable. Further analysis revealed that the dendritic paths trajectories was reduced also by 35% (Article 2 table 3) as well as the length of the terminals segment. These observations concur and allow us to conclude that the

dendrites of mSOD1 immediate firing motoneurons are in average about a third smaller than the dendrites of the WT ones. The dendrites of delayed motoneurons are therefore slightly longer whereas those of the immediate firing one are notably shorten.

3/ Conclusion

Comparison of motoneurons presenting the same discharge patterns yields to the proper identification of type selective alterations of the motoneurons properties during the ALS. At this early stage, both motoneurons populations are affected by the mutation already. Immediate firing motoneurons are hyperexcitable partly because of their lower voltage-spiking threshold. The dendritic tree is shrunk by a third but retains the same topology. Regarding the delayed firing motoneurons, they present no changes in their electrophysiological properties. Their morphology is similar despite of a slight elongation of the dendritic tree.

Article 2

Only spinal motoneurons that display the “immediate firing” profile are hyperexcitable in SOD1 G93A neonatal mice

Felix Leroy, Boris Lamotte d’Incamps and Daniel Zytnicki
Laboratoire de Neurophysique et Physiologie, Université Paris Descartes, Centre National de la Recherche Scientifique (UMR 8119), 45 rue des Saints-Pères, 75006 Paris, France

Abbreviated title:
Immediate firing MNs are hyperexcitable in mSOD1 neonatals

Key words: spinal motoneurones, electrical properties, ALS

Corresponding author: Daniel Zytnicki
Laboratoire de Neurophysique et Physiologie, UMR 8119
Université Paris Descartes, UMR 8119, 45 rue des Saints-Pères, 75006 Paris, France e-mail: Daniel.Zytnicki@parisdescartes.fr

Table of Contents category:
Neuroscience – cellular/molecular

Acknowledgements

The authors wish to thank Dr. Marin Manuel for helpful comments and careful scrutinizing of the manuscript and Ms. Rebecca Manuel for mouse breeding and genotyping. Financial supports provided by the Agence Nationale pour la Recherche (HYPER-MND, ANR-2010-BLAN-1429-01), the NIH-NINDS (R01NS077863) and the Thierry Latran Fundation (OHEX Project) are gratefully acknowledged. Felix Leroy is recipient of a “Contrat Doctoral” from the Ecole Normale Supérieure, Cachan.

Abstract

Numerous electrical and geometrical abnormalities have been observed in spinal motoneurons of mSOD1 mice during the second post-natal week but the results were somehow contradictory. However, we have shown that, at this age, the population of spinal motoneurons is heterogeneous. In neonatals, spinal motoneurons exhibit two distinct firing modes. In most of them the discharge in response to a liminal pulse of current is delayed (delayed firing pattern) whereas for other motoneurons the discharge starts at the onset of the pulse (immediate firing pattern). The present work aims at investigating whether the immediate and delayed firing motoneurons are equally affected by the SOD1 mutation. We show that this is not the case. The delayed firing motoneurons have a larger input conductance, a higher rheobase, a narrower action potential, a shorter AHP and a more complex dendritic arbor than the immediate firing motoneurons in both WT and mSOD1 mice. However, we found that the SOD1 mutation induced a decrease in the rheobase and a hyperpolarization of the voltage threshold only in the immediate firing motoneurons, thereby making them more excitable than in WT mice. Furthermore the dendrites of the immediate firing motoneurons are substantially shorter (about 35%) in the mSOD1 animals than in the WT animals. In sharp contrast, the excitability of the delayed firing motoneurons is unchanged and the dendritic tree is nearly unaffected (the dendrites only undergo a 10% elongation).

Introduction

Several studies revealed early alterations in the electrical and geometrical properties of spinal motoneurons of embryonic and SOD1 G93A neonatal mice, a standard model of Amyotrophic Lateral Sclerosis. Some motoneurons from embryos recorded in culture (Pieri *et al.*, 2003) (Kuo *et al.*, 2005) are hyperexcitable. They are recruited at lower current and display higher F-I gain than in WT mice. Recently Martin *et al.* (2013) found, in an *in vitro*

preparation of embryonic cord, that motoneurons are also hyperexcitable but this was due to an increase in the motoneuron input resistance, leading to a decrease of their rheobase. This change in input resistance was attributed to a reduction in the dendritic length. If all studies pointed out to a hyperexcitable state in embryos, the results were somehow contradictory in neonatal animals. Hypoglossal motoneurons of neonatal mice were found to be hyperexcitable (the F-I gain is increased) and an early pruning of dendrites was detected (van Zundert *et al.*, 2008). On the other hand, Pambo-Pambo *et al.* (2009) did not observe any change in input resistance, rheobase, or stationary gain of spinal motoneurons suggesting that their excitability was unchanged. In sharp contrast, spinal motoneurons were found to be hypoexcitable in Bories *et al.* (2007) as shown by a decrease in input conductance and F-I gain. Quinlan *et al.* (2011) found that the excitability of spinal motoneurons was homeostatically maintained despite an increase in their input conductance (recruitment current and F-I gain unchanged). This increase in input conductance was partly accounted for by an over-branching of the dendritic tree (Amendola & Durand, 2008; Elbasiouny *et al.*, 2010). Most studies agreed on an increase in sodium and persistent inward currents (PICs, (Kuo *et al.*, 2004; Kuo *et al.*, 2005; van Zundert *et al.*, 2008; Pambo-Pambo *et al.*, 2009; Quinlan *et al.*, 2011). The evolution of the shape of the action potential was also controversial. In mSOD1 mice it was found to be wider (Pambo-Pambo *et al.*, 2009), narrower (Quinlan *et al.*, 2011) or unchanged (Bories *et al.*, 2007) than in WT mice depending on the study.

These discrepancies might be due to the location of the mutation on the SOD1 gene (G93A or G83R), the number of transgenes (high or low), the preparation that differ from one work to another, or other factors. One factor that has not been taken into account so far is that the population of spinal motoneurons, even in neonatal animals, is intrinsically heterogeneous. They innervate different types of muscle fibers but also display different patterns of discharge underlied by different panoplies of currents. Indeed, the firing behavior of motoneurons is heterogeneous during the second postnatal week as revealed by patch-clamp recordings in slices (Russier *et al.*, 2003; Pambo-Pambo *et al.*, 2009). In P1-P13 rats, most abducens motoneurons displayed a bursting pattern with a frequency adaptation in response to a current pulse whereas the discharge of other motoneurons is delayed and displayed a progressive acceleration of the frequency (Russier *et al.*, 2003). Similarly, two modes of discharge initiation have also been observed in mouse spinal motoneurons at P6-P10 (Pambo-Pambo *et al.*, 2009). For liminal current pulses, the discharge starts at the current onset in some motoneurons (immediate firing pattern) but it is delayed in others (delayed firing pattern). In a previous work we identified the ionic currents that underlie the delayed firing pattern and we showed that it is caused by a combination of an A-like potassium

current that acts on a short time scale and of a slowly inactivating potassium current that acts to delay the discharge on a much longer time scale (Leroy *et al.*, 2012). These two potassium currents contribute to the recruitment threshold and shape the F-I function of the delayed firing motoneurons.

The present work aims at investigating whether immediate and delayed motoneurons are equally affected by the SOD1 mutation in neonatal mice. We show that this is not the case: we found that only the immediate firing motoneurons are hyperexcitable because of a more hyperpolarized voltage threshold for spiking. Moreover, the length of their distal dendrites is reduced by about 35%. In sharp contrast, the excitability of the delayed firing motoneurons is unchanged and the dendritic tree is nearly unaffected (the dendrites only undergo a 10% elongation).

Materials and Methods

Animals and slice preparation

The experiments were performed in accordance with French legislation and were approved by Paris Descartes University ethics committee. Six to ten days old B6.Cg-Tg(SOD1-G93A)1Gur/J and their non-transgenic littermates of either sex were used (JAX reference 004435, The Jackson Laboratory, Bar Harbor, ME, USA). Genotyping was done following the protocol given by the Jackson Laboratory. Slices were prepared as described by Lamotte d'Incamps *et al.* (Lamotte d'Incamps *et al.*, 2012). The slices were transferred into artificial cerebrospinal fluid (ACSF) containing (in mM): NaCl 130, KCl 2.5, $CaCl_2$ 2, $MgCl_2$ 1, NaH_2PO_4 1, $NaHCO_3$ 26, glucose 25, ascorbic acid 0.4, Na-pyruvate 2, bubbled with 95% O_2 and 5% CO_2 (pH 7.4).

Electrophysiology

The recording chamber was continuously perfused with ACSF at a rate of 1-2 ml/min, at room temperature. The slices used were those containing a ventral rootlet of sufficient length to be mounted on a suction stimulation electrode, a glass pipette with a tip size adapted to the diameter of the rootlet (40-170 µm) and filled with ACSF. Single biphasic stimulation of the ventral rootlet (1-50 V, 0.1-0.3 ms) was used to elicit antidromic action potential in the recorded cells of the ventral cord. The motoneurons were found in the ventral horn and patched in the whole-cell configuration under visual control using a video-camera (Scientifica, Uckfield, UK). Identification of the cell as motoneuron was based on the recording of an antidromic action potential following stimulation of the ventral root. We retained for analysis motoneurons exhibiting a resting potential equal or below -50 mV, an

overshooting action potential and that could maintain firing during 5 s at least. In addition, since we targeted cells whose soma area was in the range 270 - 1000 μm^2, it is likely that there were alpha motoneurons since their soma sizes were already larger than the gamma motoneurons investigated at P14 by Friese *et al.* (2009).

Patch pipettes had an initial open-tip resistance of 3 to 6 MΩ. The internal solution contained (in mM): K-gluconate 140, KCl 6, HEPES 10, EGTA 1, $CaCl_2$ 0.1, Mg-ATP 4, Na_2GTP 0.3. The pH was adjusted to 7.3 with KOH, and the osmolarity to 285-295 mOsm. An AxoClamp 700B (Molecular Device, Sunnyvale, CA, USA) amplifier was used for data acquisition. Whole-cell recordings were filtered at 3 kHz, digitized at 10 kHz using a CED 1401 and monitored using the Signal 5 software (Cambridge Electronic Design Limited, Cambridge, UK). Bridge resistance compensation was applied in current-clamp mode. Liquid junction potential (15 mV) was corrected offline. Cells were maintained at -80 mV unless specified otherwise.

Intracellular labeling and 3D-reconstruction

For neurobiotin injection, intracellular solution was supplemented with 2% neurobiotin (Vector Labs, Burlingame, CA, USA) and the motoneurons were recorded for at least 30 min to allow diffusion of the dye. After carefully removing the electrode from the cell, the slice was bathed in 0.4% PBS with 4% paraformaldehyde for 1 h. Blocking solution containing 0.25% pork gelatin and 0.3% Triton X100 in PBS was applied for 1h. Slices were incubated overnight at 4°C with streptavidin-Cy3 conjugated antibody diluted at 1/500 in the blocking solution and then mounted with fluoromount. Acquisition was performed on a confocal microscope lsm 510 (Carl Zeiss, Oberkochen, Germany) and the dendritic tree of the motoneuron was reconstructed using Neurolucida software (MBF Bioscience, Williston, VT, USA). Analysis of the dendritic tree included only the radial dendrites that remained in the same plane as the slice and that do not plunge deeper than 50 µm below the surface of the slice. We were able to reconstruct the geometry of these dendrites up to their terminal branches.

Data analysis

Analysis of the recordings was performed using custom programs in Signal 5 (Cambridge Electronic Design Limited, Cambridge, England). Input conductance was the inverse of the slope of the I-V curve obtained by injecting small 500 ms pulses of currents (-100 pA to +20 pA, 30 pA steps repeated 10 times). The *rheobase* was the minimal current required to elicit a discharge in response to a 5 s square pulse (the current was incremented by 50 - 100pA steps). We measured the *voltage spiking threshold* on the first spike of the 5 s pulses as the

voltage for which the first derivative value went over 10 mV/ms. We also measured the *recruitment current* (I_{on}) for which the first action potential was fired during a 0.1 nA/s current ramp (average of 3 trials). Single action potentials were elicited by 1 ms square pulses. Their height, width at half-amplitude and relaxation time constant of their AHP were measured on the average of 30 successive trials. The relaxation time constant of the AHP was determined using a mono-exponential fit. Morphological analysis of labeled motoneurons was conducted with Neurolucida software and summary data was collected in Microsoft Excel (Microsoft, Redmont, WA, USA). We measured the following parameters: *primary dendrites number* (including only the reconstructed dendrites, see above), *branching points number* (number of dendritic bifurcations in the reconstructed dendrites), *total dendritic length* (sum of the length of all reconstructed dendrites), *terminal segment length* and *dendritic paths* (paths realized when starting from the tip of every terminal segment and coming back to the soma). We used two-tailed *Mann-Whitney U tests* to assess the difference between two properties while two-tailed *Fischer exact tests* were used on contingency tables. Data in the tables are expressed as mean ± SD with the range and the number of observations.

Results

The proportion of delayed and immediate motoneurons is similar in mSOD1 and WT mice

The mSOD1 motoneurons display the same two discharge patterns as the WT motoneurons (Figure 1). In the example of Figure 1A1, the mSOD1 motoneuron did not fire at the onset of a 1.2 nA square pulse. Instead the motoneuron depolarized slowly and it started to fire only 3.1 s after the pulse onset when the potential finally reached the voltage threshold for spiking (-52 mV). Once the firing started, the discharge displayed an increasing frequency. This pattern is very similar to the one exhibited by the WT motoneuron shown in Figure 1A2. Most of the mSOD1 motoneurons (31 out of 49, i.e. 63%) exhibit a *delayed firing* pattern at rheobase. This is similar to the 67% of the recorded WT motoneurons (63 out of 94 recorded) found to exhibit the *delayed firing* pattern. The other motoneurons display the so-called *immediate firing* pattern: at rheobase, the motoneuron discharged at the pulse onset without any delay (Figure 1B). The spiking frequency remained constant with little variability. 18 out of the 49 SOD1 motoneurons (i.e. 37%, Figure 1B1) and 31 out of the 94 WT motoneurons (i.e. 33%, Figure 1B2) displayed the immediate firing pattern. The proportion of delayed and immediate motoneurons is not different between mSOD1 and WT mice (Fischer exact test, p=0.54).

The input conductance is unchanged in mSOD1 mice when analysing separately the delayed firing and the immediate firing motoneurons

In both mSOD1 and WT mice, the input conductance is, on average, larger in the delayed firing motoneurons than in the immediate firing ones (Figure 2B, table 1). However, the input conductance of the delayed firing motoneurons is not significantly different in mSOD1 mice and in WT mice. Similarly we do not observe any significant difference in input conductance between the immediate firing motoneurons of mSOD1 mice and the immediate firing motoneurons of WT mice. These results indicate that there is no change in the input conductance in mSOD1 mice when separately comparing the two subpopulations of spinal motoneurons.

The mSOD1 mutation selectively increases the excitability of the immediate firing motoneurons

Despite the unchanged input conductance, the SOD1 mutation increases the excitability of the immediate firing motoneurons but not of the delayed firing ones. A major determinant of the cell excitability is the current that the cell must receive in order to elicit spiking (rheobase). The rheobase is smaller in the immediate firing motoneurons than in the delayed firing motoneurons both in WT mice and in SOD1 mice (Figure 2C, Table 1). However, we found that, in the immediate firing motoneurons, the rheobase is even smaller in mSOD1 mice compared to WT mice (Figure 2C, Table 1). In sharp contrast the rheobase of the delayed firing motoneurons is not affected by the mutation (Figure 2C, Table 1). Figure 2A shows that the rheobase increases with the input conductance. However, in mSOD1 mice, the relationship between the rheobase and the input conductance is affected only in the immediate firing motoneurons. For any given value of input conductance, the rheobase tends to be smaller in the immediate firing motoneuron of mSOD1 mice (Figure 2A2) but not in the delayed firing motoneurons (Figure 2A1). This indicates that the immediate firing motoneurons, but not the delayed firing ones, are more excitable in mSOD1 mice than in WT mice.

The rheobase lowering in the immediate firing motoneurons of mSOD1 mice is partly accounted for by a change in the voltage threshold for spike generation. Indeed, the spike threshold is more hyperpolarized in the immediate firing motoneurons than in the delayed firing ones both in mSOD1 and WT mice (Figure 2D, Table 1). However, in the case of the immediate firing motoneurons, the spike threshold is even more hyperpolarized in mSOD1 mice than in WT mice (Table 1, Figure 1B and Figure 2D). As a consequence, a smaller amount of current is required to reach the voltage threshold for spiking in the immediate firing motoneurons of mSOD1 mice.

Firing behavior is unaffected in mSOD1 motoneurons

The firing behavior of motoneurons was assessed on their responses to slow triangular ramps of currents. The response in the ascending branch is a fairly good approximation of the stationary F-I function, and its comparison with the response to the descending branch allows us to assess the hysteretic properties of the cell. The delayed and the immediate firing motoneurons do not display the same hysteretic profiles (see Leroy *et al.*, 2012 for the WT motoneurons). The response of immediate firing motoneurons is either symmetrical (overlapping frequencies with same recruitment and derecruitment currents) during the ascending and descending ramps (Figure 3 type A) or it is hysteretic with the derecruitment current on the descending branch higher than the recruitment current on the ascending branch (Figure 3 type B). Remarkably, the immediate firing motoneurons display the same proportion of these two profiles in SOD1 and WT mice (9 type A and 8 type B for WT, 6 type A and 10 type B for SOD1, exact Fisher test p=0.3, Figure 3). In sharp contrast, most of the delayed firing motoneurons display a hysteretic response in which the derecruitment current is smaller than the recruitment one (Figure 3 type C). However a few delayed firing motoneurons display the symmetric profile (type A) or the hysteretic profile with derecruitment current larger than the recruitment current (type B). The proportion of these three profiles among the population of delayed firing motoneurons is again the same in SOD1 and in WT mice (6 type A, 6 type B and 39 type C for WT, 4 type A and 3 type B and 23 type C for SOD1, exact Fisher test p=0.9, Figure 3).

Interestingly, the recruitment current during the ascending branch of the delayed firing motoneurons was the same in SOD1 mice than in WT mice (all three profiles during the slow triangular ramps pooled, Table 1). In contrast the recruitment current of the immediate firing motoneurons was smaller in mSOD1 mice than in WT mice (two profiles pooled, table 1). This is in keeping with the differences that we observed in the rheobase measured with long pulses, confirming that the immediate firing motoneurons are more excitable in the mSOD1 mice than in the WT mice (see above).

Action potentials are unaffected in the mSOD1 mice

The delayed firing and the immediate firing motoneurons display differences in the shape of their action potentials. The action potentials are narrower and the duration of their AHPs is shorter in the delayed firing motoneurons compared to the immediate firing motoneurons (see Figure 4 and Table 2). However, the SOD1 mutation has no significant effect on the duration of the action potential and the duration of the AHP in either the delayed or immediate motoneurons (Table 2). Therefore, the shape of the action potential and its after-

hyperpolarization depend on the mode of firing displayed by the motoneuron but they are unaffected in the mSOD1 mice.

The SOD1 mutation affects differentially the dendritic tree of delayed firing and immediate firing motoneurons

In order to investigate the morphological differences between the delayed firing and immediate firing motoneurons, and in order to study whether the morphology is affected by the SOD1 mutation, we filled motoneurons of both types with neurobiotin in WT and mSOD1 mice. We were able to follow and to reconstruct the dendrites that remained in the slice plane (Figure 4). Only these dendrites were considered in the following analysis. In these conditions, the number of primary dendrites (and thereby dendritic trees) per motoneuron is similar in the immediate firing motoneurons and in the delayed firing ones in both WT and SOD1 mice (Table 3). This allows us to make quantitative morphological comparisons. In the examples shown in Figure 5, it is immediately apparent that the dendritic arborization extends much further in the delayed firing motoneuron than in the immediate firing one in both WT (compare Figure 5A and Figure 5B) and mSOD1 mice (compare Figure 5C and Figure 5D). The delayed firing motoneurons in WT mice have more branching points (i.e. a more complex topology) and longer total dendritic length than the immediate firing motoneurons (Table 3).

In mSOD1 mice, the morphology of the dendritic tree is not affected the same way in the delayed vs. immediate firing motoneurons. Figure 6A1 shows the relationship between the number of branching points and the total dendritic length for WT and mSOD1 mice: the more branching points (and therefore branches), the longer the total dendritic length. This relationship largely overlaps for the WT delayed firing motoneurons and most of the mSOD1 delayed firing motoneurons. However, one out of the fifteen investigated mSOD1 motoneuron (black arrowhead in Figure 7A1) displays more branching points and a longer total dendritic length than the largest WT motoneurons. This particular motoneuron thereby displays an overbranching of its dendritic tree. In the 14 other mSOD1 motoneurons, the number of branching points is in the same range as in WT motoneurons (Figure 7A1 and Table 3). Moreover, in these 14 mSOD1 motoneurons the morphometric parameters of the dendritic tree are almost unchanged. The small elongation of the total dendritic length (10% longer in mSOD1 motoneurons compared to WT) is not statistically significant (Figure 3). However, the small elongation of the dendritic paths and the terminal segments (14% and 11% on average, Table 3, the overbranching motoneuron was excluded) reach significativity because of the large sample sizes.

The immediate firing motoneurons undergo more profound changes in mSOD1 mice. Their total dendritic length is 35% smaller in mSOD1 motoneurons despite the fact that they display the same number of branching points as WT motoneurons (Figure 7A2, Table 3). Consistently, the total dendritic lengths and the dendritic paths are shorter (35% on average) in the mSOD1 mice (Figure 7B2, Table 3). The intermediate and terminal segments are shortened in the mSOD1 mice (terminal segments 34% shorter in the mSOD1 mice, Table 3). Altogether, the dendrites of immediate firing motoneurons are substantially shorter in mSOD1 mice than in WT mice.

Discussion

Here we provide evidence that the electrical and morphological alterations of spinal motoneurons in neonatal mSOD1 mice are not the same in immediate vs. delayed motoneurons. Indeed, these two subtypes of motoneurons display, on average, numerous differences in both WT and mSOD1 mice: the delayed firing motoneurons have a larger input conductance, a higher rheobase, a narrower action potential, a shorter AHP but a more complex dendritic tree than the immediate firing motoneurons. However, when comparing separately the delayed firing motoneurons and the immediate firing ones between WT and mSOD1 animals, we found that the mutation affects specifically the immediate firing motoneurons by decreasing the rheobase and hyperpolarizing the voltage threshold for spiking. This shows that these motoneurons are more excitable in mSOD1 mice than in WT mice. Furthermore, the dendritic segments of the immediate firing motoneurons are shorter in mSOD1 animals than in the WT animals. In sharp contrast, the electrical and geometrical properties of the delayed firing motoneurons are quite similar in mSOD1 and WT animals although a slight 10% elongation of the dendrites could be detected.

Immediate vs. delayed firing pattern: a factor not taken into account in ALS research so far

In previous studies in neonatal animals, no distinction was made between the immediate and delayed firing motoneurons and data coming from these two subpopulations were pooled together (Bories *et al.*, 2007; Amendola & Durand, 2008; Pambo-Pambo *et al.*, 2009; Quinlan *et al.*, 2011). However the input conductance, the rheobase, the shape of the action potential and its AHP, and the morphology of the dendritic tree are different in immediate and delayed firing motoneurons. Therefore, average values, standard deviations and all other statistics for each individual property was heavily dependent on the proportion of immediate and delayed firing motoneurons present in the sample. If these proportions differ substantially in the samples from WT and mSOD1 mice, this might obfuscate the conclusions that are raised on

the impact of the disease. In the same line, the delayed firing motoneurons have a larger dendritic tree than the immediate firing ones. One must therefore be careful to sort these two categories of motoneurons when comparing morphological differences between WT and mSOD1 neonatal mice (Amendola & Durand, 2008; Filipchuk & Durand, 2012). We suggest that the discharge pattern-related specific effects have to be been taken into consideration in ALS research.

Origin of the intrinsic hyperexcitability in the immediate firing motoneurons in P6-P10 mSOD1 mice

The reduction in rheobase, which is restricted to the immediate firing motoneurons, indicates that only these motoneurons are hyperexcitable in mSOD1 mice. This occurred despite of the fact that their input conductance was unchanged. The average 5 mV hyperpolarization of the voltage threshold for spiking likely accounts for the decrease in the rheobase. Such a hyperpolarization might arise either from an increase in the sodium current responsible for spiking or a decrease in the delayed rectifier potassium current (Dai *et al.*, 2002). A shift in the activation curves would facilitate the sodium current activation or impede the delayed rectifier potassium current activation (Dai *et al.*, 2002). The increase in sodium persistent inward current observed in the second postnatal week (Quinlan *et al.*, 2011) might also contribute to hyperpolarize the spiking threshold. In sharp contrast, no change in the intrinsic excitability was observed in the motoneurons that exhibit a delayed firing pattern. We previously showed that this type of firing is due to the specific presence in these motoneurons of two potassium currents that act at two time scales: an A-current and a slowly activating and inactivating potassium current (Leroy *et al.*, 2012). It is possible that the presence of these two currents prevent the spiking threshold to be hyperpolarized and thereby the recruitment current to be lowered.

The origin of the hyperexcitability in the immediate firing motoneurons seems to be different from the mechanism at work in late embryonic motoneurons. In the embryonic motoneurons, hyperexcitability is likely to arise from the alterations of their dendritic tree (Martin *et al.*, 2013) see also (van Zundert *et al.*, 2008). Numerical simulations suggested that the shortening of the terminal segments of embryonic spinal motoneurons accounts for the decrease in input conductance and consequently for the decrease in rheobase (Martin *et al.*, 2013). The cause of the shortening of the dendritic tree in embryonic motoneurons is unclear. One possibility is that it results from an increased synaptic activity. Indeed, during a critical developmental period, the morphology of the neuronal dendritic tree depends on the synaptic activity on the dendrites (Spitzer, 2006; Cline & Haas, 2008). It was shown that an increase in the density of synaptic inputs on dendrites might lead to a shortening of the

dendrites (Tripodi *et al.*, 2008). In embryos there is a spontaneous rhythmic activity in the spinal cord (Yvert *et al.*, 2004) but we do not know whether it is increased in mSOD1 mice.

During the postnatal development, the dendritic trees of spinal motoneurons are growing a lot. However, we found that the dendrites of the immediate firing motoneurons in neonatals are substantially shorter (about 35%) in mSOD1 mice than in WT mice. This is reminiscent of embryonic spinal motoneurons in mSOD1 mice (Martin *et al.*, 2013). Contrary to embryonic motoneurons, these morphological changes do not decrease the input conductance. This might be due to the larger overall size of the motoneuron dendritic tree in the second postnatal week, which limits the influence of morphological alterations on the input conductance measured at the soma. Another possibility would be that the dendritic shortening is compensated by a decrease of the specific membrane resistivity. In sharp contrast, we found almost no change (only a slight dendritic elongation) in most of the delayed firing motoneurons. It is unclear why the geometry of the two motoneuron sub-types is differentially affected in the mSOD1 mice.

It is interesting to compare our results in ALS with those obtained in mouse models of the spinal muscular atrophy (SMA), another motoneuron degenerative disease. In neonatal SMA mice, the spinal motoneurons lost their proprioceptive synapses and display a lower rheobase than motoneurons of control mice (Mentis *et al.*, 2011). This indicates an increased excitability. In these animals the hyperexcitability is caused both by a hyperpolarization of the voltage threshold for spiking and an increase of the input conductance (Mentis *et al.*, 2011).

Is the discharge pattern related to specific motoneuron subpopulations?

A link between the discharge properties of the motoneuron and their muscle targets cannot be established in our experimental conditions. However, it is likely that all cells were alpha motoneurons since their soma areas were in majority larger (113 - 998 μm^2) than the soma areas of gamma motoneurons at P14 (Friese *et al.*, 2009). Furthermore, the delayed and immediate firing motoneurons belong to the same, or closely related motor pools since we have frequently encountered the two types in close proximity in the same slice. We showed that the delayed firing motoneurons present, on average, larger input conductances, higher recruitment currents, and shorter AHP. In adults, it is long known that motoneurons innervating fast-contracting motor units (F type) and those innervating slow-contracting motor units (S type) display similar differences in cats (Burke, 1981; Zengel *et al.*, 1985), rats (Beaumont & Gardiner, 2002; Button *et al.*, 2006) and mice (Manuel & Heckman, 2011). Furthermore, F type motoneurons display a larger dendritic tree than S type motoneurons (Burke *et al.*, 1982; Cullheim *et al.*, 1987). One seducing assumption is then that delayed

motoneurons will become F type motoneuron whereas immediate firing motoneurons will become S type. This hypothesis remains however to be experimentally tested.

Excitability of motoneurons and degeneration of motor units in ALS

In mSOD1 mice, the degeneration of neuromuscular junctions does not start before P50 and it has been shown that F type motor units degenerate before the S type motor units (Pun *et al.*, 2006; Hegedus *et al.*, 2008). Recent data shows that none of spinal motoneurons are hyperexcitable in mSOD1 mice prior their neuromuscular junctions start to degenerate (Delestrée *et al.*, SfN 2012). One might therefore question whether intrinsic hyperexcitability is contributing by itself to degeneration (Ilieva *et al.*, 2009). Indeed, it was recently shown that increasing motoneuron excitability has surprisingly the opposite effect: it rather prolongs the animal survival (Saxena *et al.*, 2013). If the immediate firing motoneurons are bound to S type motoneurons, their hyperexcitability in neonates might thereby contribute to their low vulnerability during ALS.

References

Amendola J & Durand J. (2008). Morphological differences between wild-type and transgenic superoxide dismutase 1 lumbar motoneurons in postnatal mice. *The Journal of comparative neurology* **511,** 329-341.

Beaumont E & Gardiner P. (2002). Effects of daily spontaneous running on the electrophysiological properties of hindlimb motoneurones in rats. *J Physiol* **540,** 129-138.

Bories C, Amendola J, Lamotte d'Incamps B & Durand J. (2007). Early electrophysiological abnormalities in lumbar motoneurons in a transgenic mouse model of amyotrophic lateral sclerosis. *The European journal of neuroscience* **25,** 451-459.

Burke RE. (1981). *Motor units: anatomy, physiology, and functional organization*. Am. Physiol. Soc., Bethesda, MD.

Burke RE, Dum RP, Fleshman JW, Glenn LL, Lev-Tov A, O'Donovan MJ & Pinter MJ. (1982). A HRP study of the relation between cell size and motor unit type in cat ankle extensor motoneurons. *The Journal of comparative neurology* **209,** 17-28.

Button DC, Gardiner K, Marqueste T & Gardiner PF. (2006). Frequency-current relationships of rat hindlimb alpha-motoneurones. *J Physiol* **573,** 663-677.

Cline H & Haas K. (2008). The regulation of dendritic arbor development and plasticity by glutamatergic synaptic input: a review of the synaptotrophic hypothesis. *J Physiol* **586,** 1509-1517.

Cullheim S, Fleshman JW, Glenn LL & Burke RE. (1987). Membrane area and dendritic structure in type-identified triceps surae alpha motoneurons. *The Journal of comparative neurology* **255,** 68-81.

Dai Y, Jones KE, Fedirchuk B, McCrea DA & Jordan LM. (2002). A modelling study of locomotion-induced hyperpolarization of voltage threshold in cat lumbar motoneurones. *J Physiol* **544,** 521-536.

Elbasiouny SM, Amendola J, Durand J & Heckman CJ. (2010). Evidence from computer simulations for alterations in the membrane biophysical properties and dendritic processing of synaptic inputs in mutant superoxide dismutase-1 motoneurons. *The Journal of neuroscience : the official journal of the Society for Neuroscience* **30,** 5544-5558.

Filipchuk AA & Durand J. (2012). Postnatal dendritic development in lumbar motoneurons in mutant superoxide dismutase 1 mouse model of amyotrophic lateral sclerosis. *Neuroscience* **209,** 144-154.

Friese A, Kaltschmidt JA, Ladle DR, Sigrist M, Jessell TM & Arber S. (2009). Gamma and alpha motor neurons distinguished by expression of transcription factor Err3. *Proceedings of the National Academy of Sciences of the United States of America* **106,** 13588-13593.

Hegedus J, Putman CT, Tyreman N & Gordon T. (2008). Preferential motor unit loss in the SOD1 G93A transgenic mouse model of amyotrophic lateral sclerosis. *J Physiol* **586,** 3337-3351.

Ilieva H, Polymenidou M & Cleveland DW. (2009). Non-cell autonomous toxicity in neurodegenerative disorders: ALS and beyond. *The Journal of cell biology* **187,** 761-772.

Kuo JJ, Schonewille M, Siddique T, Schults AN, Fu R, Bar PR, Anelli R, Heckman CJ & Kroese AB. (2004). Hyperexcitability of cultured spinal motoneurons from presymptomatic ALS mice. *Journal of neurophysiology* **91,** 571-575.

Kuo JJ, Siddique T, Fu R & Heckman CJ. (2005). Increased persistent Na(+) current and its effect on excitability in motoneurones cultured from mutant SOD1 mice. *J Physiol* **563,** 843-854.

Lamotte d'Incamps B, Krejci E & Ascher P. (2012). Mechanisms shaping the slow nicotinic synaptic current at the motoneuron-renshaw cell synapse. *The Journal of neuroscience : the official journal of the Society for Neuroscience* **32,** 8413-8423.

Lamotte d'Incamps B, Krejci E & Ascher P. (2012). Mechanisms shaping the slow nicotinic synaptic current at the motoneuron-renshaw cell synapse. *The Journal of neuroscience : the official journal of the Society for Neuroscience* **32,** 8413-8423

Leroy F, Lamotte d'Incamps B & Zytnicki D. (2012). Two types of spinal motoneurons in neonatal mice: Delayed and immediate motoneurons. Progr. No. 272.15. *Neuroscience Meeting Planner. New-Orleans, LO: Soc. Neurosci. http://www.sfn.org/am2012/.*

Martin E, Cazenave W, Cattaert D & Branchereau P. (2013). Embryonic alteration of motoneuronal morphology induces hyperexcitability in the mouse model of amyotrophic lateral sclerosis. *Neurobiology of disease* **54,** 116-126.

Mentis GZ, Blivis D, Liu W, Drobac E, Crowder ME, Kong L, Alvarez FJ, Sumner CJ & O'Donovan MJ. (2011). Early functional impairment of sensory-motor connectivity in a mouse model of spinal muscular atrophy. *Neuron* **69,** 453-467.

Pambo-Pambo A, Durand J & Gueritaud JP. (2009). Early excitability changes in lumbar motoneurons of transgenic SOD1G85R and SOD1G(93A-Low) mice. *Journal of neurophysiology* **102,** 3627-3642.

Pieri M, Albo F, Gaetti C, Spalloni A, Bengtson CP, Longone P, Cavalcanti S & Zona C. (2003). Altered excitability of motor neurons in a transgenic mouse model of familial amyotrophic lateral sclerosis. *Neuroscience letters* **351,** 153-156.

Pun S, Santos AF, Saxena S, Xu L & Caroni P. (2006). Selective vulnerability and pruning of phasic motoneuron axons in motoneuron disease alleviated by CNTF. *Nature neuroscience* **9,** 408-419.

Quinlan KA, Schuster JE, Fu R, Siddique T & Heckman CJ. (2011). Altered postnatal maturation of electrical properties in spinal motoneurons in a mouse model of amyotrophic lateral sclerosis. *J Physiol* **589,** 2245-2260.

Russier M, Carlier E, Ankri N, Fronzaroli L & Debanne D. (2003). A-, T-, and H-type currents shape intrinsic firing of developing rat abducens motoneurons. *J Physiol* **549,** 21-36.

Saxena S, Roselli F, Singh K, Leptien K, Julien JP, Gros-Louis F & Caroni P. (2013). Neuroprotection through Excitability and mTOR Required in ALS Motoneurons to Delay Disease and Extend Survival. *Neuron* **80,** 80-96.

Spitzer NC. (2006). Electrical activity in early neuronal development. *Nature* **444,** 707-712.

Tripodi M, Evers JF, Mauss A, Bate M & Landgraf M. (2008). Structural homeostasis: compensatory adjustments of dendritic arbor geometry in response to variations of synaptic input. *PLoS biology* **6,** e260.

van Zundert B, Peuscher MH, Hynynen M, Chen A, Neve RL, Brown RH, Jr., Constantine-Paton M & Bellingham MC. (2008). Neonatal neuronal circuitry shows hyperexcitable disturbance in a mouse model of the adult-onset neurodegenerative disease amyotrophic lateral sclerosis. *The Journal of neuroscience : the official journal of the Society for Neuroscience* **28,** 10864-10874.

Yvert B, Branchereau P & Meyrand P. (2004). Multiple spontaneous rhythmic activity patterns generated by the embryonic mouse spinal cord occur within a specific developmental time window. *Journal of neurophysiology* **91,** 2101-2109.

Zengel JE, Reid SA, Sypert GW & Munson JB. (1985). Membrane electrical properties and prediction of motor-unit type of medial gastrocnemius motoneurons in the cat. *Journal of neurophysiology* **53,** 1323-1344.

Figure Legends

Figure 1: Delayed and immediate firing patterns of discharge are present among WT and SOD1 motoneurons.
A1-2: Responses of mSOD1 **(A1)** and WT **(A2)** delayed firing motoneurons to long lasting pulses (5 seconds) of increasing amplitude. Bottom: injected-current (square pulses), middle: voltage-response and top: instantaneous firing frequency. **B1-2:** Same with SOD1 **(B1)** and WT **(B2)** immediate firing motoneurons.

Figure 2: Only the immediate firing motoneurons recruitment is affected by the SOD1 mutation.
A: Plot of the input conductance as a function of the current threshold for delayed (**A1**) and immediate (**A2**) firing motoneurons. **B-D:** Bar and whisker diagrams of the input conductance (**B**), the rheobase (**C**) and the voltage thresholds (**D**) of the different populations.

Figure 3: Same types of F-I curves in WT and SOD1 motoneurons.
Types A, B and C: For each type, the left panel shows the response to triangular ramp of currents (slope ± 0.1 nA/s, Bottom: injected-current, top: voltage-responses). On the right panel, the instantaneous firing frequency is plotted in function of the injected current during the ascending (black empty squares) and descending (red filled circles) ramps. **F-I curves type repartition within each of the motoneurons population** (pie charts on the bottom right part of the figure)**:** Note that the repartition of the different types of F-I curves is unchanged in mutants

Figure 4: Delayed and immediate firing motoneurons exhibit different action potentials.
A1-2: Responses of delayed (black line) and immediate (grey line) firing WT motoneurons to a square pulse of current (1-10 nA, 1 ms duration). Dashed lines are the exponential fits of the AHP relaxation. **B1-2:** Same for SOD1 motoneurons.

Figure 5: Reconstructed motoneurons of each population.
Each motoneuron was injected with 2% neurobiotin and revealed using a Cy3-streptavidin conjugated antibody. Reconstructed dendritic tree includes only the radial dendrites that remain in the same plane as the slice and that do not go deeper than 50 µm below the surface of the slice. The axon was not reconstructed. Reconstructions are projected in the section plane. We were able to reconstruct the geometry of these dendrites up to their terminal branches. **A:** WT delayed firing motoneuron. **B:** WT immediate firing motoneuron. **C:** SOD1 delayed firing motoneuron. **D:** SOD1 immediate firing motoneuron.

Figure 6: Delayed and immediate firing motoneurons morphology is differentially affected by the SOD1 mutation
A1, A2: Plots of the number of branching points in function of the total dendritic length for WT and SOD1 delayed firing motoneurons (**A1**) and WT and SOD1 immediate firing motoneurons (**A2**). Arrowhead points at the over-branching SOD1 delayed motoneuron **B1-B2:** Distribution of the dendritic paths for delayed (**B1**) and immediate firing motoneurons (**B2**). Distributions between WT and mSOD1 dendritic paths are significantly different (Kolmogorov-Smirnov bilateral test) for delayed firing motoneurons ($p=0.00012$) and for immediate firing motoneurons ($p<0.0001$).

Table 1: Excitability properties

		WT mice	mSOD1 mice	significativity
Input conductance (nS)	Delayed firing MNs	51.8 ± 28,0 10 / 151.5 N=63	53.8 ± 29,6 21.6 / 153 N=31	0.8
	Immediate firing MNs	33.2 ± 23.8 5.7 / 98 N=31	32.6 ± 16.2 6.3 / 62.5 N=18	0.6
	significativity	0.0007	0.01	
Rheobase (pA)	Delayed firing MNs	1199 ± 613 300 / 2800 N=57	1055 ± 503 300 / 2600 N=30	0.4
	Immediate firing MNs	593 ± 404 50 / 1600 N=29	284 ± 150 100 / 550 N=16	0.008
	significativity	<0.0001	<0.0001	
Recruitment current on ramp (pA)	Delayed firing MNs	1082 ± 649 149 / 2876 N=51	1076 ± 533 298 / 2533 N=29	0.8
	Immediate firing MNs	620 ± 473 67 / 1965 N=25	335 ± 306 69 / 1007 N=15	0.02
	significativity	0.001	<0.001	
Voltage threshold (mV)	Delayed firing MNs	-48.0 ± 7.3 -62 / -31 N=59	-46.4 ± 9.7 -65 / -25 N=31	0.7
	Immediate firing MNs	-59,5 ± 6,9 -75 / -41 N=30	-64,0 ± 5,6 -75 / -55 N=17	0.03
	significativity	<0.001	<0.001	

Table 2: Action potential properties

		WT mice	mSOD1 mice	significativity
Action Potential amplitude (mV)	Delayed firing MNs	89.1 ± 13.2 66.4 / 121.1 N=29	87.1 ± 11.3 71.2 / 111.1 N=19	0.5
	Immediate firing MNs	84.2 ± 10.7 65.9 / 103.7 N=21	80.8 ± 15.2 61.3 / 110 N=13	0.4
	significativity	0.2	0.2	
Action potential width (ms)	Delayed firing MNs	1.42 ± 0.54 0.66 / 2.50 N=29	1.30 ± 0.44 0.58 / 2.21 N=19	0.6
	Immediate firing MNs	1.73 ± 0.45 1.13 / 2.87 N=21	1.80 ± 0.59 0.90 / 3.12 N=13	0.7
	significativity	0.04	0.01	
AHP relaxation time constant (ms)	Delayed firing MNs	27.2 ± 9.0 11.3 / 49.9 N=21	23.2 ± 5.2 14.7 / 33.9 N=12	0.2
	Immediate firing MNs	41.7 ± 12.5 20.9 / 60.2 N=11	48.5 ± 27.0 19.2 / 91 N=7	1
	significativity	0.004	0.02	

Table 3: Morphological properties

		WT mice	mSOD1 mice	significativity
Primary dendrites	Delayed firing MNs	6.4 ± 2.0 N=14	6.7 ± 1.3 N=14	0.3
	Immediate firing MNs	6.2 ± 2.4 N=9	6.4 ± 4.0 N=5	0.9
	significativity	1	0.5	
Branching points	Delayed firing MNs	42.7 ± 13.6 N=14	43.6 ± 18.8 N=14	1
	Immediate firing MNs	26.7 ± 14.3 N=9	28.0 ± 13.7 N=5	0.7
	significativity	0.002	0.1	
Total dendritic length (mm)	Delayed firing MNs	7.9 ± 3.2 N=14	8.7 ± 3.8 N=14	0.5
	Immediate firing MNs	5.5 ± 1.3 N=9	3.6 ± 0.3 N=5	0.03
	significativity	0.03	0.001	
Terminal segment length (µm)	Delayed firing MNs	105 ± 90 N=598	117 ± 104 N=696	0.03
	Immediate firing MNs	108 ± 89 N=281	71 ± 79 N=164	<0.0001
	significativity	0.7	<0.0001	
Dendritic paths (µm)	Delayed firing MNs	289±135 N=598	329±149 N=696	<0.0001
	Immediate firing MNs	252±141 N=281	165±127 N=164	<0.0001
	significativity	0.0004	<0.0001	

Note that the “overbranching motoneuron” (arrowhead on Figure 6A1) is excluded for analysis.

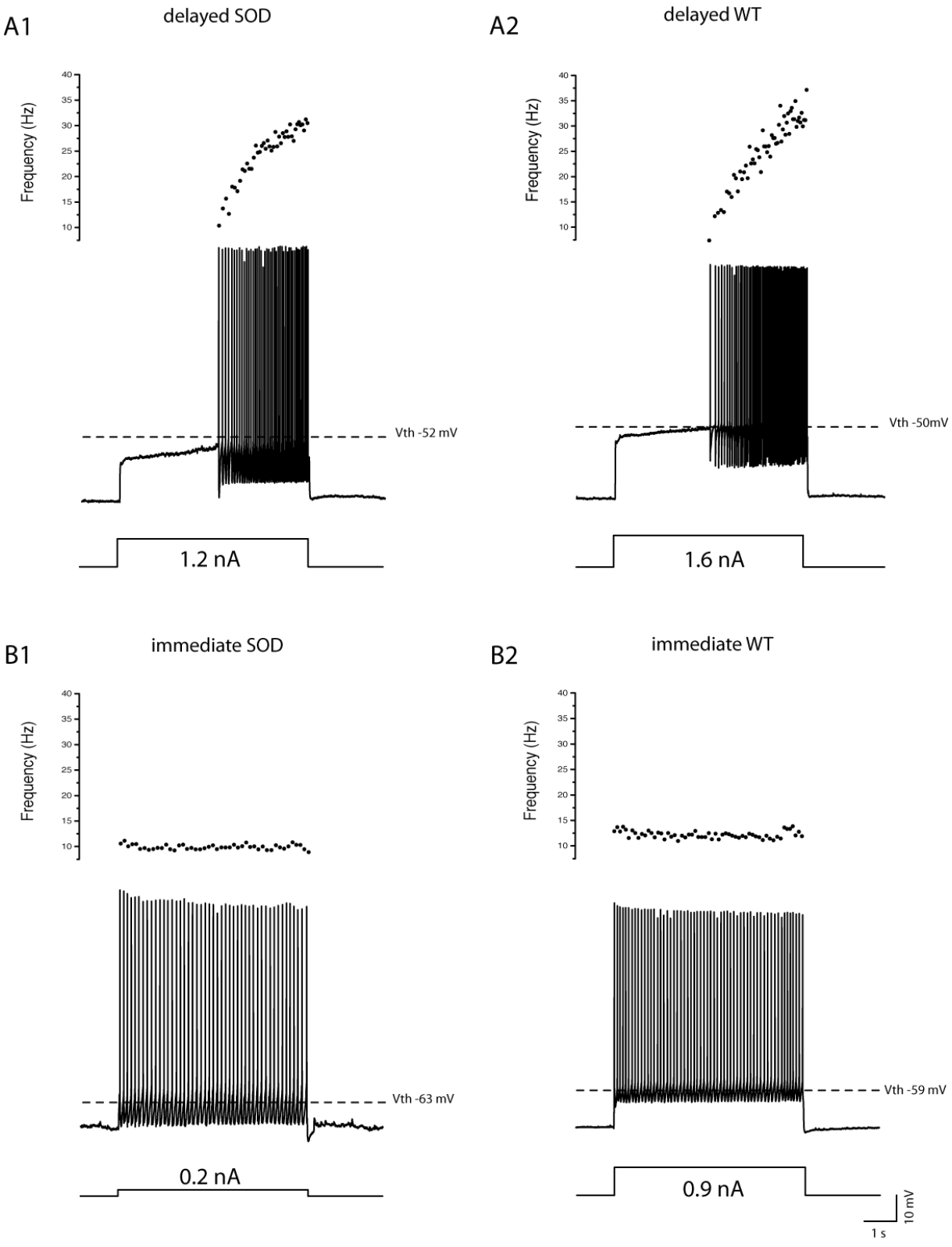

Article 2 Figure 1

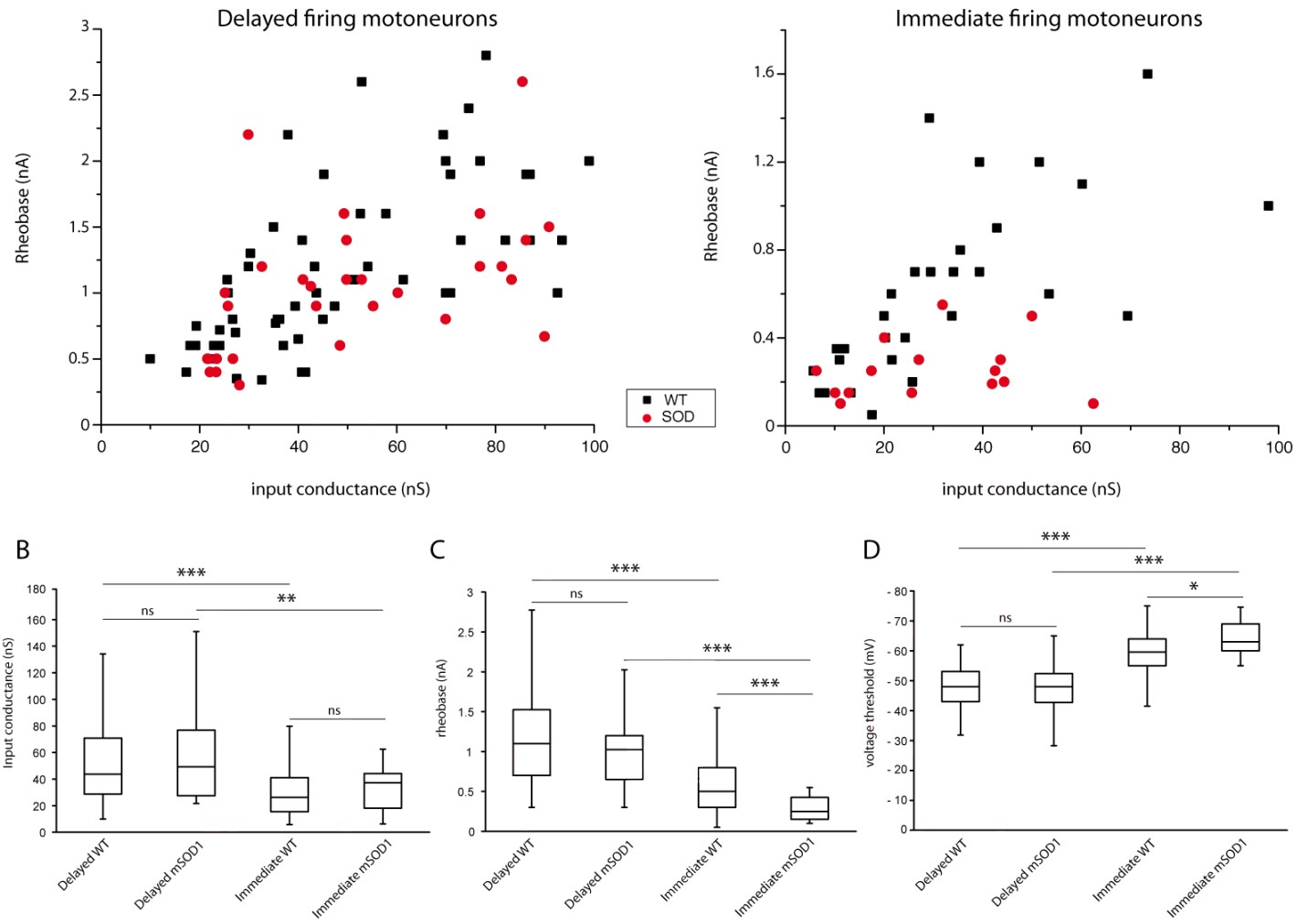

Article 2 Figure 2

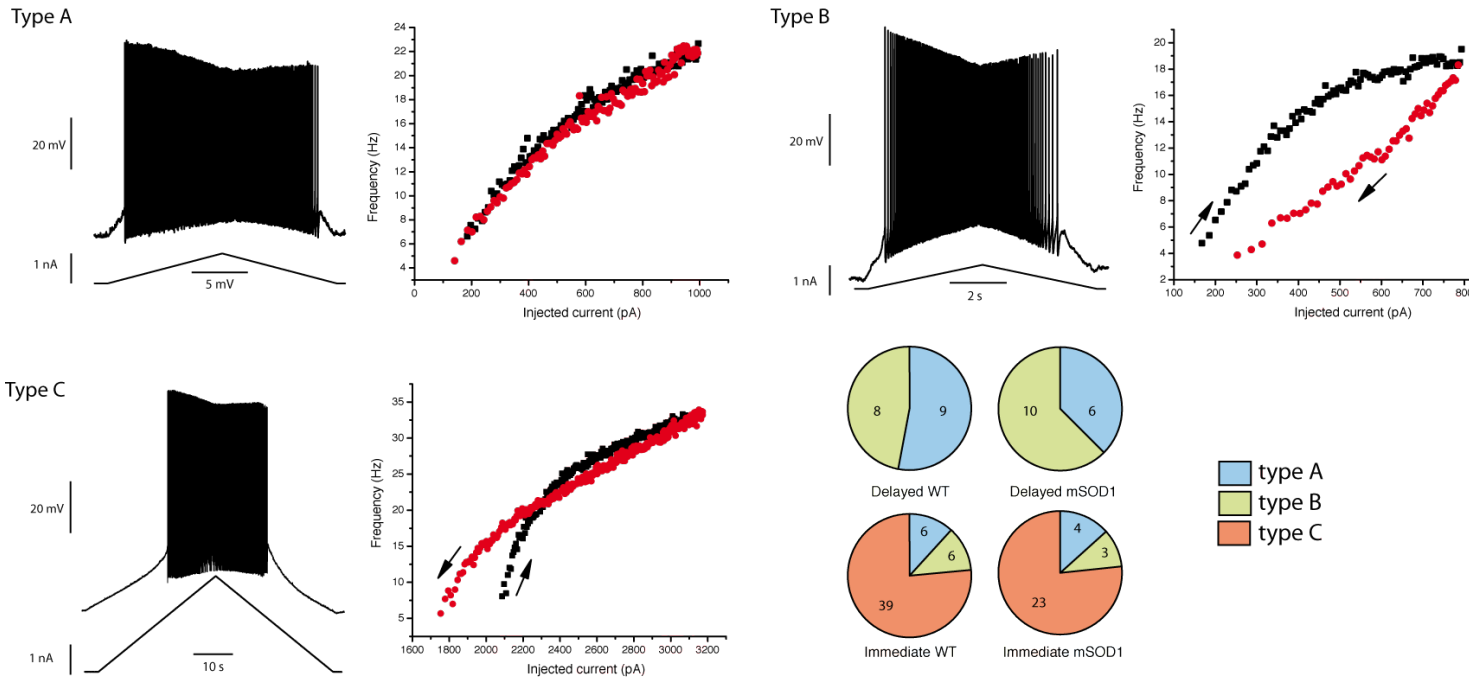

Article 2 Figure 3

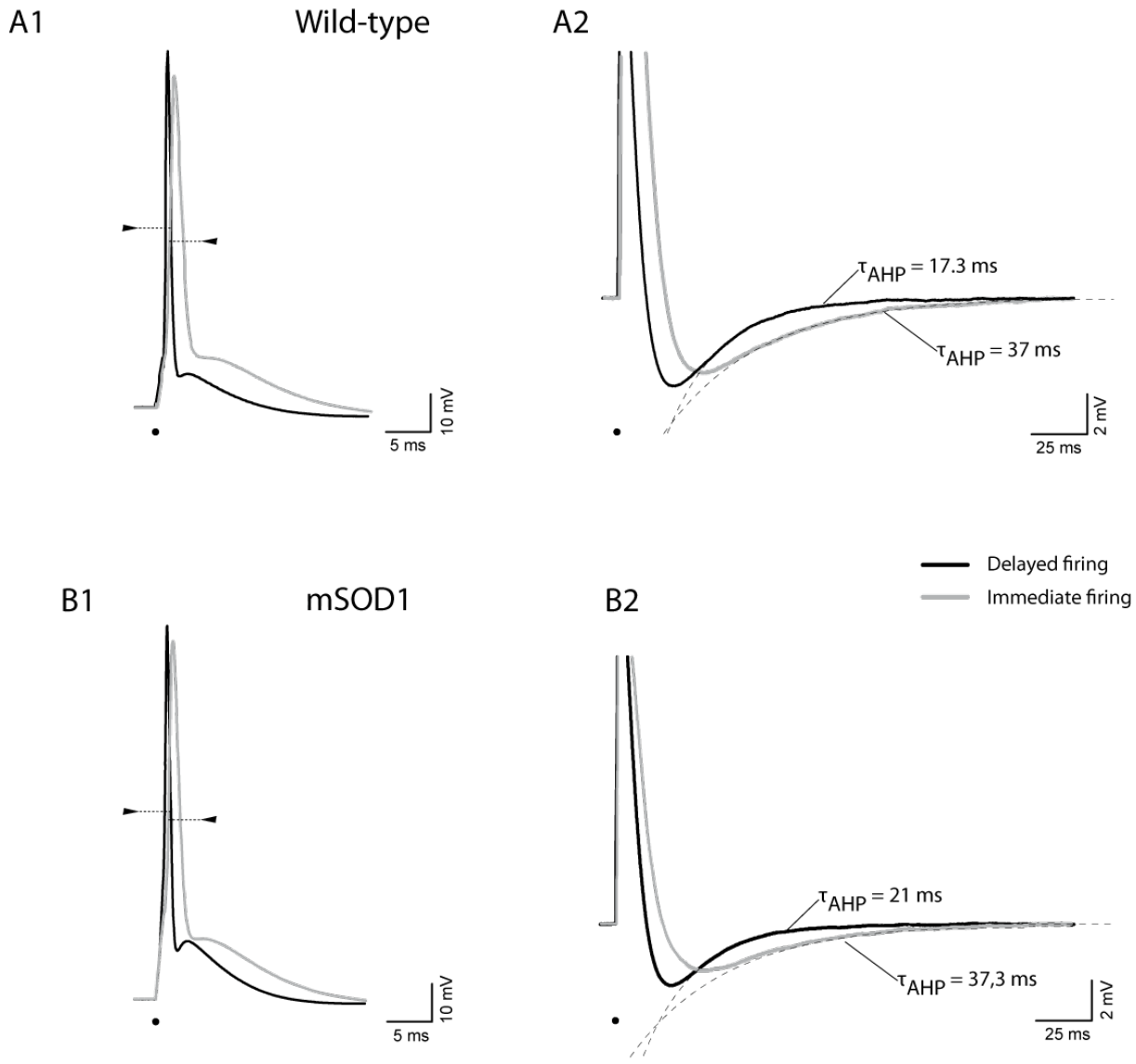

Article 2 Figure 4

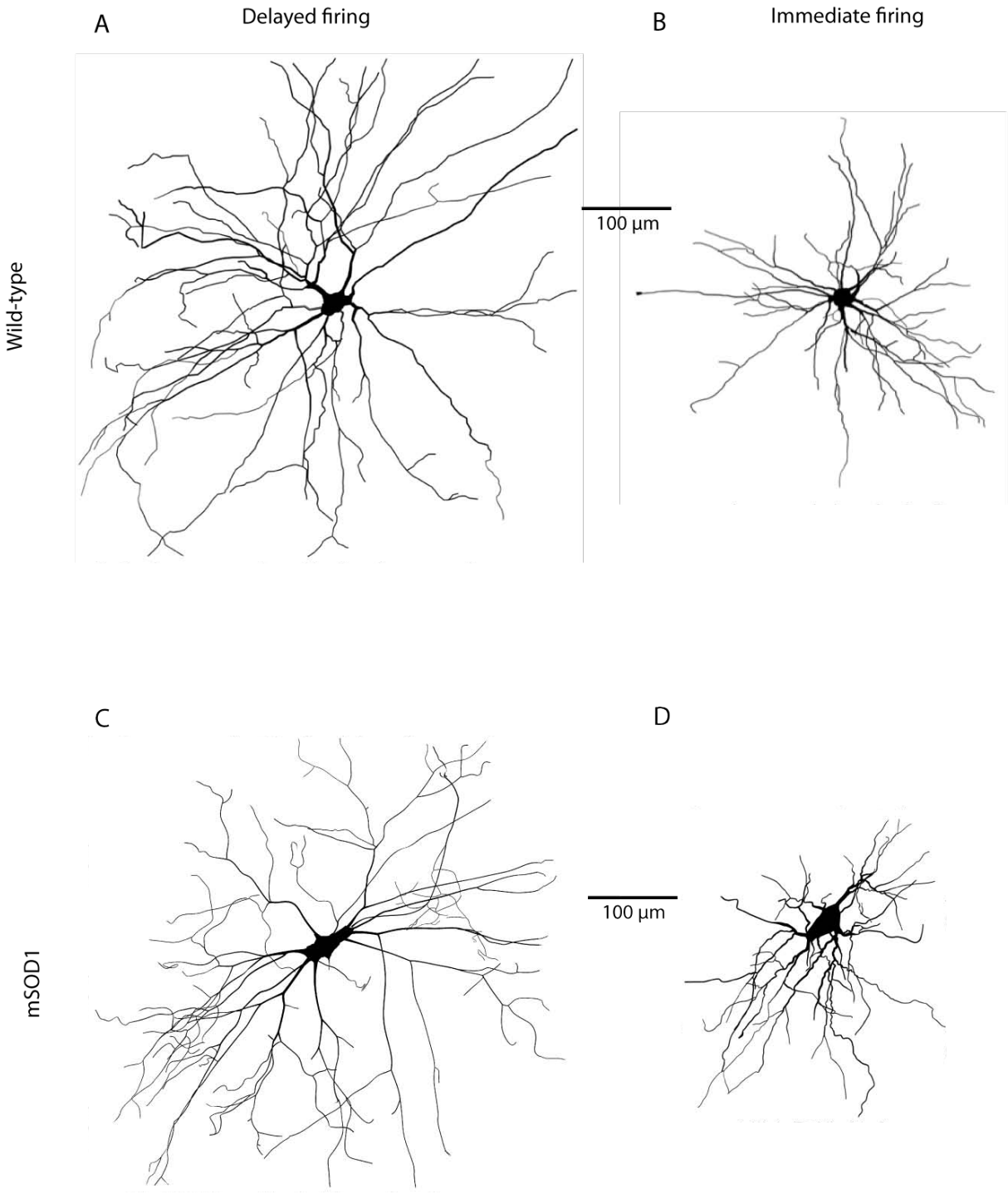

Article 2 Figure 5

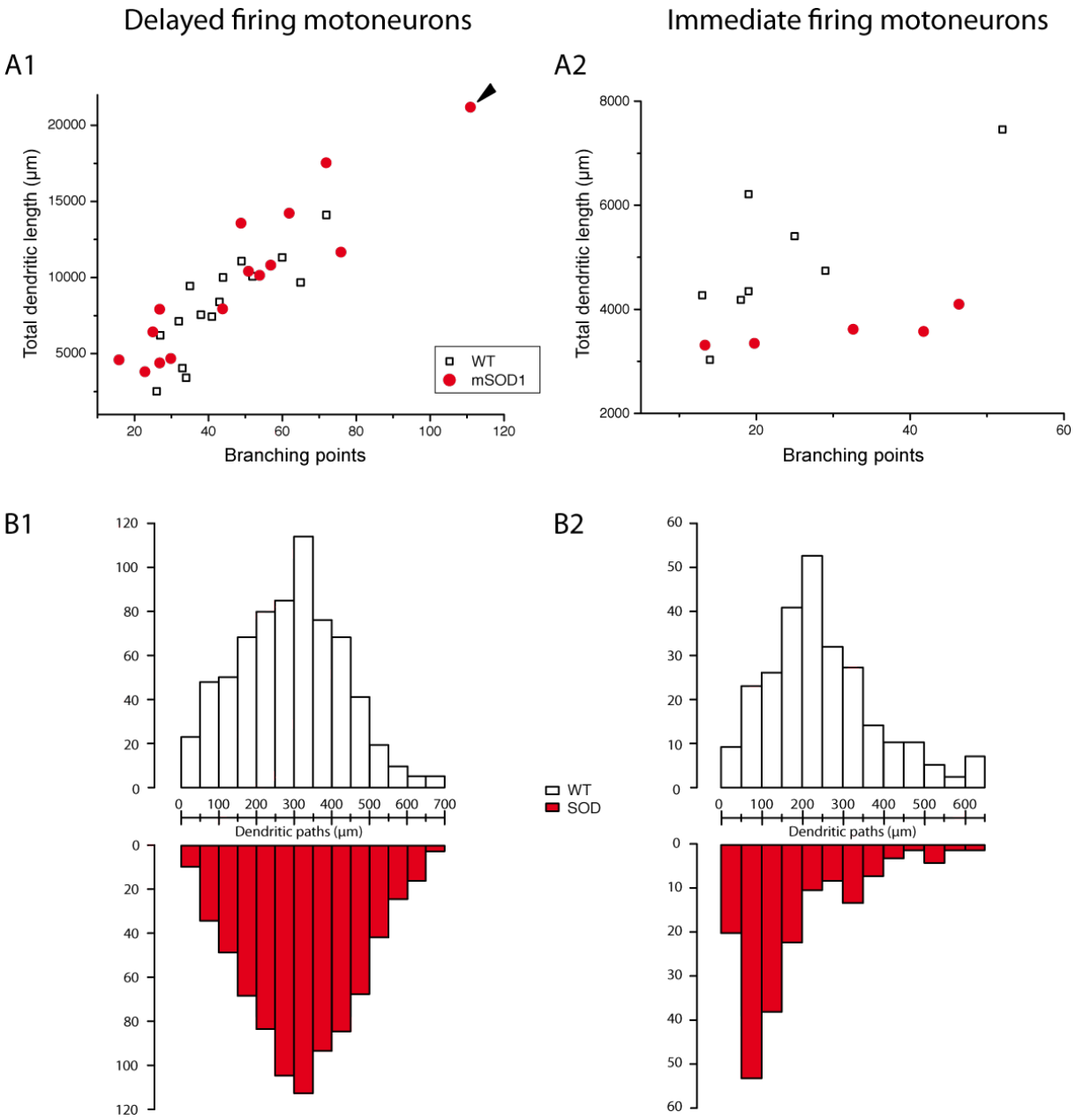

Article 2 Figure 6

Discussion

The aim of my thesis was primarily to look for alterations of the electrophysiological properties due to the SOD1 G93A mutation going along the idea of the neurotoxicity hypothesis. At first, I characterized in the WT motoneurons two populations exhibiting different discharge patterns and tried to correlate them with known physiological sub-types. Based on a bundle of clues I ascribed the immediate firing motoneurons to the slow motoneurons and the delayed firing motoneurons to the fast motoneurons. Then I moved on to study separately the effect of the SOD1 mutation on each motoneuron population.

1/ Lack of tonic synaptic inputs in the slice preparation

Prior to record the intrinsic properties of spinal motoneurons I inquired whether they could be subjected to some tonic synaptic inputs that would alter the correct measurements of the intrinsic properties.

Synaptic inputs can affect in many ways the motoneurons intrinsic properties. To begin with inhibitory inputs can produce shunting inhibition. Brizzi *et al.* (2004) mimicked an increase in tonic synaptic activity thanks to dynamic-clamp. By setting the reversal potential of the injected current at the resting membrane potential they elicit a constant increase in input conductance without changing the membrane voltage. The resulting shunting inhibition reduced the firing frequency in the primary range without affecting its slope. The shift in the F-I curve was proportional to the amount of current injected and dependent on an intrinsic property called shunting potential. Additionally the inhibitory synaptic inputs can exert considerable control over the discharge by regulating intrinsic PIC activation/deactivation, especially due to a shunting effect when the synapses colocalize with PIC channels (Bui *et al.*, 2008). In turn, PIC activation substantially amplifies both synaptic excitation and inhibition and is critical for the dynamic transformation of synaptic inputs to motoneuron frequency code (Lee & Heckman, 2000; Prather *et al.*, 2001; Hultborn *et al.*, 2003). Using modelization Venugopal *et al.* (2011) showed that dendritic

inhibition and more specifically the one mediated by GABAAR could regulate the PIC activation/inactivation and modify the shape of the F-I curve. In their model dendritic inhibition could linearized the F-I curve that was previously counter-clockwise due to the PIC activation. Evidence displayed in supplementary material 1 clearly demonstrate that passive and active properties of the motoneurons are not affected by the application of a cocktail of synaptic blockers. Consequently the study of the motoneurons intrinsic properties in the spinal cord slice preparation can be undertaken without blocking the synaptic inputs.

2/ Motor units maturation

We have shown that, at P6-P10, a majority of spinal motoneurons display a delayed firing pattern in response to long square pulses of current. The delayed discharge is caused by the combined action of a fast A-like current and a slow-inactivating potassium current. These potassium currents contribute to shaping the F-I function of the delayed firing motoneurons. The slow-inactivating current is responsible for memory effects that have a strong impact on motoneuron excitability.

a/ Expression of potassium currents during the postnatal development

My results show that 2 potassium currents, an A-like and a slow one are expressed in 66% of the spinal motoneurons between P6 and P10. They act by preventing the discharge and delaying its initiation conferring to the motoneurons the delayed pattern of discharge. This pattern is transient as no delay in the discharge was ever observed in adults spinal motoneurons upon liminal pulses injection motoneurones (Barrett *et al.*, 1980; Kernell, 2006). Similarly Russier *et al.* (2003) reported a delayed firing pattern in a sub-population of rat abducens motoneurons between P4 and P9. Transient expression of an A-like current during development is a common feature of developing motoneurons (reviewed in Perrier and Hounsgard 2000). More generally transient expression of potassium current during development was reported not only in spinal motoneurons (Gao & Ziskind-Conhaim, 1998) but also in brainstem motoneurons (Lape & Nistri, 1999; Russier *et al.*, 2003).

To our knowledge, this is the first time that this specific slow-inactivating current is described although slow currents have also been observed in other types of neurons

such as the adult rat hippocampal neurons (Storm, 1988; Lüthi *et al.*, 1996) and the thalamic relay neurons (Huguenard *et al.*, 1991).

b/ Firing properties of the motoneurons are shaped by the potassium currents

The most obvious effect of the potassium currents expression is their ability to delay the initiation of the discharge. In our recordings, most of the motoneurons started to discharge several seconds after the onset of the pulse. This is much longer than the delay shown by Russier et al. (2003) and Pambo-Pambo et al. (2009). The second effect is the acceleration of the discharge following its initiation. Such acceleration has been observed only in the delayed firing motoneurones (Russier *et al.*, 2003; Pambo-Pambo *et al.*, 2009 and present work). We show that the membrane potential increase responsible for this is due to the inactivation of the slow potassium current. Based on their different time constants the two potassium currents act mostly one after another. At spike onset, the fast A-like current hyperpolarizes the membrane potential and prevents the initiation of the first spikes. This gives time to the slow current to fully activate and maintain the membrane potential below spiking threshold while the A-like is inactivating. The slow inactivation then allows for the membrane to reach the spiking threshold and for the discharge to begin. However the inactivation of the slow current continues thus depolarizing the membrane and causing an acceleration in the discharge. In contrast, the immediate firing motoneurons never display an acceleration of the discharge. In adult motoneurons, the firing frequency is always decreasing during a pulse (Viana *et al.*, 1995; Brownstone, 2006; Manuel *et al.*, 2009). We must keep in mind that the delayed accelerating discharge only occurs upon injection of long liminal pulse.

Delayed and immediate firing motoneurons also present differences in the shape of their action potentials. The action potential of delayed motoneurons is notably narrower. The activation of the A-like current might contribute to the faster repolarization and a more narrow spike. As a result the amount of calcium entering the cell during the spike is smaller and the activation of the SK Ca^{2+} dependent channels is reduced. This is likely to link with our observation that AHPs of delayed firing motoneurons is shorter than for the immediate firing motoneurons.

The effects of the potassium currents are also visible upon injection of current ramps at a slow velocity. In adults motoneurons the shapes of the F-I relationships have been extensively characterized and categorized (Hounsgaard *et al.*, 1988; Lee & Heckman, 1998b; Bennett *et al.*, 2001; Button *et al.*, 2006). The shape can be put in relation with the slow currents expressed by the adults motoneurons, notably the calcium persistent inward current and the slow-inactivating sodium current. Such classification cannot however applied to neonatal motoneurons given the different panoply of currents they express. The virtual lack of persistent inward currents (Quinlan *et al.*, 2011) and the expression of the slow potassium current at this age confers to some of the delayed firing motoneurons F-I relationships a specific shape never described before. After a rapid acceleration of the discharge, a clear deceleration occurs. We correlated this inflexion with the complete inactivation of all potassium current. After the point, discharge acceleration relies solely on the membrane depolarization driven by the ramp and do not benefit anymore from the membrane depolarization due to the slow potassium inactivation. The inactivation of the sodium persistent current may further slow down the discharge during the increasing ramp. The gain of the F-I relationship is much more linear during the decreasing ramp. Given that the potassium current is still inactivated, the discharge continues for lower intensities than it started. Altogether the shape of the F-I curves for delayed firing motoneurons mostly relies on the interaction between the slow inactivation of the potassium current and the slow inactivation of the sodium current. Immediate firing motoneurons F-I relationship is much more conventional and mostly depends of the amount of sodium inactivation occurring during the increasing part of the ramp. A strong inactivation resulting in a clockwise hysteresis.

Although the smaller input conductance of the immediate firing motoneurons already suggests that they are recruited earlier than the delayed firing ones, the expression of potassium currents in the later enhances even more the differential recruitment by increasing the recruitment threshold of delayed motoneurons. Once again the two potassium currents act on different time-scales; the A-like current would increase the recruitment threshold for brief synaptic inputs (several tens of milliseconds) whereas the slow potassium current would increase the threshold during steady synaptic inputs. Thus the specific expression of the potassium currents in the biggest

population of motoneurons strengthened the orderly recruitment proposed by Henneman *et al.* (1957).

c/ Impact of the different discharge patterns on the maturation of the motor units.

Although muscle fibers are already differentiated between fast and slow types during the second week after birth (Schiaffino & Reggiani, 2011), very little is known about the differentiation of the fast and slow-types motoneurons. In the work presented, motoneurons were recorded in an in vitro slice preparation and such preparation precluded me to correlate the motoneurons properties with those of the motor units they innervate. Therefore in order to dissect the sub-types of motoneurons I analyzed whether some sub-populations would cluster along key intrinsic properties Additionally, I tried recurring to newly described molecular markers. If we assume that the neonatal motoneurons properties segregate similarly to the adult then the delayed firing motoneurons being the motoneurons with the larger dendritic tree, the larger input conductance and the smaller AHP are likely to become fast-type motoneurons while the immediate firing ones would become slow-type motoneurons. The results obtained with the fast-type motoneurons marker Chodl (Enjin *et al.*, 2010) concurs to indicate that at least part of the delayed firing motoneurons will become fast-type motoneurons.

Under this assumption, we may contemplate how the lower recruitment probability of the delayed compared to the immediate firing motoneurons would contribute to the maturation of the slow and fast motor units.

First, although the muscle fibers properties are already well-differentiated during our recording window (Close, 1967) they still express a cocktail of different embryonic, neonatal and adult myosin heavy chain isoforms (Agbulut *et al.*, 2003). In the adult fiber, the profile of myosin heavy chain expressed eventually falls to one isoform only. This maturation process takes place during the few weeks following birth (Schiaffino & Reggiani, 2011) and it is known that the motoneurons activity is one of the factors controlling it (Lowrie *et al.*, 1989; Goldspink *et al.*, 1992; Picquet *et al.*, 1998, Agbulut *et al.,* 2009). Blocking the activity of the muscle during development leads to a prolong expression of the myosin embryonic isoforms as well as the

incorrect expression of fast isoforms in slow fibers (Lowrie *et al.*, 1989; Goldspink *et al.*, 1992; Picquet *et al.*, 1998). Considering that the slow muscle fibers are the first to express their adult myosin heavy chain isoform this would go along the fact they are innervating in by the most active motoneurons (the most easily recruited).

Second, during our recording window, an intensive reorganization of the motoneurons connectivity to the muscle takes place (Jansen & Flatby, 1990). After reaching a plateau of poly-innervation during the first week after birth, the fibers innervation falls to a unique axon terminal coming from a motoneuron whose properties match the fibers properties. How the elimination of supernumerary neuro-muscular junctions take place remains quite mysterious. However we know that as early as after birth motor units are mostly homogenous in their fiber types composition at this age. Therefore each motoneurons population probably competes against motoneurons from the same population for the maintenance of its NMJ. Nonetheless the competition between the two populations remains plausible for a significant minority of muscle fibers innervated by motoneuron from the two populations. The motoneurons activity also controls the rate of elimination of the poly-innervation (Thompson, 1985). Indeed, chronic application of electrical stimulations extensively sped up the loss of supernumerary synapse (O'Brien *et al.*, 1978). Conversely, reducing proprioceptive inputs to motoneurones (Benoit & Changeux, 1975) or reducing inputs to muscle fibres by partial axotomy (Brown *et al.*, 1976) delays the elimination of poly-innervation. Building on these results and theoretical works many authors have suggested that motoneurones with less active neuromuscular junctions will innervate larger territories than motoneurones with more active ones (Callaway *et al.*, 1987; Barber & Lichtman, 1999; Nowik *et al.*, 2012). Furthermore, F motoneurons torritories are bigger than slow ones. We may wonder to what extent this is the result of the lower activation of the delayed motoneurons. When competing against immediate firing motoneurons the delayed one would then innervate larger sub-set of muscle fibers.

3/ Differential effect of the SOD1 G93A mutation on the two populations

In the second part of my work we provide evidence that the electrical and morphological alterations of spinal motoneurons in neonatal SOD1 mice are not the same in the immediate firing motoneurons and in the delayed firing ones. Indeed, the two motoneuron subtypes display, on average, numerous differences both in WT and mSOD1 mice: the delayed firing motoneurons have a larger input conductance, a higher threshold current, a briefer action potential, a shorter AHP but a more complex dendritic tree than the immediate firing motoneurons. However, when comparing separately the delayed firing motoneurons and the immediate firing ones between WT and mSOD1 animals, we found that the immediate firing motoneurons display a smaller threshold current and a more hyperpolarized voltage threshold for spiking in the mSOD1 mice than in the WT mice. This suggests that these motoneurons are more excitable in the mSOD1 mice than in the WT mice. Furthermore the dendritic segments of the immediate firing motoneurons are shorter in the mSOD1 animals than in the WT animals. In sharp contrast, the electrical properties of the delayed firing motoneurons are similar in WT and mSOD1 animals and their dendrites are slightly elongated.

a/ Categorization of the motoneurons sub-type is crucial when studying the ALS.

We know that, in the ALS, all motoneurons are not equal when facing the ALS. Some motor pools remain unaffected until the very last stages of the disease (Onufs, trochlear, oculomotor). Even within those that degenerate, the degenerative process begins with FF motoneurons expanding later to FR ones while S ones continue to function long after most of the F motoneurons are gone (Hegedus *et al.*, 2008). Indirect observations suggest that most gamma motoneurons are spared contrary to alpha motoneurons.

Sor far, every studies on the motoneurons intrinsic properties performed in neonatal mice pooled every motoneurons recorded and didn't take into account the heterogeneity between sub-types (Bories *et al.*, 2007; Amendola & Durand, 2008; Pambo-Pambo *et al.*, 2009; Quinlan *et al.*, 2011; Filipchuk & Durand, 2012). Any average property computed when pooling motoneurons coming from these two populations therefore heavily relies on the proportion of the two populations in the sample. Any significant variation between the proportion of the two populations might

therefore obscure the results and invalidate the conclusions drawn from the comparison of WT and mSOD1 motoneurons. This might explain conflictual results between different studies. Additionally, in several studies motoneurons sampling was also biased toward the bigger ones given that the authors only relied on the soma size and its location to assert the nature of the recorded cell. I propose the motoneuron discharge patterns to be taken into account in ALS studies.

b/ Opposed effect on delayed and immediate firing motoneurons.

When comparing separately the delayed and immediate firing motoneurons electrical properties we found a differential effect of the SOD mutation. Immediate firing motoneurons are hyper-excitable when the delayed firing ones retain the same excitability. The specific hyperpolarization of the voltage threshold probably comes from a change in the sodium / potassium balance controlling the spike initiation. It could either be due to a shift in the activation curves or in the total conductances amplitude (Dai *et al.*, 2002). Regarding the delayed firing motoneurons, it is possible that the expression of the A-like current hinders the hyper-excitability.

The mSOD1 differential effects on the morphology was even more striking since the dendritic tree of immediate firing motoneurons shrinks by 35% whereas the dendritic tree of the delayed firing motoneurons expands by 10. These changes in morphology had however no impact on the motoneurons input conductances. This is somewhat surprising since the change concern the entire tree and not just the distal part of it (the entire dendritic path is shorter in mSOD1 imemdiate firing motoneurons than in the WT counter-parts). We may infer that the immediate firing motoneurons shrinkage is compensated by a lowering of the cell membrane specific conductance. Some homeostatic modification of the membrane intrinsic permeability may be at stake to maintain the input conductance. This would explain the contradictory result of having a shorter dendritic tree but no effect on the cell input conductance. The need for this homeostatic regulation may come from the necessity to finely control the orderly recruitment of the different motoneurons sub-types. Without compensation of the membrane specific conductance, putative slow motoneurons would be recruited much more often than putative fast ones. Regarding the delayed firing motoneurons, one mSOD1 delayed firing motoneuron markedly overbranches. The overbranching delayed motoneuron might be put in relation with the larger input

conductance (Delestrée *et al., SfN 2012*) observed in adult spinal motoneurons. The reason why different motoneurons sub-types undergo opposed morphological alteration remains to be elucidated.

c/ Putative slow motoneurons are affected first by the mutation

A surprising result of my study is that the putative slow motoneurons (the immediate firing ones) seem to be the first affected by the mutation. They are clearly hyper-excitable, a change that has always been previously linked to the excitotoxicity hypothesis (Ilieva *et al.*, 2009) and therefore thought to be detrimental to the cell. However, hyperexcitability could be an epiphenomenon or, more provocatively, a protective mechanism (Saxena *et al.*, 2013). In a recent study Saxena *et al.* (2013) demonstrated that the relatively higher resilience of FR and S motoneurons correlates to their higher excitabilities compared to FF motoneurons low-excitability. As soon as between P7 and P14 the FF motoneurons display increasing accumulation of misfolded SOD1 protein as well as activation of the mTOR neuroprotective pathway. FF motoneurons are therefore already markedly subjected to alteration of their fonctionnement. The reason why they do not display hyper-excitability could be that it's already too late for them to cope with the disease progression. On the other hand, the increased excitability display by the putative slow motoneurons could protect them from the degenerescence. Although we cannot exclude a putative excitotoxic role of the increased level of activity, their hypothesis provide a framework to explain why the less active motoneurons die first. In addition, recent data shows that none of the adult spinal motoneurons are hyperexcitable in mSOD1 mice prior their neuromuscular junctions start to degenerate (Delestrée *et al.*, SfN 2012). Another role for hyper-excitability has been suggested by a work done in a mouse model of the spinal muscular atrophy (SMA). Indeed, Mentis *et al.* (2011) reported that following the loss of the proprioceptive inputs, the motoneurons input resistance is increased and their voltage threshold becomes hyperpolarized. It is tempting to view in this hyper-excitability a homeostatic mechanism allowing the motoneurons to maintain a similar level of activity by maintaining its position in the orderly recruitment. To conclude, hyperexcitability may trigger, prevent or simply be an homeostatic epiphenomenon to the degenerescence. Further studies will be needed to disambiguate between the different scenarios.

4/ Possible change in excitation leading to morphological alterations

It has long been proposed that shift toward excessive excitation of the balanced inhibitory/excitatory synaptic inputs received by the motoneurones may induce a glutamate-mediated excitotoxicity in ALS (Rothstein *et al.*, 1995; Van Den Bosch *et al.*, 2006). A decreased amplitude of glycinergic minis was reported in a cultured motoneuron preparation (Chang & Martin, 2011). Similarly to what happens during the SMA (Mentis *et al.*, 2011) sensory inputs coming from the ventral roots could be altered. Bories *et al.* (2007) reported a decreased amplitude for sensory PSPs (mixed inhibitory and excitatory) evoked in motoneurons by dorsal root stimulation. Furthermore, during a critical developmental period in embryos, the morphology of the neuronal dendritic tree depends on the synaptic activity on the dendrites (Spitzer, 2006; Cline & Haas, 2008). It was shown that an increase of the density of synaptic inputs on dendrites may led to a shortening of the dendrite length (Tripodi *et al.*, 2008). In keeping with this, Martin *et al.* (2013) found that the terminal segments are shorter in E17.5 spinal motoneurons recorded from mSOD1 mice. Early pruning of the dendritic tree was also observed by van Zundert *et al.* (2008) in mSDO1 hypoglossal motoneurons at P2.

In this framework, it would be interesting to investigate whether there is a shift in the balance between excitation and inhibition. Recordings should be done during the pre- and post-natal periods and coupled with cells reconstruction to determine if the alteration of synaptic inputs precedes the change in morphology. As we did for intrinsic properties, synaptics inputs impinging on either delayed or immediate firing motoneurons should be analyzed separately.

I propose to record minis in voltage-clamp as well as dorsal root-evoked potentials. In order to analyse the minis, two technical difficulties must be overcome. First, each motoneuron receives various degrees of synaptic inputs in our slice preparation. Second, we need to isolate properly space-clamped proximal event from filtered distal ones. The first issue can be overcome by a large sampling and the second by looking at the faster event only to get rid of the filtered ones. The recordings will be

done after assessing the different categories of events that can be recorded. Preliminary recordings show that we have no spontaneous cholinergic or GABAergic activity in our recorded motoneurons while many characteristic AMPA or NMDA receptor-mediated glutamatergic events can be seen as well as glycinergic ones. Synaptic blockers will be used to appropriately isolate each category of events. We now need to assess whether the frequency, amplitude, rising or decaying times of the fastest events in each category are altered in delayed and immediate firing motoneurons. Building on our results from the minis as well as those from dorsal root stimulation, we might pinpoint some pre- or post-synaptic modifications occuring in the motoneurons inputs.

References

Agbulut O, Noirez P, Beaumont F & Butler-Browne G. (2003). Myosin heavy chain isoforms in postnatal muscle development of mice. *Biology of the cell / under the auspices of the European Cell Biology Organization* **95,** 399-406.

Agbulut O, Vignaud A, Hourde C, Mouisel E, Fougerousse F, Butler-Browne GS & Ferry A. (2009). Slow myosin heavy chain expression in the absence of muscle activity. *American journal of physiology Cell physiology* **296,** C205-214

Alessandri-Haber N, Paillart C, Arsac C, Gola M, Couraud F & Crest M. (1999). Specific distribution of sodium channels in axons of rat embryo spinal motoneurones. *J Physiol* **518 (Pt 1),** 203-214.

Alexianu ME, Ho BK, Mohamed AH, La Bella V, Smith RG & Appel SH. (1994). The role of calcium-binding proteins in selective motoneuron vulnerability in amyotrophic lateral sclerosis. *Annals of neurology* **36,** 846-858.

Amendola J & Durand J. (2008). Morphological differences between wild-type and transgenic superoxide dismutase 1 lumbar motoneurons in postnatal mice. *The Journal of comparative neurology* **511,** 329-341.

Atkin JD, Farg MA, Walker AK, McLean C, Tomas D & Horne MK. (2008). Endoplasmic reticulum stress and induction of the unfolded protein response in human sporadic amyotrophic lateral sclerosis. *Neurobiology of disease* **30,** 400-407.

Bakels R & Kernell D. (1993a). Average but not continuous speed match between motoneurons and muscle units of rat tibialis anterior. *Journal of neurophysiology* **70,** 1300-1306.

Bakels R & Kernell D. (1993b). Matching between motoneurone and muscle unit properties in rat medial gastrocnemius. *J Physiol* **463,** 307-324.

Barber MJ & Lichtman JW. (1999). Activity-driven synapse elimination leads paradoxically to domination by inactive neurons. *The Journal of neuroscience : the official journal of the Society for Neuroscience* **19,** 9975-9985.

Barrett EF & Barret JN. (1976). Separation of two voltage-sensitive potassium currents, and demonstration of a tetrodotoxin-resistant calcium current in frog motoneurones. *J Physiol* **255,** 737-774.

Barrett EF, Barrett JN & Crill WE. (1980). Voltage-sensitive outward currents in cat motoneurones. *J Physiol* **304,** 251-276.

Beaumont E & Gardiner P. (2002). Effects of daily spontaneous running on the electrophysiological properties of hindlimb motoneurones in rats. *J Physiol* **540,** 129-138.

Beers DR, Ho BK, Siklos L, Alexianu ME, Mosier DR, Mohamed AH, Otsuka Y, Kozovska ME, McAlhany RE, Smith RG & Appel SH. (2001). Parvalbumin overexpression alters immune-mediated increases in intracellular calcium, and delays disease onset in a transgenic model of familial amyotrophic lateral sclerosis. *Journal of neurochemistry* **79,** 499-509.

Bendotti C, Calvaresi N, Chiveri L, Prelle A, Moggio M, Braga M, Silani V & De Biasi S. (2001). Early vacuolization and mitochondrial damage in motor neurons of FALS mice are not associated with apoptosis or with changes in cytochrome oxidase histochemical reactivity. *Journal of the neurological sciences* **191,** 25-33.

Bennett DJ, Hultborn H, Fedirchuk B & Gorassini M. (1998). Synaptic activation of plateaus in hindlimb motoneurons of decerebrate cats. *Journal of neurophysiology* **80,** 2023-2037.

Bennett DJ, Li Y & Siu M. (2001). Plateau potentials in sacrocaudal motoneurons of chronic spinal rats, recorded in vitro. *Journal of neurophysiology* **86,** 1955-1971.

Bennett MR & Pettigrew AG. (1974). The formation of synapses in striated muscle during development. *J Physiol* **241,** 515-545.

Benoit P & Changeux JP. (1975). Consequences of tenotomy on the evolution of multiinnervation in developing rat soleus muscle. *Brain research* **99,** 354-358.

Berger AJ, Bayliss DA, Bellingham MC, Umemiya M & Viana F. (1995). Postnatal development of hypoglossal motoneuron intrinsic properties. *Advances in experimental medicine and biology* **381,** 63-71.

Berger AJ & Takahashi T. (1990). Serotonin enhances a low-voltage-activated calcium current in rat spinal motoneurons. *The Journal of neuroscience : the official journal of the Society for Neuroscience* **10,** 1922-1928.

Boillee S, Vande Velde C & Cleveland DW. (2006a). ALS: a disease of motor neurons and their nonneuronal neighbors. *Neuron* **52,** 39-59.

Boillee S, Yamanaka K, Lobsiger CS, Copeland NG, Jenkins NA, Kassiotis G, Kollias G & Cleveland DW. (2006b). Onset and progression in inherited ALS determined by motor neurons and microglia. *Science* **312,** 1389-1392.

Bories C, Amendola J, Lamotte d'Incamps B & Durand J. (2007). Early electrophysiological abnormalities in lumbar motoneurons in a transgenic mouse model of amyotrophic lateral sclerosis. *The European journal of neuroscience* **25,** 451-459.

Brizzi L, Meunier C, Zytnicki D, Donnet M, Hansel D, Lamotte D'Incamps B & Van Vreeswijk C. (2004). How shunting inhibition affects the discharge of lumbar motoneurones: a dynamic clamp study in anaesthetized cats. *J Physiol* **558,** 671-683.

Brown MC, Jansen JKS & Van Essen D. (1976). Polyneural innervation of skeletal muscle in new-born rats and its elimination during maturation. *J Physiol* **261,** 387-422.

Brownstone RM. (2006). Beginning at the end: repetitive firing properties in the final common pathway. *Progress in neurobiology* **78,** 156-172.

Bruijn LI, Becher MW, Lee MK, Anderson KL, Jenkins NA, Copeland NG, Sisodia SS, Rothstein JD, Borchelt DR, Price DL & Cleveland DW. (1997). ALS-linked SOD1 mutant G85R mediates damage to astrocytes and promotes rapidly progressive disease with SOD1-containing inclusions. *Neuron* **18,** 327-338.

Bui TV, Grande G & Rose PK. (2008). Multiple modes of amplification of synaptic inhibition to motoneurons by persistent inward currents. *Journal of neurophysiology* **99,** 571-582.

Burke RE. (1981). *Motor units: anatomy, physiology, and functional organization*. Am. Physiol. Soc., Bethesda, MD.

Burke RE. (1982). Motor units in cat muscles: anatomical considerations in relation to motor unit types. *Advances in neurology* **36,** 31-45.

Burke RE, Levine DN, Tsairis P & Zajac FE, 3rd. (1973). Physiological types and histochemical profiles in motor units of the cat gastrocnemius. *J Physiol* **234,** 723-748.

Burke RE, Levine DN & Zajac FE, 3rd. (1971). Mammalian motor units: physiological-histochemical correlation in three types in cat gastrocnemius. *Science* **174,** 709-712.

Butler JE & Gandevia SC. (2008). The output from human inspiratory motoneurone pools. *J Physiol* **586,** 1257-1264.

Button DC, Gardiner K, Marqueste T & Gardiner PF. (2006). Frequency-current relationships of rat hindlimb alpha-motoneurones. *J Physiol* **573,** 663-677.

Callaway EM, Soha JM & Van Essen DC. (1987). Competition favouring inactive over active motor neurons during synapse elimination. *Nature* **328,** 422-426.

Callaway EM, Soha JM & Van Essen DC. (1989). Differential loss of neuromuscular connections according to activity level and spinal position of neonatal rabbit soleus motor neurons. *The Journal of neuroscience : the official journal of the Society for Neuroscience* **9,** 1806-1824.

Chakkalakal JV, Nishimune H, Ruas JL, Spiegelman BM & Sanes JR. (2010). Retrograde influence of muscle fibers on their innervation revealed by a novel marker for slow motoneurons. *Development* **137,** 3489-3499.

Chang Q & Martin LJ. (2011). Glycine receptor channels in spinal motoneurons are abnormal in a transgenic mouse model of amyotrophic lateral sclerosis. *The Journal of neuroscience : the official journal of the Society for Neuroscience* **31,** 2815-2827.

Cheroni C, Marino M, Tortarolo M, Veglianese P, De Biasi S, Fontana E, Zuccarello LV, Maynard CJ, Dantuma NP & Bendotti C. (2009). Functional alterations of the ubiquitin-proteasome system in motor neurons of a mouse model of familial amyotrophic lateral sclerosis. *Human molecular genetics* **18,** 82-96.

Chiu AY, Zhai P, Dal Canto MC, Peters TM, Kwon YW, Prattis SM & Gurney ME. (1995). Age-dependent penetrance of disease in a transgenic mouse model of familial amyotrophic lateral sclerosis. *Molecular and cellular neurosciences* **6,** 349-362.

Clarac F, Brocard F & Vinay L. (2004). The maturation of locomotor networks. *Progress in brain research* **143,** 57-66.

Cline H & Haas K. (2008). The regulation of dendritic arbor development and plasticity by glutamatergic synaptic input: a review of the synaptotrophic hypothesis. *J Physiol* **586,** 1509-1517.

Close R. (1964). Dynamic Properties of Fast and Slow Skeletal Muscles of the Rat during Development. *J Physiol* **173,** 74-95.

Close R. (1967). Properties of motor units in fast and slow skeletal muscles of the rat. *J Physiol* **193,** 45-55.

Condon K, Silberstein L, Blau HM & Thompson WJ. (1990). Development of muscle fiber types in the prenatal rat hindlimb. *Developmental biology* **138,** 256-274.

Connor JA & Stevens CF. (1971). Voltage clamp studies of a transient outward membrane current in gastropod neural somata. *J Physiol* **213,** 21-30.

Conway BA, Hultborn H, Kiehn O & Mintz I. (1988). Plateau potentials in alpha-motoneurones induced by intravenous injection of L-dopa and clonidine in the spinal cat. *J Physiol* **405,** 369-384.

Cope TC & Sokoloff AJ. (1999). Orderly recruitment among motoneurons supplying different muscles. *Journal of physiology, Paris* **93,** 81-85.

Cullheim S, Fleshman JW, Glenn LL & Burke RE. (1987a). Membrane area and dendritic structure in type-identified triceps surae alpha motoneurons. *The Journal of comparative neurology* **255,** 68-81.

Cullheim S, Fleshman JW, Glenn LL & Burke RE. (1987b). Three-dimensional architecture of dendritic trees in type-identified alpha-motoneurons. *The Journal of comparative neurology* **255,** 82-96.

Dai Y, Jones KE, Fedirchuk B, McCrea DA & Jordan LM. (2002). A modelling study of locomotion-induced hyperpolarization of voltage threshold in cat lumbar motoneurones. *J Physiol* **544,** 521-536.

Dasen JS & Jessell TM. (2009). Hox networks and the origins of motor neuron diversity. *Current topics in developmental biology* **88,** 169-200.

De Vos KJ, Chapman AL, Tennant ME, Manser C, Tudor EL, Lau KF, Brownlees J, Ackerley S, Shaw PJ, McLoughlin DM, Shaw CE, Leigh PN, Miller CC & Grierson AJ. (2007). Familial amyotrophic lateral sclerosis-linked SOD1 mutants perturb fast axonal transport to reduce axonal mitochondria content. *Human molecular genetics* **16,** 2720-2728.

De Winter F, Vo T, Stam FJ, Wisman LA, Bar PR, Niclou SP, van Muiswinkel FL & Verhaagen J. (2006). The expression of the chemorepellent Semaphorin 3A is selectively induced in terminal Schwann cells of a subset of neuromuscular synapses that display limited anatomical plasticity and enhanced vulnerability in motor neuron disease. *Molecular and cellular neurosciences* **32,** 102-117.

Deardorff AS, Romer SH, Deng Z, Bullinger KL, Nardelli P, Cope TC & Fyffe RE. (2013). Expression of postsynaptic Ca2+-activated K+ (SK) channels at C-bouton synapses in mammalian lumbar -motoneurons. *J Physiol* **591,** 875-897.

DeJesus-Hernandez M, Mackenzie IR, Boeve BF, Boxer AL, Baker M, Rutherford NJ, Nicholson AM, Finch NA, Flynn H, Adamson J, Kouri N, Wojtas A, Sengdy P, Hsiung GY, Karydas A, Seeley WW, Josephs KA, Coppola G, Geschwind DH, Wszolek ZK, Feldman H, Knopman DS, Petersen RC, Miller BL, Dickson DW, Boylan KB, Graff-Radford NR & Rademakers R. (2011). Expanded GGGGCC hexanucleotide repeat in noncoding region of C9ORF72 causes chromosome 9p-linked FTD and ALS. *Neuron* **72,** 245-256.

Delgado-Lezama R, Perrier JF & Hounsgaard J. (1999). Local facilitation of plateau potentials in dendrites of turtle motoneurones by synaptic activation of metabotropic receptors. *J Physiol* **515 (Pt 1),** 203-207.

Dengler R, Konstanzer A, Kuther G, Hesse S, Wolf W & Struppler A. (1990). Amyotrophic lateral sclerosis: macro-EMG and twitch forces of single motor units. *Muscle & nerve* **13,** 545-550.

Dennis MJ, Ziskind-Conhaim L & Harris AJ. (1981). Development of neuromuscular junctions in rat embryos. *Developmental biology* **81,** 266-279.

Desmedt JE & Godaux E. (1977). Fast motor units are not preferentially activated in rapid voluntary contractions in man. *Nature* **267,** 717-719.

Duchen LW & Tonge DA. (1973). The effects of tetanus toxin on neuromuscular transmission and on the morphology of motor end-plates in slow and fast skeletal muscle of the mouse. *J Physiol* **228,** 157-172.

Edstrom L & Kugelberg E. (1968). Histochemical composition, distribution of fibres and fatiguability of single motor units. Anterior tibial muscle of the rat. *Journal of neurology, neurosurgery, and psychiatry* **31,** 424-433.

Eken T & Kiehn O. (1989). Bistable firing properties of soleus motor units in unrestrained rats. *Acta physiologica Scandinavica* **136,** 383-394.

Elbasiouny SM, Amendola J, Durand J & Heckman CJ. (2010). Evidence from computer simulations for alterations in the membrane biophysical properties and dendritic processing of synaptic inputs in mutant superoxide dismutase-1 motoneurons. *The Journal of neuroscience : the official journal of the Society for Neuroscience* **30,** 5544-5558.

Enjin A, Leao KE, Mikulovic S, Le Merre P, Tourtellotte WG & Kullander K. (2012). Sensorimotor function is modulated by the serotonin receptor 1d, a novel marker for gamma motor neurons. *Molecular and cellular neurosciences* **49,** 322-332.

Enjin A, Rabe N, Nakanishi ST, Vallstedt A, Gezelius H, Memic F, Lind M, Hjalt T, Tourtellotte WG, Bruder C, Eichele G, Whelan PJ & Kullander K. (2010). Identification of novel spinal cholinergic genetic subtypes disclose Chodl and Pitx2 as markers for fast motor neurons and partition cells. *The Journal of comparative neurology* **518,** 2284-2304.

Feiereisen P, Duchateau J & Hainaut K. (1997). Motor unit recruitment order during voluntary and electrically induced contractions in the tibialis anterior. *Experimental brain research Experimentelle Hirnforschung Experimentation cerebrale* **114,** 117-123.

Ferrucci M, Spalloni A, Bartalucci A, Cantafora E, Fulceri F, Nutini M, Longone P, Paparelli A & Fornai F. (2010). A systematic study of brainstem motor nuclei in a mouse model of ALS, the effects of lithium. *Neurobiology of disease* **37,** 370-383.

Filipchuk AA & Durand J. (2012). Postnatal dendritic development in lumbar motoneurons in mutant superoxide dismutase 1 mouse model of amyotrophic lateral sclerosis. *Neuroscience* **209,** 144-154.

Fischer LR, Culver DG, Tennant P, Davis AA, Wang M, Castellano-Sanchez A, Khan J, Polak MA & Glass JD. (2004). Amyotrophic lateral sclerosis is a distal axonopathy: evidence in mice and man. *Experimental neurology* **185,** 232-240.

Flatby T & Jansen JKS. (1990). Development of homogeneous fast and slow motor units in the neonatal mouse soleus muscle. *Development* **109,** 723-732.

Forsgren S, Bergh A, Carlsson E & Thornell LE. (1993). Calcitonin gene-related peptide expression at endplates of different fibre types in muscles in rat hind limbs. *Cell and tissue research* **274,** 439-446.

Frey D, Schneider C, Xu L, Borg J, Spooren W & Caroni P. (2000). Early and selective loss of neuromuscular synapse subtypes with low sprouting competence in motoneuron diseases. *The Journal of neuroscience : the official journal of the Society for Neuroscience* **20,** 2534-2542.

Friese A, Kaltschmidt JA, Ladle DR, Sigrist M, Jessell TM & Arber S. (2009). Gamma and alpha motor neurons distinguished by expression of transcription factor Err3. *Proceedings of the National Academy of Sciences of the United States of America* **106,** 13588-13593.

Gao BX & Ziskind-Conhaim L. (1998). Development of ionic currents underlying changes in action potential waveforms in rat spinal motoneurons. *Journal of neurophysiology* **80,** 3047-3061.

Gardiner PF. (1993). Physiological properties of motoneurons innervating different muscle unit types in rat gastrocnemius. *Journal of neurophysiology* **69,** 1160-1170.

Gizzi M, DiRocco A, Sivak M & Cohen B. (1992). Ocular motor function in motor neuron disease. *Neurology* **42,** 1037-1046.

Goetz CG. (2000). Nineteenth century studies of atypical parkinsonism: Charcot and his Salpetriere School. *Advances in neurology* **82,** 1-8.

Goldspink G, Scutt A, Loughna PT, Wells DJ, Jaenicke T & Gerlach GF. (1992). Gene expression in skeletal muscle in response to stretch and force generation. *The American journal of physiology* **262,** R356-363.

Gorassini MA, Bennett DJ & Yang JF. (1998). Self-sustained firing of human motor units. *Neuroscience letters* **247,** 13-16.

Gordon T, Tyreman N, Li S, Putman CT & Hegedus J. (2010). Functional over-load saves motor units in the SOD1-G93A transgenic mouse model of amyotrophic lateral sclerosis. *Neurobiology of disease* **37,** 412-422.

Gould TW, Buss RR, Vinsant S, Prevette D, Sun W, Knudson CM, Milligan CE & Oppenheim RW. (2006). Complete dissociation of motor neuron death from motor dysfunction by Bax deletion in a mouse model of ALS. *The Journal of neuroscience : the official journal of the Society for Neuroscience* **26,** 8774-8786.

Gurney ME, Pu H, Chiu AY, Dal Canto MC, Polchow CY, Alexander DD, Caliendo J, Hentati A, Kwon YW, Deng HX & et al. (1994). Motor neuron degeneration in mice that express a human Cu,Zn superoxide dismutase mutation. *Science* **264,** 1772-1775.

Hall ZW & Sanes JR. (1993). Synaptic structure and development: the neuromuscular junction. *Cell* **72 Suppl,** 99-121.

Hamson DK, Hu JH, Krieger C & Watson NV. (2002). Lumbar motoneuron fate in a mouse model of amyotrophic lateral sclerosis. *Neuroreport* **13,** 2291-2294.

Harris AJ. (1981). Embryonic growth and innervation of rat skeletal muscles. I. Neural regulation of muscle fibre numbers. *Philosophical transactions of the Royal Society of London Series B, Biological sciences* **293,** 257-277.

Harvey PJ, Li Y, Li X & Bennett DJ. (2006). Persistent sodium currents and repetitive firing in motoneurons of the sacrocaudal spinal cord of adult rats. *Journal of neurophysiology* **96,** 1141-1157.

Heckman CJ & Enoka RM. (2012). Motor unit. *Comprehensive Physiology* **2,** 2629-2682.

Hegedus J, Putman CT & Gordon T. (2007). Time course of preferential motor unit loss in the SOD1 G93A mouse model of amyotrophic lateral sclerosis. *Neurobiology of disease* **28,** 154-164.

Hegedus J, Putman CT, Tyreman N & Gordon T. (2008). Preferential motor unit loss in the SOD1 G93A transgenic mouse model of amyotrophic lateral sclerosis. *J Physiol* **586,** 3337-3351.

Henneman E. (1957). Relation between size of neurons and their susceptibility to discharge. *Science* **126,** 1345-1347.

Henneman E. (1985). The size-principle: a deterministic output emerges from a set of probabilistic connections. *The Journal of experimental biology* **115,** 105-112.

Henneman E & Mendell LM. (1981). Functional organization of motoneuron pool and its inputs. *In: Brooks VB, editor Handbook of Physiology, The Nervous System, Motor Control Bethesda, MD: American Physiological Society,* **,** 423-507.

Henneman E, Somjen G & Carpenter DO. (1965). Functional Significance of Cell Size in Spinal Motoneurons. *Journal of neurophysiology* **28,** 560-580.

Hivert B, Bouhanna S, Diochot S, Camu W, Dayanithi G, Henderson CE & Valmier J. (1995). Embryonic rat motoneurons express a functional P-type voltage-dependent calcium channel. *International journal of developmental neuroscience : the official journal of the International Society for Developmental Neuroscience* **13,** 429-436.

Horcholle-Bossavit G, Jami L, Thiesson D & Zytnicki D. (1990). Postnatal development of peroneal motoneurons in the kitten. *Brain research Developmental brain research* **54,** 205-215.

Hounsgaard J, Hultborn H, Jespersen B & Kiehn O. (1988). Bistability of alpha-motoneurones in the decerebrate cat and in the acute spinal cat after intravenous 5-hydroxytryptophan. *J Physiol* **405,** 345-367.

Hounsgaard J & Mintz I. (1988). Calcium conductance and firing properties of spinal motoneurones in the turtle. *J Physiol* **398,** 591-603.

Howland DS, Liu J, She Y, Goad B, Maragakis NJ, Kim B, Erickson J, Kulik J, DeVito L, Psaltis G, DeGennaro LJ, Cleveland DW & Rothstein JD. (2002). Focal loss of the

glutamate transporter EAAT2 in a transgenic rat model of SOD1 mutant-mediated amyotrophic lateral sclerosis (ALS). *Proceedings of the National Academy of Sciences of the United States of America* **99,** 1604-1609.

Huguenard JR, Coulter DA & Prince DA. (1991). A fast transient potassium current in thalamic relay neurons: kinetics of activation and inactivation. *Journal of neurophysiology* **66,** 1304-1315.

Hultborn H, Denton ME, Wienecke J & Nielsen JB. (2003). Variable amplification of synaptic input to cat spinal motoneurones by dendritic persistent inward current. *J Physiol* **552,** 945-952.

Iglesias C, Meunier C, Manuel M, Timofeeva Y, Delestree N & Zytnicki D. (2011). Mixed mode oscillations in mouse spinal motoneurons arise from a low excitability state. *The Journal of neuroscience : the official journal of the Society for Neuroscience* **31,** 5829-5840.

Ilieva H, Polymenidou M & Cleveland DW. (2009). Non-cell autonomous toxicity in neurodegenerative disorders: ALS and beyond. *The Journal of cell biology* **187,** 761-772.

Ito M & Oshima T. (1965). Electrical behaviour of the motoneurone membrane during intracellularly applied current steps. *J Physiol* **180,** 607-635.

Jansen JKS & Flatby T. (1990). The perinatal reorganization of the innervation of skeletal muscle in mammals. *Progress in Neurobiology* **34,** 39-90.

Jiang Z, Rempel J, Li J, Sawchuk MA, Carlin KP & Brownstone RM. (1999). Development of L-type calcium channels and a nifedipine-sensitive motor activity in the postnatal mouse spinal cord. *The European journal of neuroscience* **11,** 3481-3487.

Jokic N, Gonzalez de Aguilar JL, Dimou L, Lin S, Fergani A, Ruegg MA, Schwab ME, Dupuis L & Loeffler JP. (2006). The neurite outgrowth inhibitor Nogo-A promotes denervation in an amyotrophic lateral sclerosis model. *EMBO reports* **7,** 1162-1167.

Jones KE, Lyons M, Bawa P & Lemon RN. (1994). Recruitment order of motoneurons during functional tasks. *Experimental brain research Experimentelle Hirnforschung Experimentation cerebrale* **100,** 503-508.

Kaminski HJ, Richmonds CR, Kusner LL & Mitsumoto H. (2002). Differential susceptibility of the ocular motor system to disease. *Annals of the New York Academy of Sciences* **956,** 42-54.

Kanda K, Burke RE & Walmsley B. (1977). Differential control of fast and slow twitch motor units in the decerebrate cat. *Experimental brain research Experimentelle Hirnforschung Experimentation cerebrale* **29,** 57-74.

Kang SH, Li Y, Fukaya M, Lorenzini I, Cleveland DW, Ostrow LW, Rothstein JD & Bergles DE. (2013). Degeneration and impaired regeneration of gray matter oligodendrocytes in amyotrophic lateral sclerosis. *Nature neuroscience* **16,** 571-579.

Kato S. (2008). Amyotrophic lateral sclerosis models and human neuropathology: similarities and differences. *Acta neuropathologica* **115,** 97-114.

Kato T, Kurita K, Seino T, Kadoya T, Horie H, Wada M, Kawanami T, Daimon M & Hirano A. (2001). Galectin-1 is a component of neurofilamentous lesions in sporadic and familial amyotrophic lateral sclerosis. *Biochemical and biophysical research communications* **282,** 166-172.

Kernell D. (2006). The motoneuron and its muscle fibers. *Oxford, UK: Oxford UP*.

Kiehn O & Eken T. (1997). Prolonged firing in motor units: evidence of plateau potentials in human motoneurons? *Journal of neurophysiology* **78,** 3061-3068.

Kiehn O & Eken T. (1998). Functional role of plateau potentials in vertebrate motor neurons. *Current opinion in neurobiology* **8,** 746-752.

Kieran D, Hafezparast M, Bohnert S, Dick JR, Martin J, Schiavo G, Fisher EM & Greensmith L. (2005). A mutation in dynein rescues axonal transport defects and extends the life span of ALS mice. *The Journal of cell biology* **169,** 561-567.

Kikuchi H, Almer G, Yamashita S, Guegan C, Nagai M, Xu Z, Sosunov AA, McKhann GM, 2nd & Przedborski S. (2006). Spinal cord endoplasmic reticulum stress associated with a microsomal accumulation of mutant superoxide dismutase-1 in an ALS model. *Proceedings of the National Academy of Sciences of the United States of America* **103,** 6025-6030.

Kong J & Xu Z. (1998). Massive mitochondrial degeneration in motor neurons triggers the onset of amyotrophic lateral sclerosis in mice expressing a mutant SOD1. *The Journal of neuroscience : the official journal of the Society for Neuroscience* **18,** 3241-3250.

Kuo JJ, Schonewille M, Siddique T, Schults AN, Fu R, Bar PR, Anelli R, Heckman CJ & Kroese AB. (2004). Hyperexcitability of cultured spinal motoneurons from presymptomatic ALS mice. *Journal of neurophysiology* **91,** 571-575.

Kuo JJ, Siddique T, Fu R & Heckman CJ. (2005). Increased persistent Na(+) current and its effect on excitability in motoneurones cultured from mutant SOD1 mice. *J Physiol* **563,** 843-854.

Lamotte d'Incamps B, Krejci E & Ascher P. (2012). Mechanisms shaping the slow nicotinic synaptic current at the motoneuron-renshaw cell synapse. *The Journal of neuroscience : the official journal of the Society for Neuroscience* **32,** 8413-8423.

Lance-Jones C. (1982). Motoneuron cell death in the developing lumbar spinal cord of the mouse. *Brain research* **256,** 473-479.

Lape R & Nistri A. (1999). Voltage-activated K+ currents of hypoglossal motoneurons in a brain stem slice preparation from the neonatal rat. *Journal of neurophysiology* **81,** 140-148.

Lee RH & Heckman CJ. (1998a). Bistability in spinal motoneurons in vivo: systematic variations in persistent inward currents. *Journal of neurophysiology* **80,** 583-593.

Lee RH & Heckman CJ. (1998b). Bistability in spinal motoneurons in vivo: systematic variations in rhythmic firing patterns. *Journal of neurophysiology* **80,** 572-582.

Lee RH & Heckman CJ. (2000). Adjustable amplification of synaptic input in the dendrites of spinal motoneurons in vivo. *The Journal of neuroscience : the official journal of the Society for Neuroscience* **20,** 6734-6740.

Li Y, Brewer D, Burke RE & Ascoli GA. (2005). Developmental changes in spinal motoneuron dendrites in neonatal mice. *The Journal of comparative neurology* **483,** 304-317.

Li Y, Gorassini MA & Bennett DJ. (2004). Role of persistent sodium and calcium currents in motoneuron firing and spasticity in chronic spinal rats. *Journal of neurophysiology* **91,** 767-783.

Liddel EGT & Sherrington CS. (1925). Recruitment and some other factors of reflex inhibition. *Proc R Soc London* **B(97)**.

Ligon LA, LaMonte BH, Wallace KE, Weber N, Kalb RG & Holzbaur EL. (2005). Mutant superoxide dismutase disrupts cytoplasmic dynein in motor neurons. *Neuroreport* **16,** 533-536.

Ling SC, Polymenidou M & Cleveland DW. (2013). Converging Mechanisms in ALS and FTD: Disrupted RNA and Protein Homeostasis. *Neuron* **79,** 416-438.

Lips MB & Keller BU. (1998). Endogenous calcium buffering in motoneurones of the nucleus hypoglossus from mouse. *J Physiol* **511 (Pt 1),** 105-117.

Lowrie MB, More AF & Vrbova G. (1989). The effect of load on the phenotype of the developing rat soleus muscle. *Pflugers Archiv : European journal of physiology* **415,** 204-208.

Lüthi A, Gahwiler BH & Gerber U. (1996). A slowly inactivating potassium current in CA3 pyramidal cells of rat hippocampus in vitro. *The Journal of neuroscience : the official journal of the Society for Neuroscience* **16,** 586-594.

Magarinos-Ascone C, Nunez A & Delgado-Garcia JM. (1999). Different discharge properties of rat facial nucleus motoneurons. *Neuroscience* **94,** 879-886.

Mannen T. (2000). Neuropathological findings of Onuf's nucleus and its significance. *Neuropathology : official journal of the Japanese Society of Neuropathology* **20 Suppl,** S30-33.

Manuel M, Iglesias C, Donnet M, Leroy F, Heckman CJ & Zytnicki D. (2009). Fast kinetics, high-frequency oscillations, and subprimary firing range in adult mouse spinal motoneurons. *The Journal of neuroscience : the official journal of the Society for Neuroscience* **29,** 11246-11256.

Manuel M, Meunier C, Donnet M & Zytnicki D. (2007). Resonant or not, two amplification modes of proprioceptive inputs by persistent inward currents in spinal motoneurons. *The Journal of neuroscience : the official journal of the Society for Neuroscience* **27,** 12977-12988.

Martin E, Cazenave W, Cattaert D & Branchereau P. (2013). Embryonic alteration of motoneuronal morphology induces hyperexcitability in the mouse model of amyotrophic lateral sclerosis. *Neurobiology of disease* **54,** 116-126.

Martin LJ, Liu Z, Chen K, Price AC, Pan Y, Swaby JA & Golden WC. (2007). Motor neuron degeneration in amyotrophic lateral sclerosis mutant superoxide dismutase-1

transgenic mice: mechanisms of mitochondriopathy and cell death. *The Journal of comparative neurology* **500,** 20-46.

McCobb DP, Best PM & Beam KG. (1989). Development alters the expression of calcium currents in chick limb motoneurons. *Neuron* **2,** 1633-1643.

McCobb DP, Best PM & Beam KG. (1990). The differentiation of excitability in embryonic chick limb motoneurons. *The Journal of neuroscience : the official journal of the Society for Neuroscience* **10,** 2974-2984.

McLennan IS. (1983). Differentiation of muscle fiber types in the chicken hindlimb. *Developmental biology* **97,** 222-228.

Mendell LM & Henneman E. (1968). Terminals of single Ia fibers: distribution within a pool of 300 homonymous motor neurons. *Science* **160,** 96-98.

Mentis GZ, Blivis D, Liu W, Drobac E, Crowder ME, Kong L, Alvarez FJ, Sumner CJ & O'Donovan MJ. (2011). Early functional impairment of sensory-motor connectivity in a mouse model of spinal muscular atrophy. *Neuron* **69,** 453-467.

Mitsumoto H, Przedborski S & Gordon PH. (2006). *Amyotrophic lateral sclerosis*. Taylor & Francis, New York.

Mourelatos Z, Gonatas NK, Stieber A, Gurney ME & Dal Canto MC. (1996). The Golgi apparatus of spinal cord motor neurons in transgenic mice expressing mutant Cu,Zn superoxide dismutase becomes fragmented in early, preclinical stages of the disease. *Proceedings of the National Academy of Sciences of the United States of America* **93,** 5472-5477.

Mullen RJ, Buck CR & Smith AM. (1992). NeuN, a neuronal specific nuclear protein in vertebrates. *Development* **116,** 201-211.

Mynlieff M & Beam KG. (1992a). Characterization of voltage-dependent calcium currents in mouse motoneurons. *Journal of neurophysiology* **68,** 85-92.

Mynlieff M & Beam KG. (1992b). Developmental expression of voltage-dependent calcium currents in identified mouse motoneurons. *Developmental biology* **152,** 407-410.

Narusawa M, Fitzsimons RB, Izumo S, Nadal-Ginard B, Rubinstein NA & Kelly AM. (1987). Slow myosin in developing rat skeletal muscle. *The Journal of cell biology* **104,** 447-459.

Nikolaev A, McLaughlin T, O'Leary DD & Tessier-Lavigne M. (2009). APP binds DR6 to trigger axon pruning and neuron death via distinct caspases. *Nature* **457,** 981-989.

Nowik I, Zamir S & Segev I. (2012). Losing the battle but winning the war: game theoretic analysis of the competition between motoneurons innervating a skeletal muscle. *Frontiers in computational neuroscience* **6,** 16.

Nunez-Abades PA & Cameron WE. (1995). Morphology of developing rat genioglossal motoneurons studied in vitro: relative changes in diameter and surface area of somata and dendrites. *The Journal of comparative neurology* **353,** 129-142.

Nunez-Abades PA, He F, Barrionuevo G & Cameron WE. (1994). Morphology of developing rat genioglossal motoneurons studied in vitro: changes in length, branching pattern,

and spatial distribution of dendrites. *The Journal of comparative neurology* **339,** 401-420.

O'Brien RA, Ostberg AJ & Vrbova G. (1978). Observations on the elimination of polyneuronal innervation in developing mammalian skeletal muscle. *J Physiol* **282,** 571-582.

Obal I, Engelhardt JI & Siklos L. (2006). Axotomy induces contrasting changes in calcium and calcium-binding proteins in oculomotor and hypoglossal nuclei of Balb/c mice. *The Journal of comparative neurology* **499,** 17-32.

Pambo-Pambo A, Durand J & Gueritaud JP. (2009). Early excitability changes in lumbar motoneurons of transgenic SOD1G85R and SOD1G(93A-Low) mice. *Journal of neurophysiology* **102,** 3627-3642.

Papadimitriou D, Le Verche V, Jacquier A, Ikiz B, Przedborski S & Re DB. (2010). Inflammation in ALS and SMA: sorting out the good from the evil. *Neurobiology of disease* **37,** 493-502.

Perrier JF & Hounsgaard J. (1999). Ca(2+)-activated nonselective cationic current (I(CAN)) in turtle motoneurons. *Journal of neurophysiology* **82,** 730-735.

Perrier JF & Hounsgaard J. (2000). Development and regulation of response properties in spinal cord motoneurons. *Brain research bulletin* **53,** 529-535.

Picquet F, Stevens L, Butler-Browne GS & Mounier Y. (1998). Differential effects of a six-day immobilization on newborn rat soleus muscles at two developmental stages. *Journal of muscle research and cell motility* **19,** 743-755.

Piehl F, Arvidsson U, Hokfelt T & Cullheim S. (1993). Calcitonin gene-related peptide-like immunoreactivity in motoneuron pools innervating different hind limb muscles in the rat. *Experimental brain research Experimentelle Hirnforschung Experimentation cerebrale* **96,** 291-303.

Pieri M, Albo F, Gaetti C, Spalloni A, Bengtson CP, Longone P, Cavalcanti S & Zona C. (2003). Altered excitability of motor neurons in a transgenic mouse model of familial amyotrophic lateral sclerosis. *Neuroscience letters* **351,** 153-156.

Pongs O, Leicher T, Berger M, Roeper J, Bahring R, Wray D, Giese KP, Silva AJ & Storm JF. (1999). Functional and molecular aspects of voltage-gated K+ channel beta subunits. *Annals of the New York Academy of Sciences* **868,** 344-355.

Prather JF, Powers RK & Cope TC. (2001). Amplification and linear summation of synaptic effects on motoneuron firing rate. *Journal of neurophysiology* **85,** 43-53.

Pun S, Santos AF, Saxena S, Xu L & Caroni P. (2006). Selective vulnerability and pruning of phasic motoneuron axons in motoneuron disease alleviated by CNTF. *Nature neuroscience* **9,** 408-419.

Quinlan KA, Schuster JE, Fu R, Siddique T & Heckman CJ. (2011). Altered postnatal maturation of electrical properties in spinal motoneurons in a mouse model of amyotrophic lateral sclerosis. *J Physiol* **589,** 2245-2260.

Raoul C, Estevez AG, Nishimune H, Cleveland DW, deLapeyriere O, Henderson CE, Haase G & Pettmann B. (2002). Motoneuron death triggered by a specific pathway

downstream of Fas. potentiation by ALS-linked SOD1 mutations. *Neuron* **35,** 1067-1083.

Redfern PA. (1970). Neuromuscular transmission in new-born rats. *J Physiol* **209,** 701-709.

Rosen DR, Siddique T, Patterson D, Figlewicz DA, Sapp P, Hentati A, Donaldson D, Goto J, O'Regan JP, Deng HX & et al. (1993). Mutations in Cu/Zn superoxide dismutase gene are associated with familial amyotrophic lateral sclerosis. *Nature* **362,** 59-62.

Rothstein JD, Van Kammen M, Levey AI, Martin LJ & Kuncl RW. (1995). Selective loss of glial glutamate transporter GLT-1 in amyotrophic lateral sclerosis. *Annals of neurology* **38,** 73-84.

Russier M, Carlier E, Ankri N, Fronzaroli L & Debanne D. (2003). A-, T-, and H-type currents shape intrinsic firing of developing rat abducens motoneurons. *J Physiol* **549,** 21-36.

Russo RE & Hounsgaard J. (1999). Dynamics of intrinsic electrophysiological properties in spinal cord neurones. *Progress in biophysics and molecular biology* **72,** 329-365.

Safronov BV & Vogel W. (1995). Single voltage-activated Na+ and K+ channels in the somata of rat motoneurones. *J Physiol* **487 (Pt 1),** 91-106.

Saxena S, Cabuy E & Caroni P. (2009). A role for motoneuron subtype-selective ER stress in disease manifestations of FALS mice. *Nature neuroscience* **12,** 627-636.

Saxena S, Roselli F, Singh K, Leptien K, Julien JP, Gros-Louis F & Caroni P. (2013). Neuroprotection through Excitability and mTOR Required in ALS Motoneurons to Delay Disease and Extend Survival. *Neuron* **80,** 80-96.

Schaefer AM, Sanes JR & Lichtman JW. (2005). A compensatory subpopulation of motor neurons in a mouse model of amyotrophic lateral sclerosis. *The Journal of comparative neurology* **490,** 209-219.

Schiaffino S, Gorza L, Pitton G, Saggin L, Ausoni S, Sartore S & Lomo T. (1988). Embryonic and neonatal myosin heavy chain in denervated and paralyzed rat skeletal muscle. *Developmental biology* **127,** 1-11.

Schiaffino S & Reggiani C. (2011). Fiber types in mammalian skeletal muscles. *Physiological reviews* **91,** 1447-1531.

Schroder HD & Reske-Nielsen E. (1984). Preservation of the nucleus X-pelvic floor motosystem in amyotrophic lateral sclerosis. *Clinical neuropathology* **3,** 210-216.

Schwindt PC & Crill WE. (1980). Properties of a persistent inward current in normal and TEA-injected motoneurons. *Journal of neurophysiology* **43,** 1700-1724.

Schwindt PC & Crill WE. (1984). Membrane properties of cat spinal motoneurones. *In: Davidoff, R A, ed Handbook of the spinal cord New York/Basel: Marcel Dekker Inc***,** 199–242.

Scutter SD & Turker KS. (1998). Recruitment stability in masseter motor units during isometric voluntary contractions. *Muscle & nerve* **21,** 1290-1298.

Shneider NA, Brown MN, Smith CA, Pickel J & Alvarez FJ. (2009). Gamma motor neurons express distinct genetic markers at birth and require muscle spindle-derived GDNF for postnatal survival. *Neural development* **4,** 42.

Spitzer NC. (2006). Electrical activity in early neuronal development. *Nature* **444,** 707-712.

Storm JF. (1988). Temporal integration by a slowly inactivating K+ current in hippocampal neurons. *Nature* **336,** 379-381.

Sumi H, Nagano S, Fujimura H, Kato S & Sakoda S. (2006). Inverse correlation between the formation of mitochondria-derived vacuoles and Lewy-body-like hyaline inclusions in G93A superoxide-dismutase-transgenic mice. *Acta neuropathologica* **112,** 52-63.

Svirskis G & Hounsgaard J. (1998). Transmitter regulation of plateau properties in turtle motoneurons. *Journal of neurophysiology* **79,** 45-50.

Theiss RD, Kuo JJ & Heckman CJ. (2007). Persistent inward currents in rat ventral horn neurones. *J Physiol* **580,** 507-522.

Thompson WJ. (1985). Activity and synapse elimination at the neuromuscular junction. *Cellular and molecular neurobiology* **5,** 167-182.

Thompson WJ, Condon K & Astrow SH. (1990). The origin and selective innervation of early muscle fiber types in the rat. *Journal of neurobiology* **21,** 212-222.

Thompson WJ, Sutton LA & Riley DA. (1984). Fibre type composition of single motor units during synapse elimination in neonatal rat soleus muscle. *Nature* **309,** 709-711.

Thuault SJ, Malleret G, Constantinople CM, Nicholls R, Chen I, Zhu J, Panteleyev A, Vronskaya S, Nolan MF, Bruno R, Siegelbaum SA & Kandel ER. (2013). Prefrontal Cortex HCN1 Channels Enable Intrinsic Persistent Neural Firing and Executive Memory Function. *The Journal of neuroscience : the official journal of the Society for Neuroscience* **33,** 13583-13599.

Tripodi M, Evers JF, Mauss A, Bate M & Landgraf M. (2008). Structural homeostasis: compensatory adjustments of dendritic arbor geometry in response to variations of synaptic input. *PLoS biology* **6,** e260.

Tu PH, Raju P, Robinson KA, Gurney ME, Trojanowski JQ & Lee VM. (1996). Transgenic mice carrying a human mutant superoxide dismutase transgene develop neuronal cytoskeletal pathology resembling human amyotrophic lateral sclerosis lesions. *Proceedings of the National Academy of Sciences of the United States of America* **93,** 3155-3160.

Turner BJ & Talbot K. (2008). Transgenics, toxicity and therapeutics in rodent models of mutant SOD1-mediated familial ALS. *Progress in neurobiology* **85,** 94-134.

Van Den Bosch L, Van Damme P, Bogaert E & Robberecht W. (2006). The role of excitotoxicity in the pathogenesis of amyotrophic lateral sclerosis. *Biochimica et biophysica acta* **1762,** 1068-1082.

Van Essen DC, Gordon H, Soha JM & Fraser SE. (1990). Synaptic dynamics at the neuromuscular junction: mechanisms and models. *Journal of neurobiology* **21,** 223-249.

van Zundert B, Peuscher MH, Hynynen M, Chen A, Neve RL, Brown RH, Jr., Constantine-Paton M & Bellingham MC. (2008). Neonatal neuronal circuitry shows hyperexcitable disturbance in a mouse model of the adult-onset neurodegenerative disease amyotrophic lateral sclerosis. *The Journal of neuroscience : the official journal of the Society for Neuroscience* **28,** 10864-10874.

Veldink JH, Bar PR, Joosten EA, Otten M, Wokke JH & van den Berg LH. (2003). Sexual differences in onset of disease and response to exercise in a transgenic model of ALS. *Neuromuscular disorders : NMD* **13,** 737-743.

Veldink JH, Kalmijn S, Van der Hout AH, Lemmink HH, Groeneveld GJ, Lummen C, Scheffer H, Wokke JH & Van den Berg LH. (2005). SMN genotypes producing less SMN protein increase susceptibility to and severity of sporadic ALS. *Neurology* **65,** 820-825.

Venugopal S, Hamm TM, Crook SM & Jung R. (2011). Modulation of inhibitory strength and kinetics facilitates regulation of persistent inward currents and motoneuron excitability following spinal cord injury. *Journal of neurophysiology* **106,** 2167-2179.

Viana F, Bayliss DA & Berger AJ. (1995). Repetitive firing properties of developing rat brainstem motoneurones. *J Physiol* **486 (Pt 3),** 745-761.

Vlug AS, Teuling E, Haasdijk ED, French P, Hoogenraad CC & Jaarsma D. (2005). ATF3 expression precedes death of spinal motoneurons in amyotrophic lateral sclerosis-SOD1 transgenic mice and correlates with c-Jun phosphorylation, CHOP expression, somato-dendritic ubiquitination and Golgi fragmentation. *The European journal of neuroscience* **22,** 1881-1894.

Wang L, Deng HX, Grisotti G, Zhai H, Siddique T & Roos RP. (2009). Wild-type SOD1 overexpression accelerates disease onset of a G85R SOD1 mouse. *Human molecular genetics* **18,** 1642-1651.

Weydert A, Barton P, Harris AJ, Pinset C & Buckingham M. (1987). Developmental pattern of mouse skeletal myosin heavy chain gene transcripts in vivo and in vitro. *Cell* **49,** 121-129.

Wong PC, Cai H, Borchelt DR & Price DL. (2002). Genetically engineered mouse models of neurodegenerative diseases. *Nature neuroscience* **5,** 633-639.

Wooley CM, Sher RB, Kale A, Frankel WN, Cox GA & Seburn KL. (2005). Gait analysis detects early changes in transgenic SOD1(G93A) mice. *Muscle & nerve* **32,** 43-50.

Wootz H, Fitzsimons-Kantamneni E, Larhammar M, Rotterman TM, Enjin A, Patra K, Andre E, Van Zundert B, Kullander K & Alvarez FJ. (2013). Alterations in the motor neuron-renshaw cell circuit in the Sod1(G93A) mouse model. *The Journal of comparative neurology* **521,** 1449-1469.

Wootz H, Hansson I, Korhonen L, Napankangas U & Lindholm D. (2004). Caspase-12 cleavage and increased oxidative stress during motoneuron degeneration in transgenic mouse model of ALS. *Biochemical and biophysical research communications* **322,** 281-286.

Yamanaka K, Boillee S, Roberts EA, Garcia ML, McAlonis-Downes M, Mikse OR, Cleveland DW & Goldstein LS. (2008). Mutant SOD1 in cell types other than motor neurons and

oligodendrocytes accelerates onset of disease in ALS mice. *Proceedings of the National Academy of Sciences of the United States of America* **105,** 7594-7599.

Yang Y, Gozen O, Watkins A, Lorenzini I, Lepore A, Gao Y, Vidensky S, Brennan J, Poulsen D, Won Park J, Li Jeon N, Robinson MB & Rothstein JD. (2009). Presynaptic regulation of astroglial excitatory neurotransmitter transporter GLT1. *Neuron* **61,** 880-894.

Yao WD & Wu CF. (1999). Auxiliary Hyperkinetic beta subunit of K+ channels: regulation of firing properties and K+ currents in Drosophila neurons. *Journal of neurophysiology* **81,** 2472-2484.

Yoshikawa M, Vinsant S, Mansfield CM, Moreno RJ, Gifondorwa DJ & al. e. (2009). Identification of changes in muscle, neuromuscular junctions and spinal cord at early presymptomatic stages in the mutant SOD1 mouse model of ALS may provide novel insight for diagnosis and treatment development. *Progr No 6325 2009 Neuroscience Meeting Planner Chicago, IL: Soc Neurosci http://wwwsfnorg/am2009/*.

Zengel JE, Reid SA, Sypert GW & Munson JB. (1985). Membrane electrical properties and prediction of motor-unit type of medial gastrocnemius motoneurons in the cat. *Journal of neurophysiology* **53,** 1323-1344.

Zhang B, Tu P, Abtahian F, Trojanowski JQ & Lee VM. (1997). Neurofilaments and orthograde transport are reduced in ventral root axons of transgenic mice that express human SOD1 with a G93A mutation. *The Journal of cell biology* **139,** 1307-1315.

Zhu J, Feng F, Ni K, Zheng Y & Zhang J. (2012). Four subtypes of motor neurons exhibiting mutually exclusive firing patterns in the spinal ventral horn. *Neuroscience letters* **525,** 163-167.

Supplementary material

1/ Synaptic inputs have no tonic effect on neonatal motoneurons recorded in slice

Venugopal *et al.* (2011) recently posited a tonic effect of the spontaneous synaptic activity in the slice on the motoneuron intrinsic properties, particularly on the shape of the F-I curve. This additional section will demonstrate the contrary. I recorded several motoneuron intrinsic properties before and after applying a cocktail of synaptic blockers (50 µM APV, 2 µM NBQX, 1 µM strychnine and 3 µM gabazine). As quantified in the tables, every measured intrinsic property remains the same with or without synaptic inputs, including the F-I relationships.

a/ Delayed firing motoneurons

In this table we compare different delayed firing motoneurons recorded with or without spontaneous synaptic inputs. On average, all properties measured while blocking the synaptic inputs are very close from the control.

	Delayed firing MNs control	Delayed firing MNs without synaptic inputs	*Mann-Whitney U test*
input conductance (nS)	51.9 ± 28,1 10 / 151.5 N=59	58.9 ± 28.7 13 / 142 N=26	n.s
resting potential (mV) non-corrected	-63.6 ± 4.2 -72 / -55 N=59	-65.1 ± 5.8 -71 / -52 N=26	n.s
recruitment current on ramp (pA)	1199 ± 613 300 / 2800 N=59	1269 ± 617 415 / 2094 N=26	n.s
gain descending ramp (Hz/nA)	19.5 ± 7.8 5.2 / 53.7 N=51	20.1 ± 5.9 13.5 / 34.7 N=22	n.s

b/ Immediate firing motoneurons

In this table we compare different immediate firing motoneurons recorded with or without synaptic inputs. On average, all properties measured while blocking the synaptic inputs are very close from the control.

	Immediate firing MNs control	Immediate firing MNs without synaptic inputs	*Mann-Whitney U test*
input conductance (nS)	33.1 ± 23.0 5.7 / 98 N=30	34.8 ± 23.3 6.1 / 69 N=10	n.s
resting potential (mV)	-64.3 ± 5,3 -79 / -53 N=30	-66.6 ± 6.3 -80 / -61 N=10	n.s
recruitment current on ramp (pA)	667 ± 517 67 / 1965 N=20	645 ± 550 149 / 2091 N=10	n.s
gain descending ramp (Hz/nA)	49.6 ± 43.32 6.4 / 157.6 N=20	46.7 ± 25.1 22.3 / 88.8 N=10	n.s

B/ Other conductances exhibited by the neonatal spinal motoneurons

a/ H-current

Adult motoneurons are known to express the H-current. However it has never been reported in neonatal spinal motoneurons so far. In my recordings, some of the neonatal motoneurons exhibited a sag response when small hyperpolarizing or depolarizing currents were applied (Figure 17 black traces). I used ZD 7288 (10 µM) to inquire the nature of the sag response. All sag disappeared after 15 min of ZD 7288 application (Figure 17 red traces, n=3). H-current was found in delayed and immediate firing motoneurons over several separated experiments. It is likely that neonatal motoneurons start to express the H-current during my recording window.

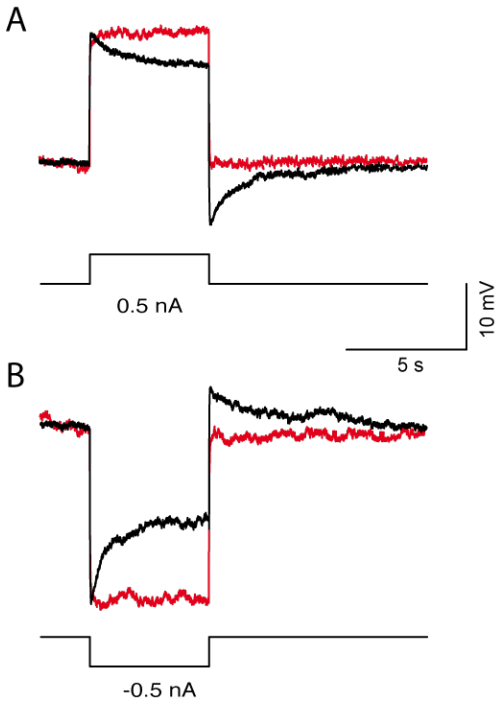

Figure 17: Some motoneurons express the H-current. Depolarizing (**A**) or hyperpolarizing (**B**) pulse of current in control condition (black trace) or following 15 min perfusion of 30 µM ZD 7288 (red trace).

b/ putative calcium-activated non-selective cation current

In some of the WT delayed firing motoneurons I noted the appearance of a depolarization following the 5 s pulses (sADP, Figure 18A and B). Duration and intensity increased with the pulse intensity and could reach spiking threshold in some

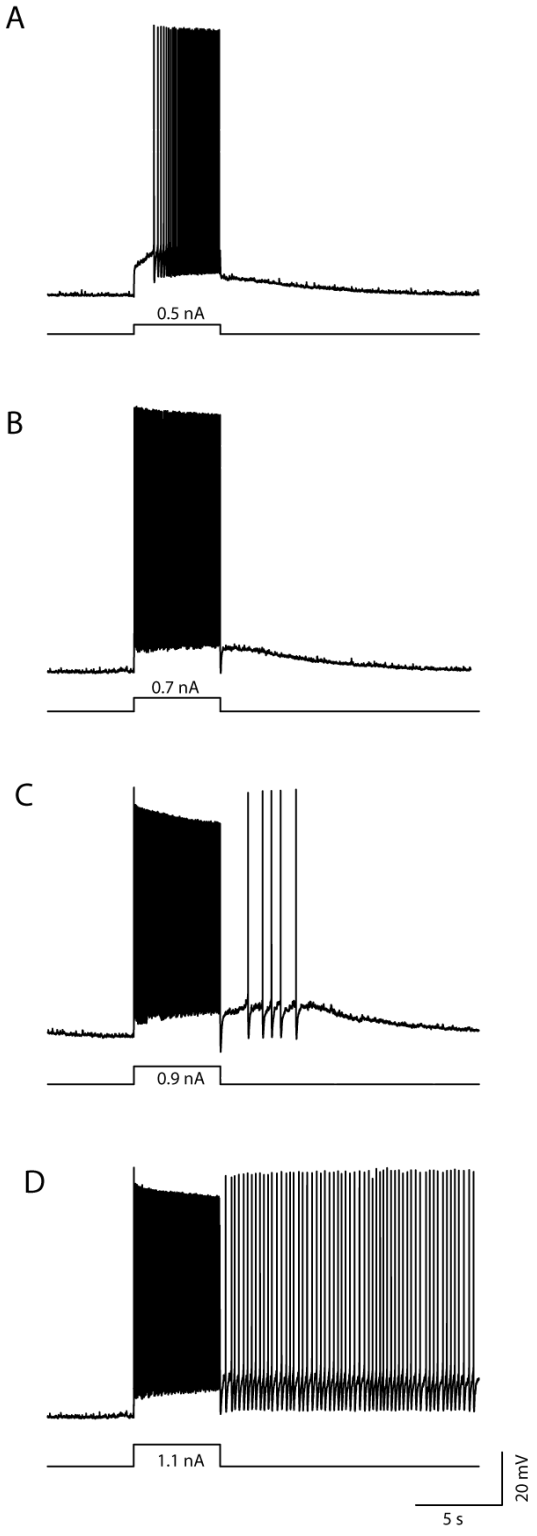

Figure 18: activation of I_{can} in delayed firing motoneuron. Increasing pulses of current. Note the increasing depolarizations following the pulses (**A** and **B**) sufficient to induce spiking (**C**) and plateau potential (**D**).

case (Figure 18C). When the motoneuron entered its up state it kept firing for several minutes (Figure 18D) or until a hyperpolarizing pulse was applied (not shown). The application of 50 µ M of Cd^{2+}, a non-specific Ca^{2+} channel blocker had no incidence on the sADP and we concluded that the calcium persistent current was not involved in the sADP. Such sADP could also be elicited in mouse pyramidal neurons through the recruitment of the calcium-activated non-selective cation current (I_{can}, Thuault *et al.*, 2013). In this work, the activation required the bath application of the acetylcholine muscarinic receptor agonist Carbachol (CCh) at 10 µm coupled with depolarizing pulses to make the motoneuron discharge and allow for Ca^{2+} entry. Furthermore, Perrier et al (1999) found I_{can} current in turtle motoneurons. This hypothesis remains however to be experimentally tested.

c/ Ca^{2+} currents

During voltage-clamp experiments a large Cd^{2+} sensitive current was detected for large depolarization following the A-current peak (Figure 19 black trace peak 2). This current was only observed in delayed motoneurons. We know that motoneurons express various high-threshold calcium channels (Mynlieff & Beam, 1992a). When present I applied 50 µM Cd^{2+} in order to better visualize the time course of the A-current (Figure 19 peak 1) and the slow potassium current (Figure 19 peak 3). Note how the amplitude of the A-current increases when the opposing current is blocked (peak 1 red trace). Further experiments using more specific drugs are however required to

properly characterized this high-threshold calcium current and its role in the motoneurons physiology.

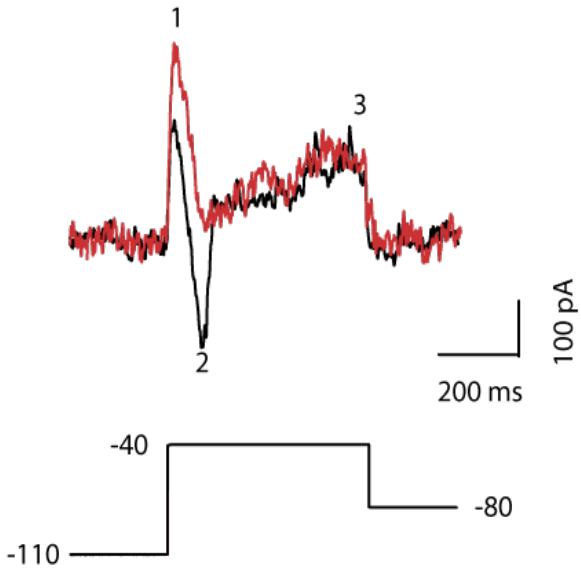

Figure 19: Ca^{2+} current in delayed firing motoneuron. Leak-substracted voltage-clamp recoding of a delayed firing motoneuron in control conditions (black trace) and following 15 min application of 50 µM Cd^{2+}

3/ Protocols

a/ ChodI *in situ* hybridization protocol for floating sections

All solutions and vials used should be RNase-free

Day 1

1. Perfuse the mouse and dissect out the spinal cord.
2. Remove the thin membrane around the spinal cord and the roots
3. Fix the spinal cord in 4% PFA o/n at 4ºC. (store at least 5 days in the fridge, but go down to 1% PFA after 24h)
4. Embed the lumbar part of the spinal cord in 4% agarose (1g agarose in 25mL PBS)
5. Section the spinal cord (60µm). Put the sections in PBS.

6. If spinal cord will be stored for longer than 2 weeks, dehydrate sections by successive washes in 25%, 50%, and 75% methanol in PBT 10 minutes each. Store in 100% methanol at -20ºC.

Day 2

1. Ask to use oven and preheat oven to 63ºC.

2. Cut the end off of a transfer pipet with RNase-free scissors.

3. Put the desired number of sections into each well by transferring them gently with the transfer pipet.

4. If dehydrated, rehydrate sections by successive washes in 75%, 50%, and 25% methanol in PBT 10 minutes each.

5. Wash with PBT 3x5 minutes.

6. Treat Samples with 0.5% Triton X in PBS for 5 min at R/T (25µL Triton X in 5mL PBS)

7. Wash with PBT 2x5 minutes.

8. Preheat the hybridization solution to 63ºC → for step 16

9. Postfix for 30 min in 4% PFA. (1g PFA in 25mL PBS)

10. Wash with PBT 3x5 minutes.

11. Prehybridize the sections in hybridization buffer for 2h at 63ºC.

12. Preheat heatblock to 80ºC. (Turn it back to 60ºC afterward – before turning heatblock off.)

13. Heat denature the probe (1ng/µL each) in hybridization buffer for 5 min at 80ºC. (1uL probe in 100uL hybridization buffer). ***It should be cooled to 63ºC: either the time it takes you to go get it and carry it back to our lab OR put on ice for 5 min. Vortex.

14. Remove the hybridization buffer carefully (the sections are transparent!) from the wells and add the denatured probed in hybridization buffer.

15. Seal the plate thoroughly with white tape to avoid evaporation.

16. Hybridize o/n at 63ºC.

Day 3

1. Wash 3x30 min with wash buffer 1 at 63ºC.
2. Wash 3x30 min with wash buffer 2 at 63ºC.
3. Wash 2x5 min with TBST (0.1% Tween-20 in 1x TBS) (50uL Tween-20 in 50mL TBS)
4. Incubate in blocking solution for 2 h at RT. (1X blocking reagent in TBST) (Add 1mL of 10X blocking reagent to 9mL of TBST)
5. Dilute anti-Dig antibody 1:5000 in blocking solution. (Add 1µL anti-Dig antibody to 5mL blocking solution)
6. Seal plate with parafilm to avoid evaporation.
7. Incubate o/n at 4ºC.

Day 4

1. Ask to use oven and preheat oven to 37ºC.
2. Wash with TBST 5x10 min.
3. Develop in BM purple AP substrate OR Fast Red for the rest of the day at 37ºC.
    - BM Purple – use straight from the bottle.
    - Fast Red – dissolve one pellet in 2mL of 0.1M Tris-HCl, pH 8.2
4. Check every 10 min to see development.
5. Wash in PBS 3x5 min when BM purple slices are labelled.
6. Mount using Fluoromount.

b/ Immuno-histochemistry

1. 4% PFA fixation for 30 min.
2. Wash with PBS 3x10 min.

3. Incubate with PBS, 0.3% Triton and 0.1% BSA for 2h.

4. Renew medium and add antibodies.

Antibody	Reference	Dilution	Incubation	Secondary antibody
Streptavidine-Cy3	Vector laboratories SP-1120	1/500	12h at 4°C	None
Anti-Errγ	R&D systems PP-H6812-00	1/100	72h at 4°C	Anti-mouse coupled to alexa 488
Anti-NeuN	Millipore ABN78	1/1000	12h at 4°C	Anti-rabbit coupled to alexa 633

5. Wash with PBS 3x30 min.

6. Incubate with PBS, 0.3% Triton and 0.1% BSA for 2h with the appropriate secondary antibody diluted at 1/500.

7. Wash with PBS 3x10 min.

c/ RT-PCR

Primers multiplex: Err beta, Err gamma, Chodl and Calca

ErrBeta b	GCCAAGCACATCCCAGGCTTCC	259bp
ErrBeta n	GATCATAAACTCTTCCTTCTCTACC	
ErrGamma a	GCAGCCAGCCAAAAAGCCATATAAC	846bp
ErrGamma m	GGCTGCATCGTACTGTGGCTG	
Calca a	GGCTGAGGGCTCTAGCTTGGACAG	462bp
Calca m	GCAAGACTAGAAGCTCTACTAGGAG	
Chodl a	GCTCCCAGTTCCGAAACTGGTAC	654bp
Chodl m	GAGAGTAACCAGGTCTCACTCAGC	

Abstract

In the second postnatal week, the locomotor behavior of mice changes from crawling to walking. This is made possible by profound changes in motor units. Yet, how the discharge properties of spinal motoneurons evolve during post-natal maturation and whether they have an effect on the motor unit maturation remains an open question. In neonates, the spinal motoneurons display two modes of discharge. For threshold pulses, 33% of the motoneurons have a discharge that start at the current onset and adapts during the pulse ("immediate firing motoneurons"). The remaining 66% motoneurons fire with a large delay and the discharge then accelerates throughout the pulse ("delayed firing motoneurons"). Though the delayed firing pattern is quite common in spinal motoneurons of neonates, the ionic mechanisms that elicit this mode of discharge have received little attention.

Using the patch-clamp technique to record P6-P10 mouse motoneurons in a spinal cord slice preparation, I characterized the ionic currents that underlie the delayed firing pattern. This is caused by a combination of an A-like potassium current that acts on a short time scale and a slow-inactivating potassium current that delays the discharge on a much longer time scale. I then investigated how these two potassium currents contribute to the recruitment threshold and how they shape the F-I function of delayed motoneurons in neonatal mice. The slow inactivating potassium current induces memory effects that have a strong impact on motoneuron excitability and on its discharge.

Building on these results, I tried to correlate the discharge pattern to known physiological sub-types. The delayed firing motoneurons have a larger input conductance, a higher rheobase, a narrower action potential, a shorter AHP and a more complex dendritic arbor than the immediate firing motoneurons. Additionally, only a sub-population of the delayed firing motoneurons expressed the chondrolectin protein, a fast motoneuron marker. Based on this body of corroborating evidence, the immediate firing motoneurons would be slow type motoneurons whereas the delayed firing motoneurons would be fast type motoneurons.

Finally, numerous electrical and geometrical abnormalities have been observed in spinal motoneurons of SOD1 G934 mice (model of the amyotrophic lateral sclerosis) during the second post-natal week but the results were somehow contradictory. In relation to the known differential sensitivity to the disease exhibited by slow and fast motoneurons, I investigated whether the immediate and delayed firing motoneurons are equally affected by the SOD1 mutation. This is not the case. I found that the SOD1 mutation induced a decrease in the rheobase and a hyperpolarization of the voltage threshold only in the immediate firing motoneurons, thereby making them more excitable than in WT mice. Furthermore, the dendrites of the immediate firing motoneurons are substantially shorter (about 35%) in the mutant than in the WT. In sharp contrast, the excitability of the delayed firing motoneurons is unchanged and the dendritic tree is nearly unaffected (the dendrites only undergo a 10% elongation). These results allow for reconsidering the link between hyperexcitability and degenerescence of the motoneurons.

Résumé

La deuxième semaine qui suit la naissance est critique pour le développement du système locomoteur de la souris. C'est pendant cette semaine que les souriceaux acquièrent leur posture et commencent à marcher. Cette transformation implique une réorganisation en profondeur des éléments composant les unités motrices. Cependant, nous ne savons encore que peu de choses sur la différenciation des propriétés intrinsèques des motoneurones innervant les fibres musculaires. Contrairement à l'adulte, où la décharge démarre au début de la stimulation, les motoneurones de souriceaux déchargent de façon hétérogène. En effet, une stimulation au seuil induit chez certains motoneurones une décharge commençant au début du créneau alors que la décharge est retardée dans d'autres motoneurones.

Par des enregistrements de motoneurones sur des tranches de moelle épinière à P6-P10, j'ai dans un premier temps caractérisé les courants sous-tendant la décharge retardée et j'ai constaté que deux conductances potassiques (l'une ressemblant au courant de type A et l'autre très lente) étaient activées autour du seuil de décharge. Lorsqu'elles s'activent, ces conductances sont capables d'hyperpolariser le potentiel de membrane et d'empêcher le motoneurone de décharger. Puis, en s'inactivant, la membrane se dépolarise et le neurone commence à décharger avec un retard pouvant aller jusqu'à plusieurs secondes après le début du créneau.

En outre, les deux populations de motoneurones présentent des propriétés électro-physiologiques et morphologiques différentes. Les motoneurones à décharge retardée possèdent un arbre dendritique plus ramifié que ceux à décharge immédiate. En conséquence, les motoneurones à décharge retardée possèdent une conductance d'entrée et un seuil de recrutement plus faible. De plus le temps de relaxation de l'hyperpolarisation suivant chaque potentiel d'action (AHP) est plus long dans les motoneurones à décharge immédiate. Enfin, une partie des motoneurones à décharge retardée exprime la protéine chondrolectine récemment décrite comme un marqueur moléculaire des motoneurones de type rapide. L'ensemble de nos résultats nous permet de faire l'hypothèse que les motoneurones à décharge retardée sont des motoneurones innervant les unités motrices de type rapide alors que ceux à décharge immédiate innervent les unités motrices de type lent.

Dans un second temps, j'ai étudié l'effet de la mutation SOD1 G93A, un modèle murin de la sclérose latérale amyotrophique, sur les motoneurones spinaux à P6-P10. Sachant que cette maladie affecte les motoneurones de façon différente à l'âge adulte, j'ai cherché à savoir si, chez les souriceaux SOD1 G93A, les motoneurones à décharge retardée et immédiate étaient affectés de la même façon. Mes résultats montrent que seuls les motoneurones à décharge immédiate sont hyperexcitables. Pour ces motoneurones, le seuil de décharge est plus hyperpolarisé et leurs dendrites sont plus courtes de 35%. Ces résultats amènent à reconsidérer le lien supposé entre hyperexcitabilité et dégénérescence des motoneurones.